DEPARTMENT OF THE INTERIOR
U.S. GEOLOGICAL SURVEY

Geoelectric characteristics of portions of the Raha fault zone and surrounding rocks, Jabal As Silsilah Quadrangle, Kingdom of Saudi Arabia

by

C. J. Zablocki[1/] and Mohammed O. Hajnour

Open-File Report 87-499

Report prepared by the U.S. Geological Survey in cooperation with the Deputy Ministry for Mineral Resources, Saudi Arabia

This report is preliminary and has not been reviewed for conformity with U.S. Geological Survey editorial standards and stratigraphic nomenclature.

1/ USGS Mission Saudi Arabia

1987

CONTENTS

ILLUSTRATIONS
[Plate in pocket]

Page

GEOELECTRIC CHARACTERISTICS OF PORTIONS OF THE RAHA FAULT ZONE AND SURROUNDING ROCKS, JABAL AS SILSILAH QUADRANGLE, KINGDOM OF SAUDI ARABIA

By

Charles J. Zablocki[1/] and Mohammed O. Hajnour

ABSTRACT

Telluric-electric and auto-magnetotelluric measurements obtained in and around the Raha fault zone in the Buqaya area indicate that it dips steeply to the southwest. Large contrasts in the electrical properties of Qarnayn and Maraghan metasedimentary rocks located on either side of the fault are characteristic of the rocks within the fault zone. However, no large electrical contrasts were detected along several segments of a southern branch of the main fault in the Shiaila area, indicating that the rocks on either side of the fault are of similar composition. Extremely low resistivity readings in the Buqaya and Shiaila areas are associated with fracturing and clay-bearing gouge that accompany known shear zones. The locations of several shallow plutons have been inferred from these studies, one of which is probably a source of gold-bearing quartz veins in the metasedimentary rocks of the Shiaila area.

INTRODUCTIONS

In mapping the geology of the Jabal as Silsilah quadrangle (sheet 26/42 D), du Bray (1984) (fig. 1) identified a major structural feature, the Raha fault zone. On the basis of physical and mineralogic considerations, du Bray (1983) and Williams (1983) suggest that the Raha fault zone may represent a fundamental structural discontinuity that penetrates the crust to a considerable depth. Preliminary geochemical sampling (du Bray, 1983) of the various rock assemblages that constitute the fault zone indicated the presence of areas of anomalous concentrations of chromium, nickel, arsenic, zinc, copper, and gold. Because of these initial findings, subproject 3.01.62 was established to assess the mineral potential in and around specific parts of the fault zone. These investigations were carried out by Smith (1985) along a 15-km segment of the fault zone near the village of Buqaya. Since mineralization would most likely be structurally controlled, and because sections of the fault zone are concealed or poorly exposed, consideration was given to assessing the applicability of geophysical techniques in order to provide insights into its subsurface structure. A detailed analysis of available aeromagnetic and gravity data may be useful in characterizing broad aspects of the fault zone, but a casual inspection of these data by the principal author did not indicate a direct correlation with the surficial expression of the

1/ USGS Mission Saudi Arabia

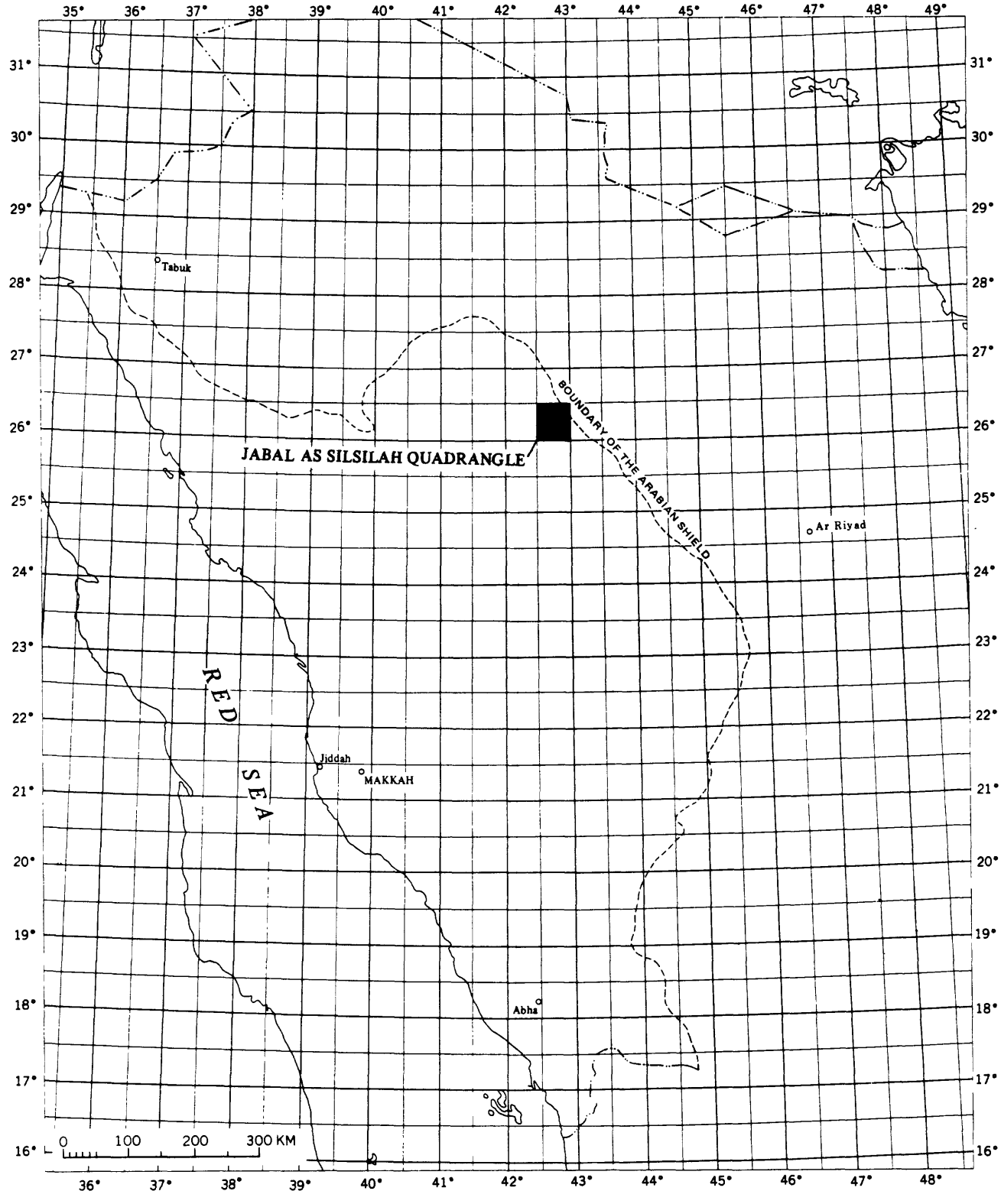

Figure 1.--*Index map of western Saudi Arabia showing the location of the Jabal as Silsilah quadrangle.*

fault zone. Earlier telluric-electric (TE) investigations by Flanigan and Zablocki (1984) across a segment of the Raha fault zone, in the Shiaila area (located about 10 km north of the Silsilah ring complex) indicated the presence of an electrical resistivity contrast between the metasedimentary rocks that bound the fault zone on either side (low resistivity on south side, higher on north side). The observed contrast was attributed to weakly metamorphosed rocks on the south side containing several percent by volume of clay minerals, whereas on the north side, the rocks were assumed to have undergone a higher degree of metamorphism where the original clay minerals have been converted to micas (principally biotite). Since clay minerals contribute significantly to rendering rocks conductive, this explanation seemed to reconcile the findings. During the same period, a similar TE profile was made across a segment of the Raha fault zone near Buqaya and the results indicated that part of the fault zone was anomalously conductive.

On the basis of the earlier electrical profiling results, and of those obtained using the audio-magnetotelluric (AMT) technique in similar types of subsurface structural problems (Zablocki and others, 1985), it was decided to apply both methods in the Buqaya area. In this report, we described the results of the investigation, as well as the results of studies made previously in other parts of the Raha fault zone.

ACKNOWLEDGMENTS

The work on which this report is based was performed in accordance with an agreement between the Saudi Arabian Ministry of Petroleum and Mineral Resources and the U.S. Geological Survey (USGS) and according to subproject 5.12.11 of the work program of the Deputy Ministry for Mineral Resources for 1404/1405. This report has benefited from technical review of an earlier version by Charles W. Smith.

METHODS AND TECHNIQUES

Telluric-electric (TE) profiling and audio-magnetotelluric (AMT) techniques have been previously described (Flanigan and Zablocki, 1984; Zablocki and others, 1985). An earlier TE-profiling traverse made in the Buqaya area used 30-second period (0.033 Hz) micropulsation electromagnetic energy as a source with electrode spacings of 250 m. In present studies, it was decided to use 140 Hz electromagnetic energy produced from spherics (distant lightning discharges) with electrode spacings of 125 m. It was felt that the higher frequency and shorter electrode spacing would provide better resolution at the scale of the features to be investigated. The AMT soundings made in the Buqaya area used the same procedures as in previous studies, except that the electric and magnetic sensors were oriented N.40°W.-S.40°E. and N.50°E.-S.50°W. instead of the usual N.-S. and E.-W. directions. This was done so that the resulting measurements would be near-parallel and perpendicular to the general strike of the major geologic structures in the area. Audio-magnetotelluric studies made in the other areas reported herein were conducted in the conventional manner, with the sensors oriented N.-S. and E.-W. Frequencies were measured from 4.5 Hz to 27 KHz at four frequencies, spaced at quasi-logarithmic intervals. Signal levels were not always persistent, particularly in the mid-band frequency range (750-Hz to 2.7

KHz), which commonly occurs because of absorption phenomena and(or) noncoherency between the electric and orthogonal magnetic fields caused by large, nearby changes in resistivities of the rocks. Never the less, data quality was good overall, which allowed us to infer several interesting aspects of the electrical characteristics of the rocks in the areas studied.

RESULTS AND DISCUSSIONS

TE PROFILES

Four TE-profiling traverses were established across several segments of the fault zone in the central part of Smith's (1985) study area. The traverses were aligned approximately normal to the surface expression of the fault zone and spaced about 1 km apart (pl. 1, map A). As mentioned previously, the earlier traverse was made using the 0.033-Hz frequency at 250-m intervals and was located about 1 km southeast of Jabal Khaslah (TE-5 in pl. 1, map B). The results from this traverse showed that the relative E-field amplitudes on the southwest side are about 30 times smaller than those on the northeast side (pl. 1). The rocks types of these areas of the traverse are mapped as Maraghan conglomerate and Qarnayn conglomerate, respectively. For a simple, two-dimensional model, the resistivity ratio would correspond to 1-to-900 (the E-field ratio is proportional to the square of the resistivity ratio). It is unlikely that the true contrast is that large; most likely, the measured fields are influenced by the proximity of the complex geologic structures that prevail here. In map B (pl. 1), the transition zone is marked by a broad solid line along the traverse, indicating the presence of a broad conductive zone about 1 km in long. Initially, it was believed that the shape of the profile suggested a simple thrust fault that dips northward. The unusually low amplitude in the vicinity of station 9 is characteristic of the extreme undershoot that results in such a simplistic model compared to the models for a dipping contact in the opposite direction or for a vertical contact (figs. 2 and 3). In detail, however, the transition zone is too broad to be treated as a simple dipping contact; it is probably related to highly variable conductive zones within the shear zone. Commonly, rocks within shear zones have very low resistivities because of their higher porosity (due to fracturing) and the presence of clay-bearing gouge material.

The higher frequency used in the subsequent TE-profiling measurements (140 Hz) senses both laterally and vertically to a lesser extent. The influence of lateral changes in resistivity, therefore, is considerably less than at the extremely low frequency used in obtaining the data from TE-5.

All of the TE profiles revealed conductive anomalies along various sections of the traverses (denoted by heavy solid lines beneath the profiles shown on plate 1 and on map B). In terms of amplitude and breadth, the major conductive anomalies are assymetrical in shape wherein the southwest side has a shallower gradient relative to the northeast side (see, for example, the following sections on plate 1: between stations 9-16 on TE-1; near stations 7 and 13 on TE-4). The consistency of the shapes of the anomalies on the profiles suggests that the attitudes of the conductive zones are not vertical, but dip steeply southwest.

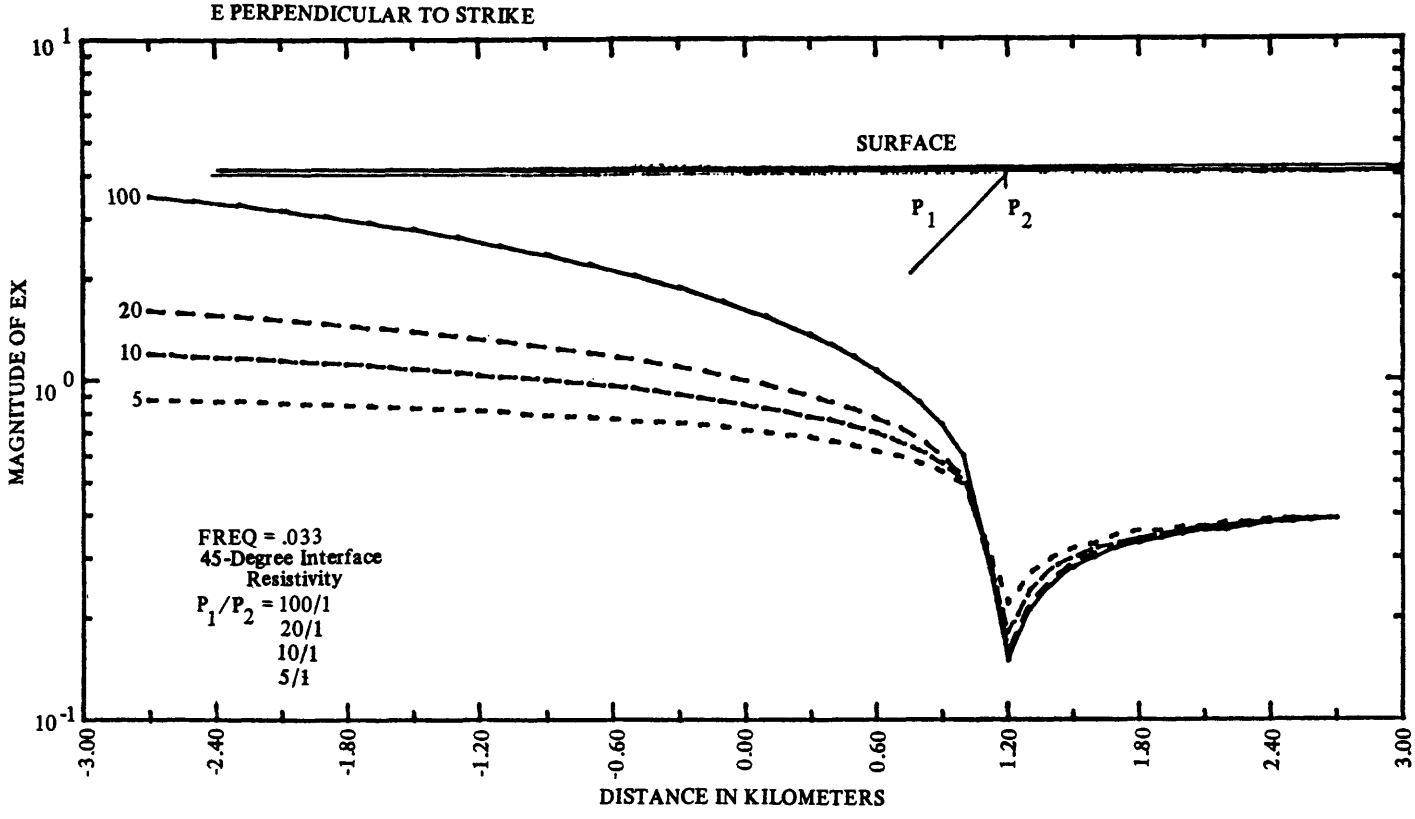

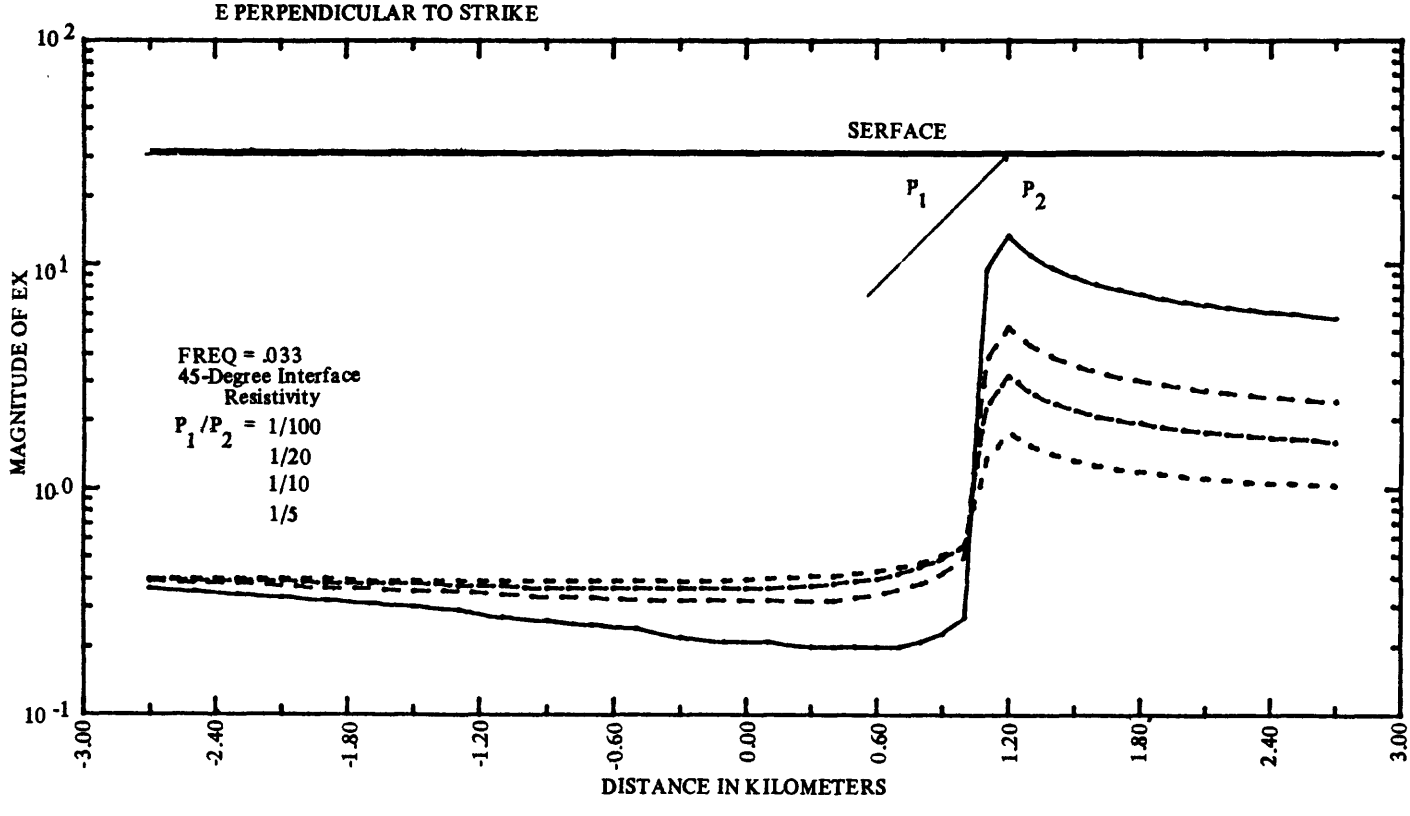

Figure 2.--*Theoretical models for E-field responses over a dipping (45°) contact for various resistivity contrasts. Computations by C. L. Long (written commun., 1985).*

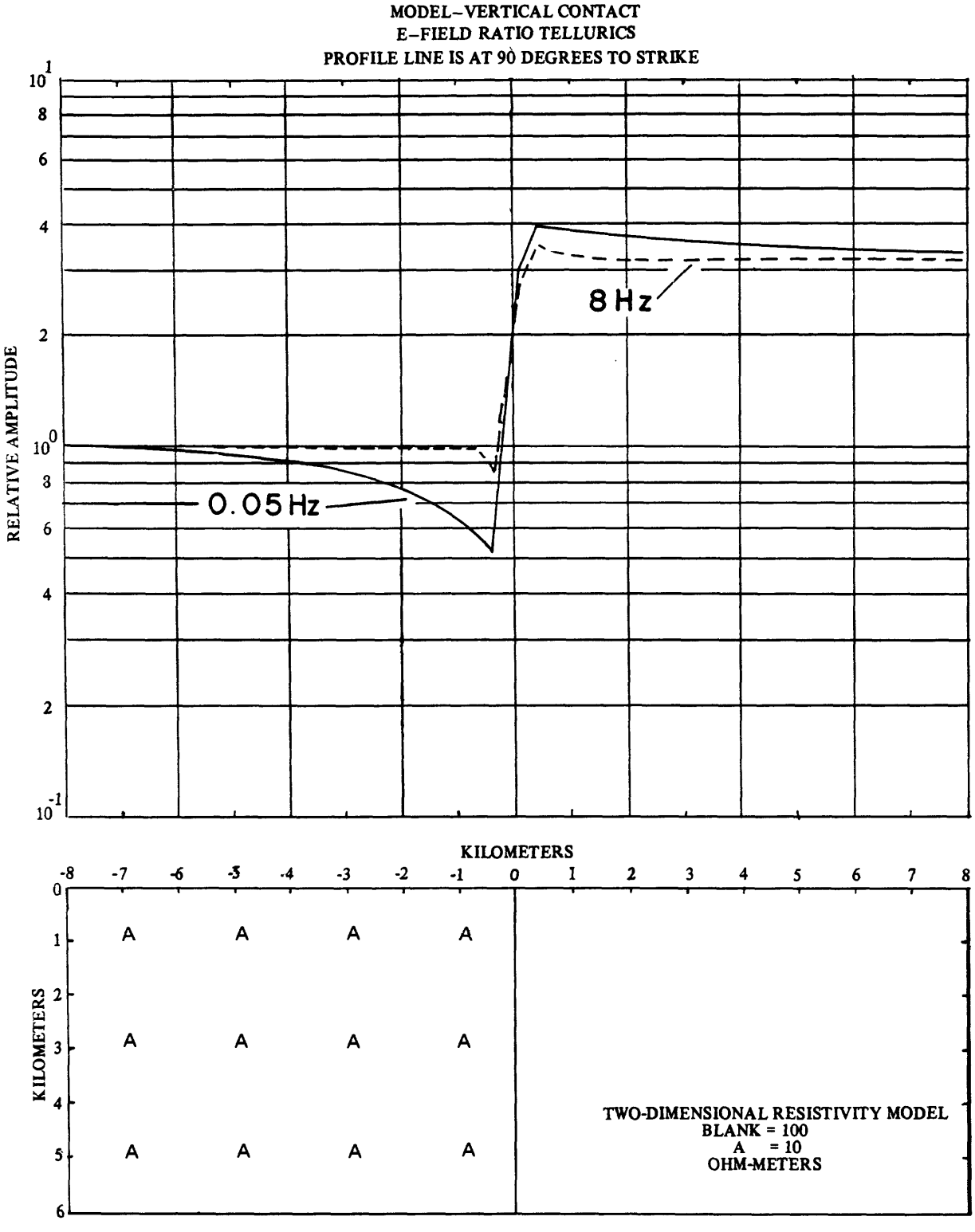

Figure 3.--*Theoretical model for E-field response for a vertical fault at 0.05 and 8 Hz. The difference in the responses reflects the difference in the sensing range, both laterally and vertically, between these two frequencies.*

The broadest and most conductive zone is located in the middle part of TE-1. The zone coincides with the locus of three known tectonic features: the Raha fault zone, a broad shear zone, and a northeast-southwest-trending lineation. It is likely that the rocks in this area are intensely fractured and altered (to clay minerals) as a result of the combined effects of these three tectonic events. The resistivities of the rocks in a part of the broad conductive zone, as determined from the AMT sounding studies, were the lowest measured in all of the studied areas.

The majority of the conductive zones are not confined to the surface expression of the southwest edge of the Raha fault (pl. 1, map B); they either straddle it and(or) extend southwest of the surface trace of the fault. This observation suggests that these areas might be influenced more by conductive zones within the shear zone than by the Raha fault alone. This suggestion is supported by some of the AMT-sounding results to be discussed in the following section. Other conductive anomalies mapped along the TE traverses are probably related to near-vertical fracture zones, rather than to changes in rock type because of their limited width.

AMT SOUNDINGS

Twenty-seven AMT soundings were made in the study area. Most were sited on or southwest of the Raha fault zone because of accessibility problems. However, five were sited northwest of the fault zone along accessible roads in several wadis that drain the area.

A geoelectric cross section derived from the soundings made along the 3-km long traverse of TE-1 revealed several notable features (fig. 4), but mainly that there is a good correlation between the TE profile and the AMT results. Toward the ends of the TE profile, away from the central conductive feature, the E-field ratio is about 2.5 to 1, being higher on the northeast side. This would correspond to a resistivity contrast of about 6 to 1. The AMT results indicate that the rocks on the northeast side of the fault zone have average resistivities of about 2,500 ohm meters at depths sensed by the TE measurements, whereas, rocks on the southwest side average about 600 ohm meters. Both the TE and AMT results indicate that the highest resistivities are associated with the Qarnayn lithic graywacke (in the vicinity of AMT station CM-37). Below several hundred meters, to depths in excess of one kilometer, the resistivity of the metasedimentary rocks can be approximately categorized as follows: Maraghan conglomerate, 1,000 ohm meters; Qarnayn lithic graywacke, 2,500 to 4,000 ohm meters; and Qarnayn conglomerate, to 10,000 ohm meters. The important factors that control the resistivities of these rocks are their porosity (fracture and interstitial) and clay-mineral content. The resistivities of these units are extremely high (sandstones, for example, normally range between 50 to 100 ohm meters) and must, therefore, reflect their high degree of induration and their low clay-mineral content. Accordingly, differences in resistivity between these metasedimentary units probably indicate differences in their physical and mineralogic make up.

The central conductive zone revealed on profile TE-1 contains resistivities of less than 16 ohm meters as measured from the AMT sounding made at station CM-19. The depth of this zone may not be as great as depicted in the cross section because of the limited depth of penetration of electromagnetic waves in

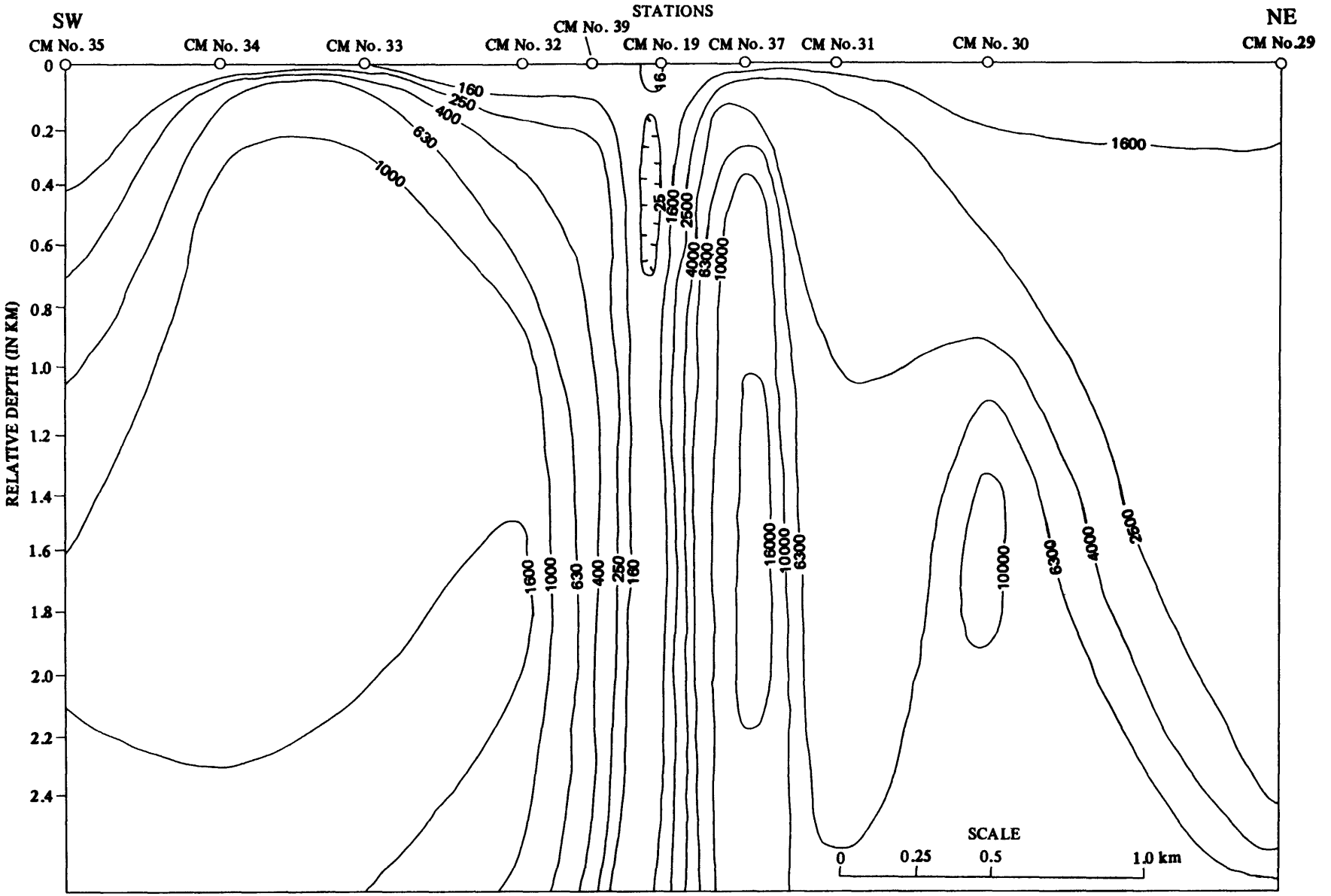
SW
STATIONS
NE
CM No. 35
CM No. 34
CM No. 33
CM No. 32
CM No. 39
CM No. 19
CM No. 37
CM No.31
CM No. 30
CM No.29
RELATIVE DEPTH (IN KM)
0
0.2
0.4
0.6
0.8
1.0
1.2
1.4
1.6
1.8
2.0
2.2
2.4
160
250
400
630
1000
1600
2500
4000
6300
10000
16000
16
25
SCALE
0
0.25
0.5
1.0 km

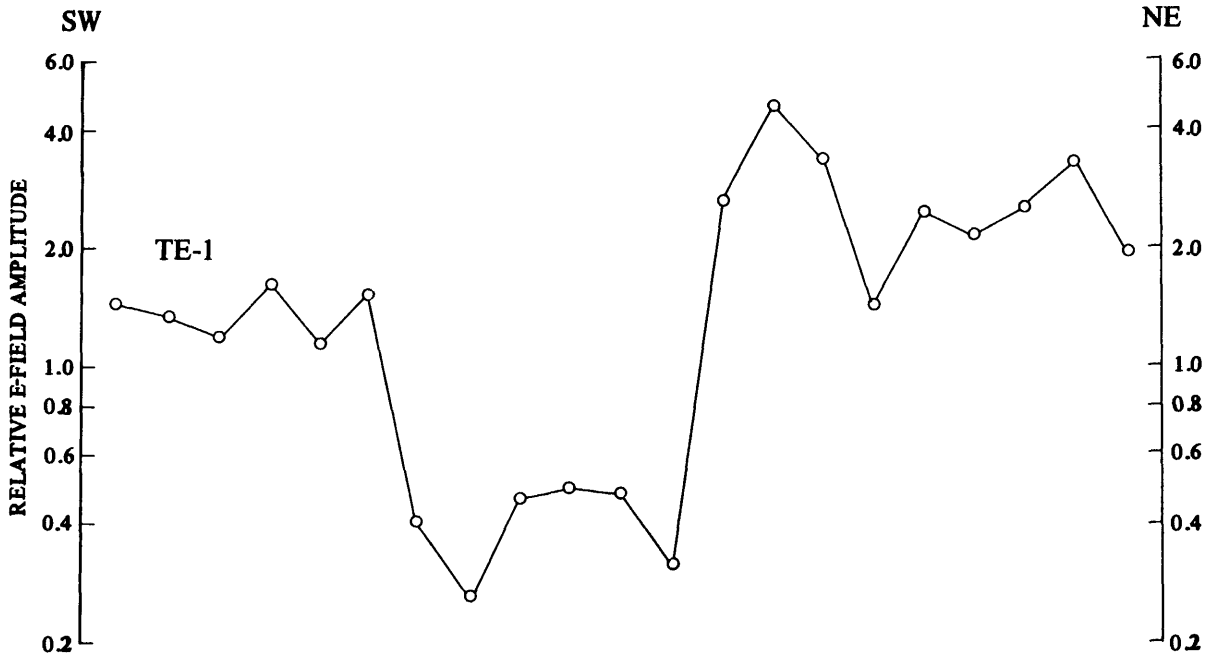

Figure 4.--*Telluric-electric profile, TE-1, and geoelectric cross section derived from AMT soundings made along the traverse. Location shown on map B, (pl. 1).*

such a conductive medium. The conductive zone probably extends to a depth of at least 800 m. As mentioned previously, this conductive zone appears to have developed from intense fracturing and clay-mineral production resulting from one or more of the tectonic features mapped in the vicinity. As seen in the geoelectric cross section, there is no indication that the attitude of the conductive zone is other than vertical or subvertical. Audio-magnetotelluric soundings were also made about 300 m northwest and southeast of station CM-19 to determine the extent of the conductive zone in these directions (CM-40 and CM-41). Both soundings gave the very low resistivities that characterize the central conductive zone (see data in appendix). Soundings located several hundred meters further to the southwest and southeast, however, indicated very high resistivities (stations CM-36 and CM-36A). Accordingly, the conductive zone appears to be a roughly circular feature about 750 m in diameter. There is no surficial evidence of argillic alteration in this area and, therefore, the possibility of this conductive zone being caused by low-temperature hydrothermal processes is remote. Again, it probably results from tectonic processes.

A geoelectric cross section derived from AMT sounding measurements made along the TE-5 traverse provided further insight into the subsurface structure in the study area (fig. 5). The rocks on the northeast side of the Raha fault zone (Qarnayn conglomerate) possess the highest resistivities measured along the section (as much as 6,300 ohm meters). Toward the southwest side of the section, the resistivities in the Maraghan conglomerate are about ten times smaller, consistent with the findings discussed earlier. The lowest resistivities are located in the vicinity of AMT station CM-52 where a shear zone was mapped. These resistivities, however, are not as low as those measured at AMT station CM-19 and may indicate that the effects from shearing here are not as intense as in the vicinity of AMT station CM-19. The general distribution of the resistivity contours shown in the cross section suggests that the lateral transition from higher to lower resistivities is not vertical, but that this transition dips steeply southeast. It is interesting to note that sounding CM-51, made near the edge of the fault zone, did not indicate any anomalously low resistivites. Similarly, a sounding made near the southwest edge of the fault zone along TE-2 (station CM-42 in pl. 1, map B) did not indicate low resistivities that might be associated with the fault. These observations reinforce the earlier suggestion that the conductive zones revealed in all of the electrical studies probably result primarily from effects of shearing and that the contact zones between the Raha fault and adjacent rocks are not intensely fractured or contain appreciable amounts of clay minerals. Indeed, the cross section derived from the AMT soundings made in the vicinity of the TE-2 traverse shows that the rocks near the southwest contact have resistivities as large as, or larger than the Qarnayn lithic graywacke (fig. 6). This cross section also shows that the resistivities of the rocks mapped as Maraghan lithic graywacke are of the same magnitude as those mapped as Maraghan conglomerate.

Smith mapped a post-tectonic diorite pluton (di, pl. 1, map B) that intrudes the Maraghan graywacke in the southeast part of the study area. The exposed part of the pluton measures approximately 1 by 1.5 km and contains gold-quartz veins that cut the pluton. Audio-magnetotelluric soundings were sited over the center of the pluton and on its flanks in the surrounding graywacke. The geoelectric cross section derived from these soundings (fig. 7) indicates that the pluton extends to at least 2.5 km and that it is very competent (few or no fractures) and devoid of clay minerals because of its exceptionally high resistivity (as much as 25,000 ohm meters). The soundings made on the flanks of the pluton show typical

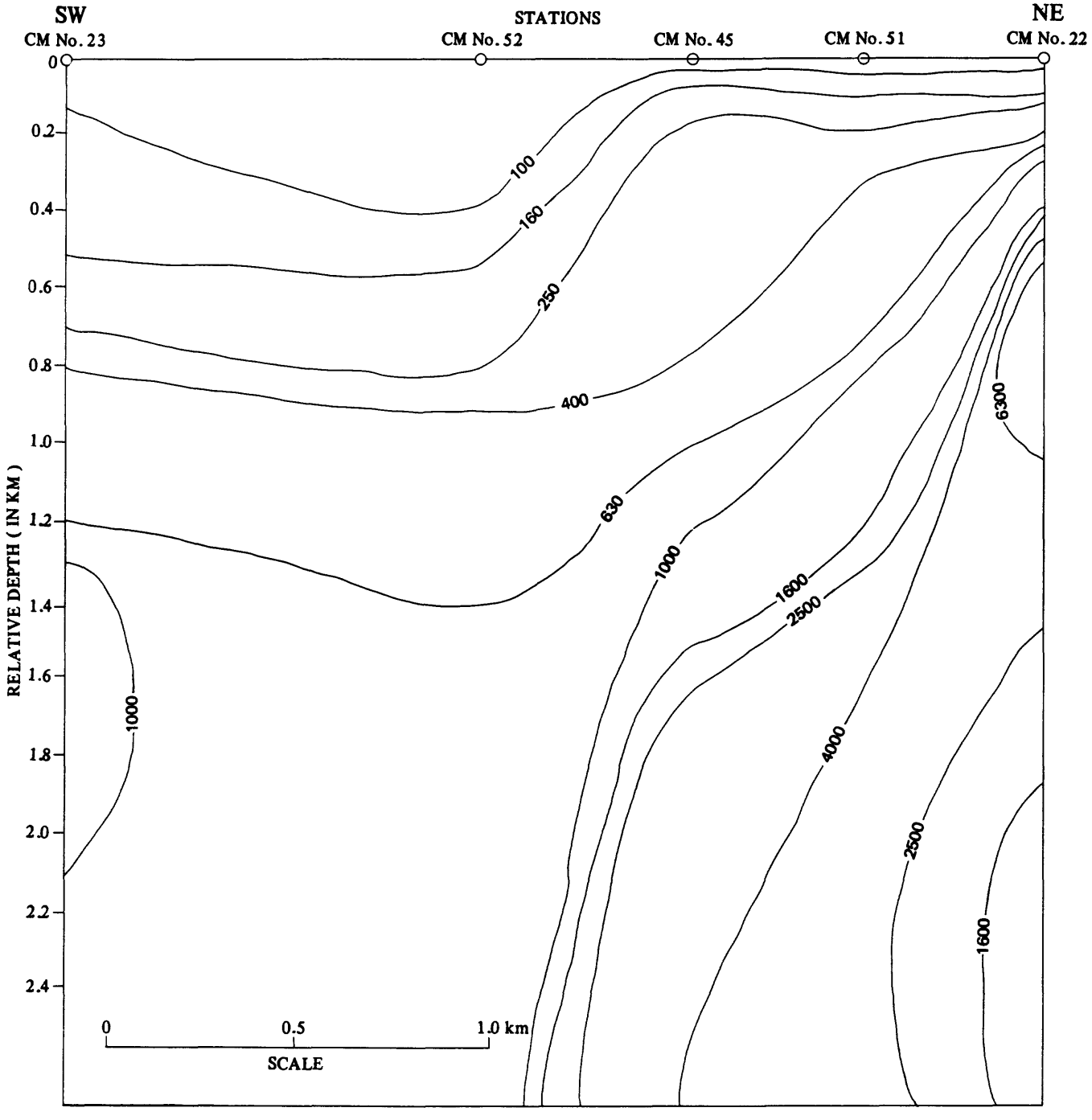

Figure 5.--*Geoelectric cross section derived from AMT soundings along TE-5. Locations shown on map B (pl. 1).*

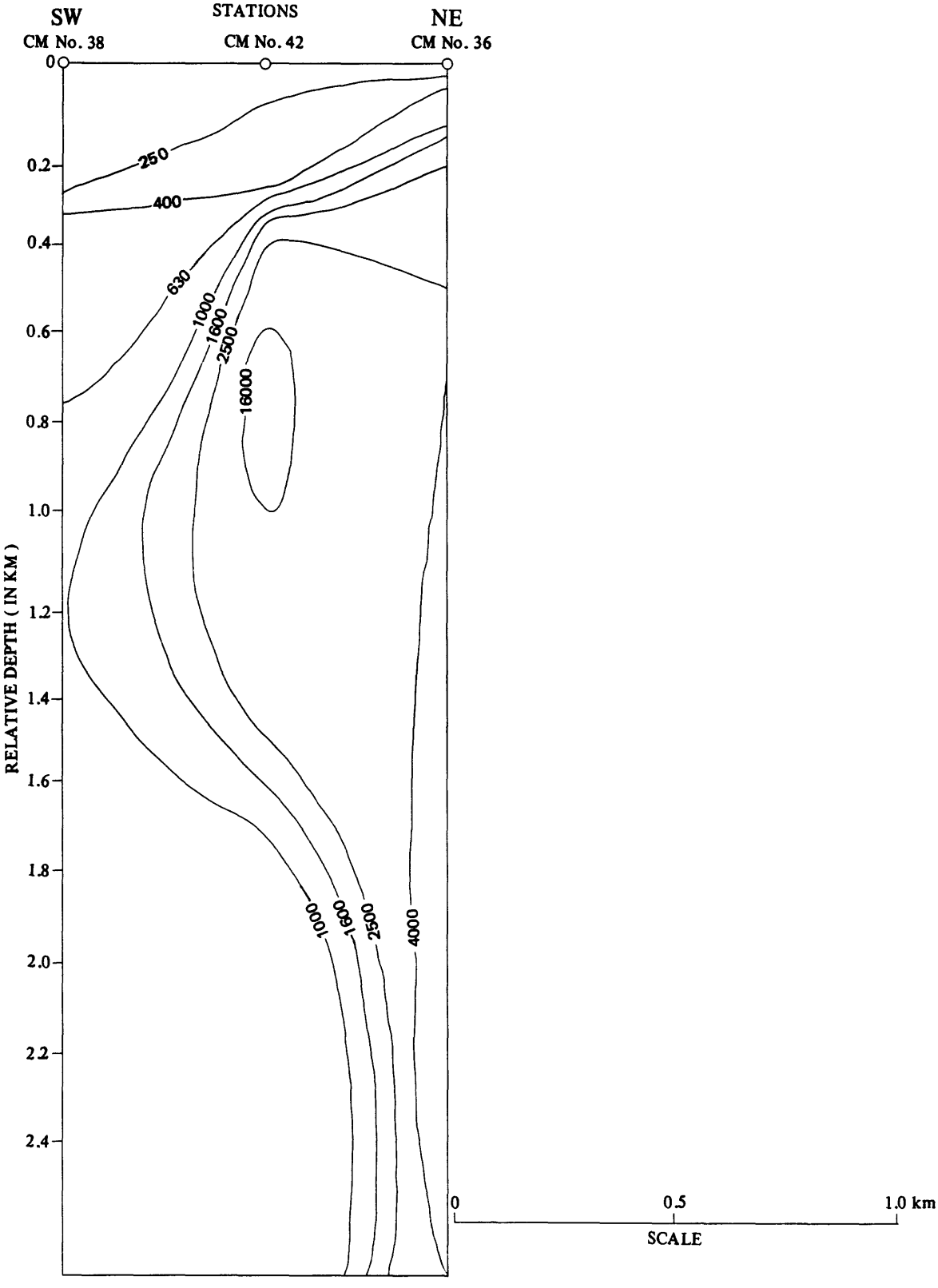

Figure 6.--*Geoelectric cross section derived from AMT soundings near TE-2. Locations shown on map B (pl. 1).*

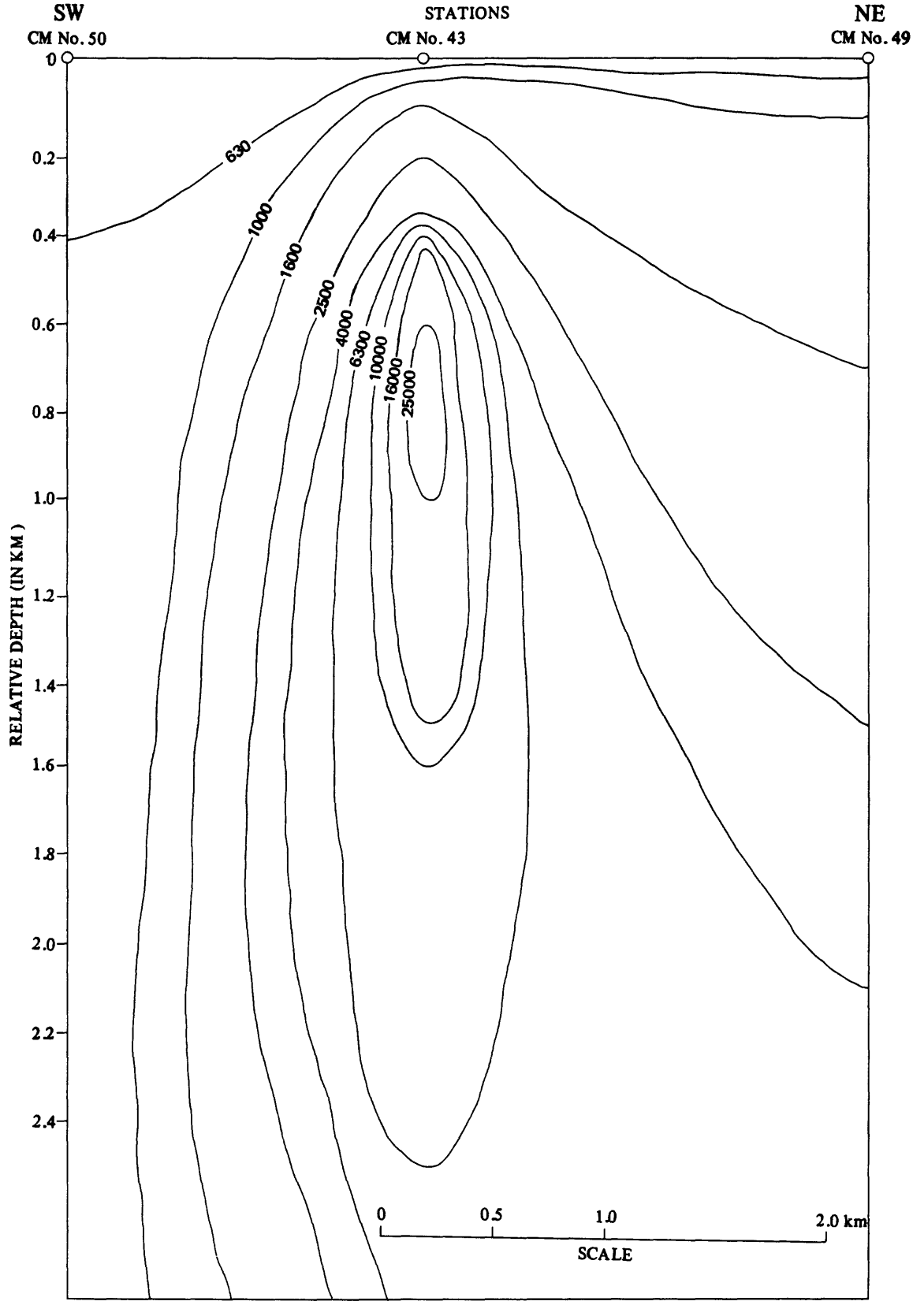

Figure 7.--*Geoelectric cross section of diorite pluton shown on map B (pl. 1).*

values for Maraghan graywacke. The data plot does not indicate that the graywacke section is thinner on the northeast side than the section on the southwest side. One possible interpretation of this fact is that these rocks dip southwest; some of the other results discussed previously also suggest this is the case.

A single sounding was made over a much smaller intrusion located southwest of the diorite pluton (station CM-44 in pl. 1, map B). The intrusive body is a medium grained plagioclase-quartz-microline monzogranite; the rock is locally argillized and contains sericite and disseminated pyrite. In contrast to the diorite pluton, the resistivity of this small boss is only about 1,000 ohm meters (see sounding data in appendix). The dimensions of the boss are small enough that the measurements at the lower frequencies may be sensing some of the lower resistivity of the graywacke host rocks. The measured resistivities at the high and intermediate frequencies, however, are probably sensing the bulk resistivities of the intrusion that are about 10 times lower than the diorite pluton. This suggests that the monzogranite may have undergone argillic alteration at depth.

In addition to studies in the Buqaya area, a 3-km long AMT transect was established in a north-south direction over a part of the Raha fault, about 15 km to the southwest (pl. 1, map A). This site was chosen because of the apparent structural and geologic simplicity of the rocks in the area (du Bray, 1983). According to du Bray, a southern segment of the fault zone is marked by several small hills composed of metagabbro that are aligned in an east-west direction. He identifies the bounding rocks on the south side as Maraghan lithic graywacke and those on the north side as Qarnayn lithic graywacke. Outcrops of the metasedimentary rocks are scarce in these areas, being largely concealed by alluvium. Eight soundings were sited along the transect at approximately 500-m intervals in the vicinity of the fault zone and at a 1-km spacing at the ends of the transect. The resulting data are displayed as a geoelectric cross section in figure 8. The high-resistivity zone indicated in the vicinity of AMT stations CM-65 and 66 is associated with gabbroic rocks whose surface expression is prominent hills immediately west and east of these stations (pl. 1, map A). The high-resistivity zone extends to a depth of at least 2.5 km and there is no indication that its attitude is other than vertical. If the gabbro is intruded into and along the plane of the Raha fault in this region, then the implication is that the Raha fault must be vertical or very steeply dipping. The relatively high resistivities measured at the south end of the transect at station CM-63 and on the north end at station CM-68 do not correlate with the surficial geology. These measurements may represent other igneous intrusive bodies at shallow depths beneath the metasedimentary cover. These data also indicate that there is no large distinction between the resistivities of the Maraghan rocks on the south side of the fault zone and Qarnayn rocks on the north side. In other areas, such as those in the Buqaya area mentioned above, a clear distinction was noted in the resistivities of these rock types. Either Qarnayn rocks are not present in this area or their character is essentially the same as those rocks that constitute the Maraghan metasedimentary rocks on the south side of the fault. Smith (1985) classified rocks in the Buqaya area immediately north and west of the metagabbroic rocks that form Jabal Khaslah and the adjacent hills to the southwest as Maraghan, and not Qarnayn, as indicated by du Bray (1983). More detailed, larger-scale geologic mapping in the area of the transect, such as Smith's (1985) in the Buqaya area (1:20,000), may help in the interpretation of the electrical data.

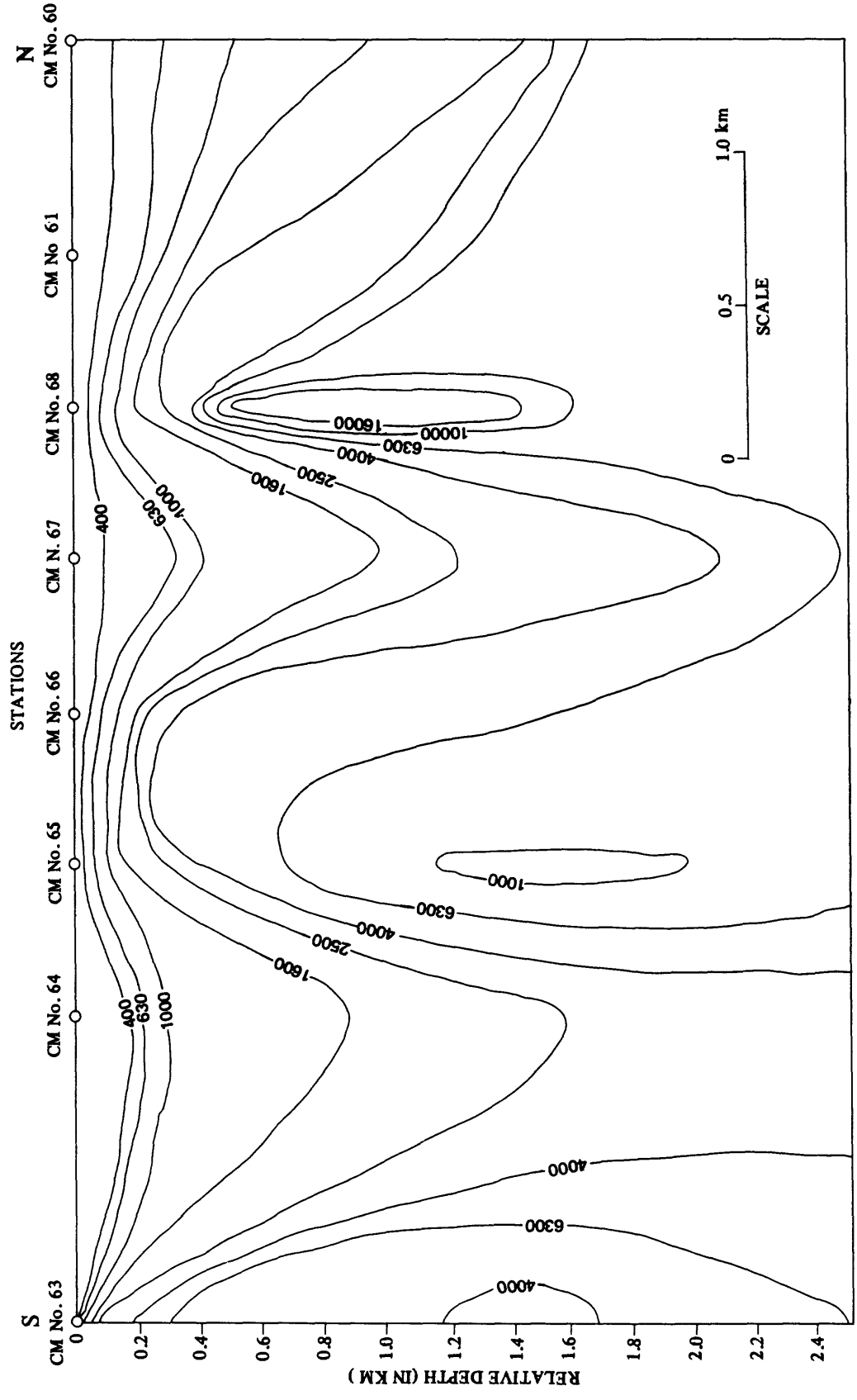

Figure 8.--*Geoelectric cross section derived from AMT soundings across Raha fault shown on map A (pl. 1).*

As mentioned earlier, several TE profiles were made previously across a section of the Raha fault zone in the Shiaila area (Flanigan and Zablocki, 1984) and one of these profiles indicated that the rocks on the north side of the fault have higher resistivities than those on the south. During this study, follow up AMT soundings were made to confirm the TE results and to obtain more information on the subsurface structure over a larger area. Eight soundings were sited along an approximate north-south transect at a nominal spacing of 2 km (pl. 1, map A). The results, displayed in a geoelectric cross section (fig. 9), revealed the following. At the extreme north end of the transect (AMT station Y-1), the average resistivities are fairly high compared to the findings from a sounding made about 1 km south (station Y-2). The variance may be due more to the presence of higher-resistivity Qarnayn metasedimentary rocks beneath station Y-1, as exposed in nearby outcrops, than to lower-resistivity metasedimentary rocks beneath station Y-2. In his geologic map, du Bray (1983) infers that the trace of the northern segment of the Raha fault trends in an east-west direction between these two sounding sites. If this is so, then the rocks of the south side of the fault, in the vicinity of station Y-2, may not be of the Qarnayn type, but rather Maraghan. Soundings made approximately 1 km north and south of the southern segment of the Raha fault (stations Y-4 and Y-5, respectively) show that the rocks at depth have lower resistivities on the south side of the fault. The contrast, however, is not as large as suggested from the earlier TE-profile results. It is probable that the TE-profile measurements, using an extremely low frequency (0.033 Hz), were influenced more by lateral changes in resistivity than were those obtained with the AMT soundings.

The most important finding of this study was the detection of an apparently shallow intrusive body in the vicinity of stations Y-6 and Y-8. This is inferred by the extremely high resistivities measured in these areas; they increase in magnitude with depth, and accordingly, suggest that the assumed intrusion extends to a great depth (more than 2.5 km). Smith (1985) reports that the source of gold-bearing quartz veins prevalent in this area may be granitic cupolas and(or) related intrusions at depth. The findings from the soundings made at Y-6 and Y-8 tend to support this conclusion. The resistivity distribution in this area suggests that the top of the inferred intrusion is very shallow, perhaps less than a few hundred meters from the surface, and that the intrusion dips steeply south. Exceptionally high resistivities were also measured at a site located about 2-km east of station Y-6 (Y-7 in pl. 1, map A). The data for this sounding are not presented here because of technical problems in printing the sounding curve. On the basis of these results, it appears that an intrusive body, several kilometers in diameter, is present at a shallow depth in the vicinity of these sounding sites.

It should be emphasized that the resistivity distributions shown in all of the geoelectric cross sections presented in this and previous reports were obtained by computing the log average of measurements made in the two horizontal and orthogonal directions. In an electrically isotropic medium (horizontally layered), computed resistivities at a given frequency will be identical. The resistivities will be different in the two directions, however, where there are lateral changes in resistivity. A good example of the later condition is found in the following sounding results. The computer print-out of the apparent resistivity vs frequency for AMT station Y-1 (see appendix) shows a significant difference in the values measured in the N-S and E-W directions. The values obtained at all frequencies in the N-S direction are about one order of magnitude larger than in the E-W direction. This large difference could be attributed to the station being located

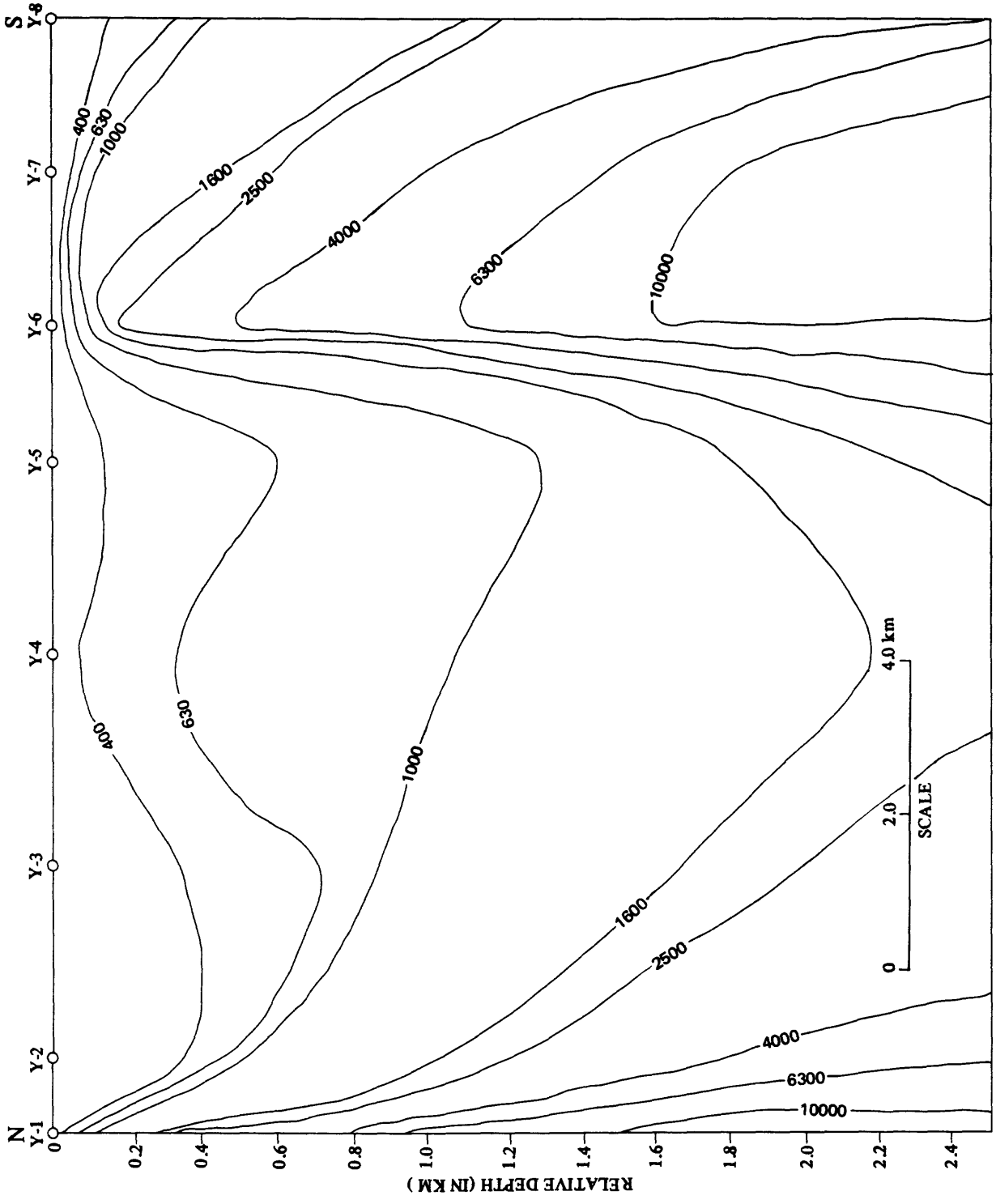

Figure 9.--*Geoelectric cross section through the Shiaila area. Locations shown on map A (pl. 1).*

close to a contact between high- and low-resistivity rocks that strikes in an east-west direction (the inferred direction of the Raha fault). The differences in resistivities measured in the N.-S. and E.-W. directions at station Y-2 are prominent only at the lower frequencies. As the measurement made at lower frequencies sense farther laterally as well as vertically, the effects of an east-west resistivity boundary are also sensed at this AMT sounding site. The other soundings along this transect do not indicate any significant differences in apparent resistivity vs frequency. Differences measured in the two directions are largely due to the inherent scatter that is characteristic of AMT data obtained with natural-source fields.

In early 1404 A.H., while carrying out AMT studies in the Jabal as Silsilah ring complex Zablocki and others (1985) sampled several areas outside of the ring complex to provide background information on the electrical responses in different geologic settings. One of the chosen areas was in the vicinity of the Raha fault zone, about 6 km west of the Shiaila area (pl. 1, map A) where five AMT soundings were made. Their locations are shown in map A (pl. 1) and the plotted results are shown in the appendix as stations SH01, SH02, SH06, SK03, and SK07. These data have not been documented previously because they were not part of a systematic study and because some of the results appeared discordant with the geology as portrayed by du Bray (1983). Recent detailed mapping by Smith and Samater (1985), however, has offered some reasonable explanations for some of the results obtained.

In the previous paragraph, we attributed the large separations between the resistivities measured in the N.-S. and E.-W. directions at station Y-1 to an east-west striking contact of contrasting resistivities that probably are related to the trace of the Raha fault in that area. The data obtained at stations SH01 and SH06, on the other hand, not only indicated a similar, but larger separation between the N.-S. and E.-W. sounding curves; further, the higher values were measured in the E.-W. directions, in direct contrast to the results obtained at station Y-1. These results implied that the soundings were sited near, or over a two-dimensional conductive structure aligned in a north-south direction. This interpretation remained unreconciled until mapping by Smith and Samater (1985) identified a major northeast-striking right-lateral shear that passes in the vicinity of these two soundings (pl. 1, map A). The zone is about 10-km long where exposed and about 1-km in width. Their observations indicated that the shearing was intense and produced a large lateral displacement between the bounding rocks. Such conditions likely created a zone of rocks with very low resistivity resulting from high fracture porosities and the generation of abundant clay-bearing gouge material. The two orders of magnitude difference in the apparent resistivities measured in the W-S and E-W directions, with values less than 10 ohm meters in the N.S.-direction, strongly suggest that they result from the proximity of the shear zone.

A sounding made near the trace of the southern segment of the Raha fault zone (station SH02; pl. 1, map A) did not show any significant differences in the measured resistivities in the two directions. Their average values (to several kilometers in depth) are fairly low (less than 1,000 ohm meters), but not low enough to suggest that they are influenced by the shear zone. The lack of any electrical anisotrophy here suggests that the rocks on either side of the fault zone are not significantly different in their electrical properties.

The two remaining soundings made in this area (station SK03, located about 2-km west of SH06, and station SK07, located about 2-km west of SK03) straddle the trace of the southern segment of the Raha fault as inferred on du Bray's (1983) geologic map. Except for higher resistivities measured at depth in excess of 3 to 4 km at station SK03, the resistivities of the rocks in these areas are not significantly different. Here, as in other areas where measurements were made across the southern segment of the Raha fault zone, there does not appear to be a large contrast in the electrical properties of the rocks on opposite sides of the fault. However, large electrical differences between the exposed Qarnayn and Maraghan metasedimentary rocks were detected in the Buqaya area.

CONCLUSIONS AND RECOMMENDATIONS

The significant findings of the electrical studies Raha fault zone are as follows: (1) Very low resistivities (less than 10 ohm meters) are associated with shear zones mapped by Smith (1985) in the Buqaya and west Shiaila areas. They most likely result from attendant fracturing and the presence of clay-rich gouge. (2) Where sufficient data were obtained, the dip of the shear zone in the Buqaya area appears to be steep; there are also indications that the shear zone dips southwest. (3) The Raha fault zone itself does not appear to contain rocks similar in character to those that comprise the shear zones because no low resistivities were measured at the contact. (4) In the Buqaya area, the Qarnayn metasedimentary rocks on the northside of the fault zone have very high resistivities compared to Maraghan metasedimentary rocks of the south side. The contrast probably reflects differences in their physical and mineralogic character. (5) In the areas where studies were made over the southern trace of the Raha fault that is shown on du Bray's (1983) geologic map, no significant differences were measured in the electrical properties of the rocks on either side of the fault zone. It is possible that the metasedimentary rocks on the north side of the inferred fault are not of the Qarnayn type, such as those exposed in the Buqaya area, but of the Maraghan type. (6) Metagabbroic rocks that include the inferred fault zone in one section of this area suggest a near-vertical attitude in the fault plane. (7) AMT soundings made over two exposed plutons in the Buqaya area showed differences in electrical properties that probably are related to differences in clay-mineral content. Other soundings made in the Shiaila area indicated the presence of a large pluton at shallow depth. The assumed pluton is also a probable source of the gold-bearing quartz veins that cut the metasedimentary rocks in this area.

No specific recommendations are offered except to point out the demonstrated utility of these electrical techniques for detecting and mapping such features as shear zones and shallow intrusions. If further studies were to be undertaken here or in similar geological settings, these methods could provide useful supplemental information in mapping the geology, particularly in areas of poor exposure or complex structure.

DATA STORAGE

DATA FILE

Data used in compiling this report are archived in the Jeddah office of the U.S. Geological Survey Mission in Data-File USGS-DF-04-46. Date include:

(1) Original field notes and field maps
(2) AMT computer printouts
(3) Magnetic tapes
(4) Preliminary data used in the preparation of this report.

MINERAL OCCURRENCE DOCUMENTATION SYSTEM (MODS)

No entries or updates have been made to the Mineral Occurrence Documentation System (MODS) data bank.

REFERENCES CITED

du Bray, E. A., 1983, Reconnaissance geology of the Jabal as Silsilah quadrangle, sheet 26/42 D, Kingdom of Saudi Arabia: Saudi Arabian Deputy Ministry for Mineral Resources map series, scale 1:100,000, 52 p., (in press).

Flanigan, V. J., and Zablocki, C. J., 1984, An evaluation of the applicability of the telluric-electric and audio-magnetotelluric methods to mineral assessment on the Arabian Shield, Kingdom of Saudi Arabia: Saudi Arabian Deputy Ministry for Mineral Resources Open-File Report USGS-OF-04-26, 61 p. Also, 1984, U.S. Geological Survey Open-File Report 84-425.

Smith, C. W., and Samater, R. M., 1985, Preliminary studies of gold deposits and rock geochemistry in the Shiaila area, Jabal as Silsilah quadrangle, Kingdom of Saudi Arabia: Saudi Arabian Deputy Ministry for Mineral Resources Open-File Report USGS-OF-05-25, 34 p. Also, 1986, U.S. Geological Survey Open-File Report 86-28.

Smith, C. W., 1985, Preliminary studies of the Raha fault zone and enclosing rocks in the Buqaya area, Jabal as Silsilah quadrangle, Kingdom of Saudi Arabia: Saudi Arabian Deputy Ministry for Mineral Resources Open-File Report USGS-OF-05-29, 21 p. Also, 1986, U.S. Geological Survey Open-File Report 86-29.

Williams, P. W., 1983, Reconnaissance geology of the Samirah quadrangle, sheet 26/42 C, Kingdom of Saudi Arabia: Saudi Arabian Deputy Ministry for Mineral Resources Open-File Report USGS-04-3, 33 p., scale 1:100,000. Also, 1984, U.S. Geological Survey Open-File Report 84-383.

Zablocki, C. J., du Bray, E. A., Long, C. L., and Tippens, C. L., 1985, Subsurface structure of the Silsilah ring complex as deduced from telluric-electric and audio-magnetotelluric investigations, Kingdom of Saudi Arabia: Saudi Arabian Deputy Ministry for Mineral Resources Open-File Report USGS-OF-05-8, 45 p. Also, 1985, U.S. Geological Survey Open-File Report 85-238.

APPENDIX

EXPLANATION

In the following, a computer printout of the AMT sounding data obtain from these studies are presented together with log-log plots of the resistivity distribution as a function of depth. These plots were derived from the inversion algorithm discussed by Flanigan and Zablocki (1984). The geoelectric cross sections presented in this report were constructed from these plots .

OUTPUT FROM PRINT

PROJECT=LINE Y

STATION ID_Y_1 NS NO FREQ= 9

FREQ	AP-RES	N OBS	STD ERR
4.5	4832.20	5	979.51
75.0	10000.00	5	429.00
136.0	9510.30	5	793.84
270.0	4919.80	4	573.07
450.0	4700.00	5	1264.40
750.0	4000.00	3	96.11
7500.0	3751.60	6	524.70
13600.0	5794.80	4	77.06
27000.0	3800.00	5	90.75

STATION ID_Y_1 EW NO FREQ= 13

FREQ	AP-RES	N OBS	STD ERR
4.5	471.74	5	65.16
7.5	765.91	4	102.44
13.6	769.20	5	61.00
27.0	659.71	5	76.73
45.0	509.75	5	19.90
75.0	468.61	5	25.74
136.0	314.21	5	70.30
270.0	326.42	4	25.50
450.0	317.00	5	283.83
750.0	310.00	5	11.93
7500.0	305.39	5	67.06
13600.0	508.94	5	11.93
27000.0	319.56	3	26.95

OUTPUT FROM PLOT

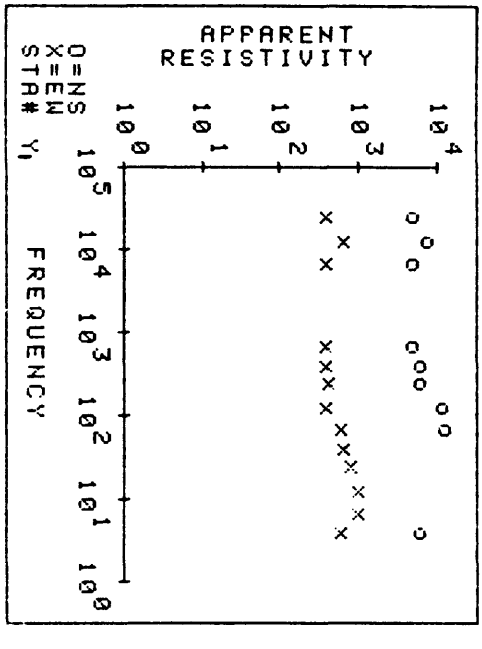

OUTPUT FROM PRINT

PROJECT=LINE Y

STATION ID_Y_2 NS NO FREQ= 11

FREQ	AP-RES	N OBS	STD ERR
4.5	4136.90	3	882.39
7.5	2324.40	4	142.10
13.6	2455.40	5	395.80
27.0	1094.60	4	175.42
45.0	1037.10	4	124.65
75.0	603.60	2	24.55
136.0	271.74	5	24.19
270.0	270.00	4	.33
450.0	170.00	3	11.70
1360.0	144.64	3	50.10
13600.0	182.49	3	6.46

STATION ID_Y_2 EW NO FREQ= 12

FREQ	AP-RES	N OBS	STD ERR
4.5	555.61	4	113.05
7.5	728.74	5	106.60
13.6	495.20	5	33.49
27.0	331.51	4	27.05
45.0	257.05	5	11.78
75.0	246.86	5	12.81
136.0	200.20	5	30.54
270.0	170.77	3	1.06
750.0	186.20	2	56.05
7500.0	107.00	4	2.88
13600.0	77.00	3	1.50
27000.0	71.31	3	2.88

OUTPUT FROM PLOT

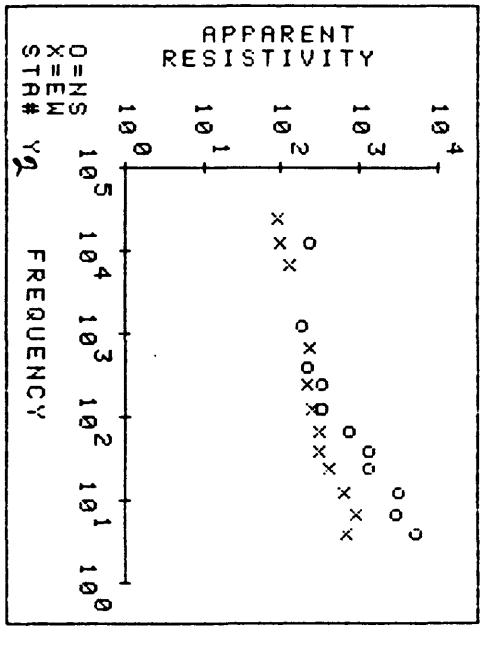

OUTPUT FROM PRINT

PROJECT=LINE Y

STATION ID_Y_3 NS NO FREQ= 9

FREQ	AP-RES	N OBS	STD ERR
4.5	1000.00	2	22.77
7.5	905.94	5	149.16
13.6	1048.40	5	225.46
27.0	384.79	3	67.60
45.0	291.94	5	47.60
75.0	296.54	5	65.21
136.0	132.04	5	6.99
270.0	129.75	5	33.14
450.0	127.00	5	117.60

STATION ID_Y_3 EW NO FREQ= 12

FREQ	AP-RES	N OBS	STD ERR
4.5	2308.70	2	220.37
7.5	1305.00	4	222.44
13.6	581.57	5	142.14
27.0	574.50	5	43.53
45.0	514.38	5	18.50
75.0	386.51	5	24.93
136.0	293.17	5	36.51
270.0	188.32	5	26.43
450.0	270.00	5	16.92
750.0	271.33	3	59.72
2700.0	260.00	2	7.89
13600.0	254.86	5	8.57

OUTPUT FROM PLOT

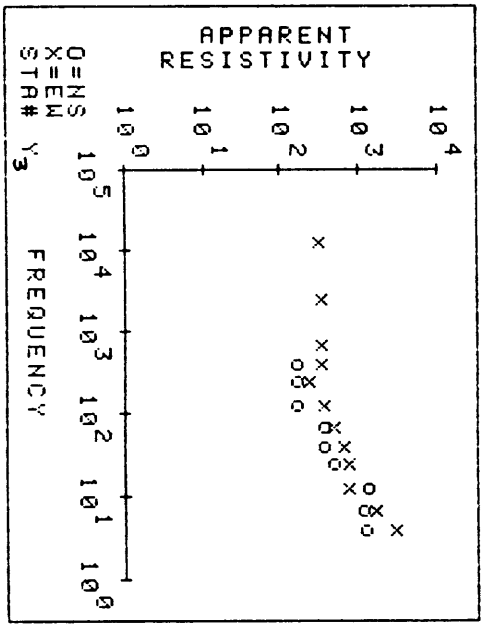

OUTPUT FROM PRINT

PROJECT=LINE Y

STATION ID_Y_4 NS NO FREQ= 10

FREQ	AP-RES	N OBS	STD ERR
4.5	1627.10	3	360.27
7.5	2896.60	5	406.96
13.6	1990.40	6	263.48
27.0	1845.10	5	316.42
45.0	909.76	5	13.30
75.0	839.45	5	231.39
136.0	449.84	6	26.76
270.0	506.81	5	24.07
450.0	500.00	4	165.58
750.0	470.00	4	20.74

STATION ID_Y_4 EW NO FREQ= 12

FREQ	AP-RES	N OBS	STD ERR
4.5	807.47	4	128.37
7.5	712.49	5	84.07
13.6	474.62	5	25.01
27.0	378.38	4	17.08
45.0	489.88	5	20.93
75.0	496.34	5	30.87
136.0	440.42	5	30.34
270.0	588.80	5	42.96
450.0	577.00	5	42.21
750.0	700.00	4	27.30
7500.0	797.82	2	173.85
13600.0	476.10	4	45.39

OUTPUT FROM PLOT

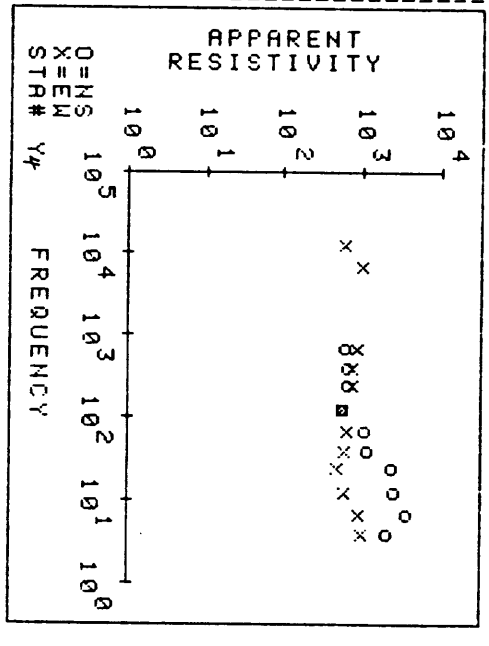

OUTPUT FROM PRINT

PROJECT=LINE Y

STATION ID_Y5 NS NO FREQ= 8

FREQ	AP-RES	N OBS	STD ERR
7.5	799.14	2	68.07
13.6	503.94	3	17.87
27.0	554.58	3	110.16
45.0	310.01	3	7.74
136.0	300.00	4	8.14
270.0	270.00	3	9.36
450.0	210.00	4	95.57
750.0	200.00	2	.68

STATION ID_Y5 EW NO FREQ= 11

FREQ	AP-RES	N OBS	STD ERR
4.5	1696.10	4	56.29
7.5	1230.80	5	83.72
13.6	868.93	4	44.92
27.0	495.96	3	43.49
45.0	598.84	5	50.39
75.0	603.28	4	28.14
136.0	516.08	3	50.40
270.0	564.86	5	21.78
450.0	540.00	5	102.18
750.0	370.00	3	4.03
13600.0	143.05	4	12.54

OUTPUT FROM PLOT

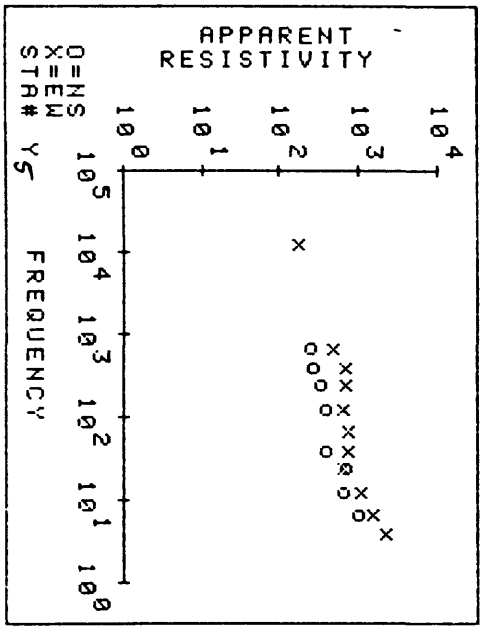

OUTPUT FROM PRINT

PROJECT=LINE Y

STATION ID_Y6 NS NO FREQ= 7

FREQ	AP-RES	N OBS	STD ERR
7.5	8870.00	4	667.80
13.6	8770.00	4	376.33
27.0	10000.00	3	603.00
45.0	10000.00	5	139.00
75.0	18763.00	3	415.80
7500.0	2800.00	3	122.36
13600.0	2777.80	3	0.00

STATION ID_Y6 EW NO FREQ= 9

FREQ	AP-RES	N OBS	STD ERR
4.5	8497.40	4	486.70
7.5	8000.00	5	332.50
13.6	7000.00	5	455.95
27.0	4339.50	2	957.60
45.0	5720.80	3	444.30
75.0	4461.70	5	538.16
136.0	3150.50	3	371.65
270.0	3000.00	4	496.70
7500.0	2000.00	5	18.38

OUTPUT FROM PLOT

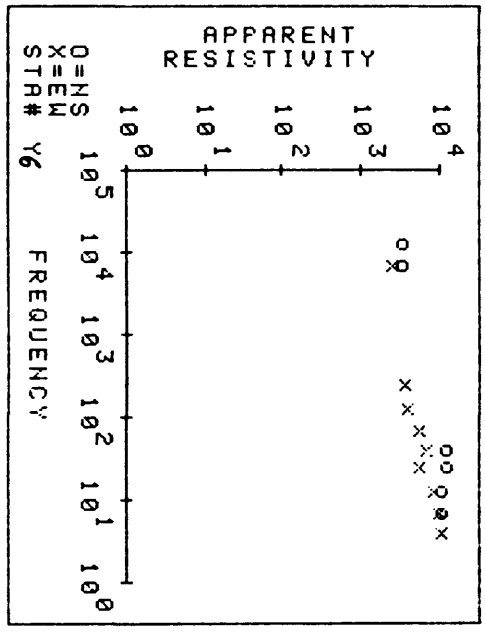

OUTPUT FROM PRINT

PROJECT=LINE Y

STATION ID_Y_7 NS NO FREQ= 13

FREQ	AP-RES	N OBS	STD ERR
4.5	1744.90	4	75.61
7.5	1674.90	4	129.49
13.6	2349.30	4	196.00
27.0	1862.30	4	90.40
45.0	1257.30	4	59.67
75.0	711.47	2	33.47
136.0	321.24	3	18.92
270.0	390.61	5	42.17
450.0	370.00	4	2.69
750.0	270.00	2	7.21
7500.0	227.00	3	10.21
13600.0	222.97	4	4.81
27000.0	200.00	4	.64

STATION ID_Y_7 EW NO FREQ= 13

FREQ	AP-RES	N OBS	STD ERR
4.5	2722.60	3	386.98
7.5	2323.90	5	345.62
13.6	1358.00	3	115.32
27.0	1211.00	4	198.24
45.0	892.63	4	42.93
75.0	573.60	3	60.82
136.0	633.56	5	33.51
270.0	602.60	5	34.45
450.0	600.00	5	8.89
750.0	570.00	5	15.11
7500.0	411.47	5	20.22
13600.0	449.37	4	42.36
27000.0	440.00	3	5.06

OUTPUT FROM PLOT

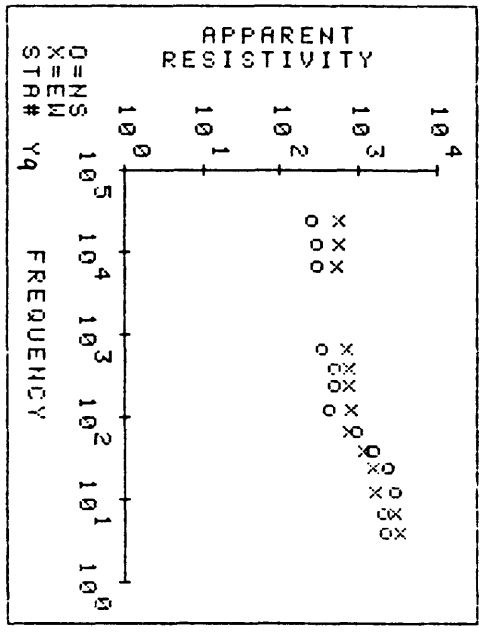

OUTPUT FROM PRINT

PROJECT=LINE Y

STATION ID_Y_8 NS NO FREQ= 12

FREQ	AP-RES	N OBS	STD ERR
4.5	3107.60	3	661.54
7.5	4457.80	5	278.17
13.6	4450.00	2	9.81
27.0	4310.80	4	488.30
45.0	2486.60	4	469.70
75.0	2605.80	4	119.68
136.0	1355.10	4	202.17
270.0	1915.90	5	166.62
450.0	1700.00	5	1825.90
750.0	953.17	3	70.66
13600.0	900.00	4	39.50
27000.0	700.00	5	31.21

STATION ID_Y_8 EW NO FREQ= 10

FREQ	AP-RES	N OBS	STD ERR
7.5	10573.00	5	1049.20
13.6	7700.00	4	401.45
27.0	6001.00	4	623.72
45.0	4079.10	2	1011.40
75.0	3199.00	4	332.13
136.0	3555.50	3	688.65
270.0	1882.30	3	408.91
450.0	1800.00	4	3560.20
7500.0	1998.20	5	176.73
13600.0	1700.00	2	161.51

OUTPUT FROM PLOT

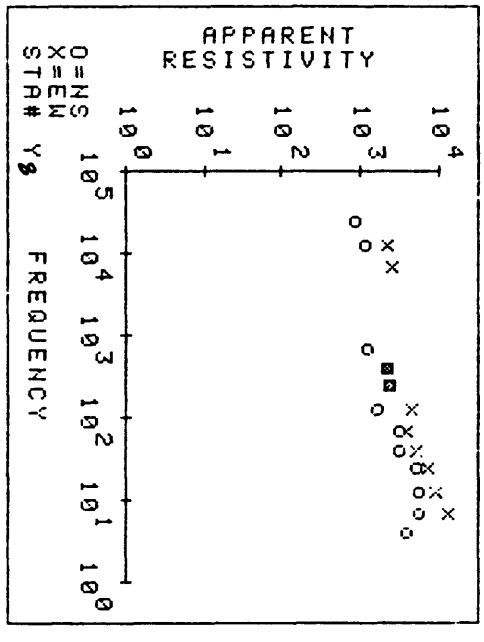

PROJECT=RAHA

STA. ID_CM#19R NS NO FREQ= 16

FREQ	AP-RES	N OBS	STD ERR
4.5	42.21	4	7.12
7.5	70.21	6	5.02
14.0	43.52	5	4.24
27.0	26.96	8	.90
45.0	21.74	7	1.12
45.0	19.11	6	2.23
75.0	15.79	7	.78
140.0	12.41	6	1.06
270.0	8.33	6	1.12
450.0	7.32	8	.67
750.0	6.38	5	.99
750.0	6.85	4	.80
4500.0	2.81	6	.29
7500.0	2.47	5	.12
14000 0	.93	5	.05
27000.0	2.05	6	.18

STA ID_CM#19R EW NO FREQ= 13

FREQ	AP-RES	N OBS	STD ERR
7 5	4.90	6	.75
14.0	4.75	6	.98
27.0	4.80	6	.85
45.0	4.34	5	1.19
75.0	4.89	5	.42
140.0	4.53	8	.62
270.0	3.89	7	.30
450.0	4.41	7	.68
750.0	6.36	3	1.30
4500.0	5.24	6	1.03
7500.0	2.74	4	.09
14000.0	2.47	6	.17
27000.0	2.92	7	.31

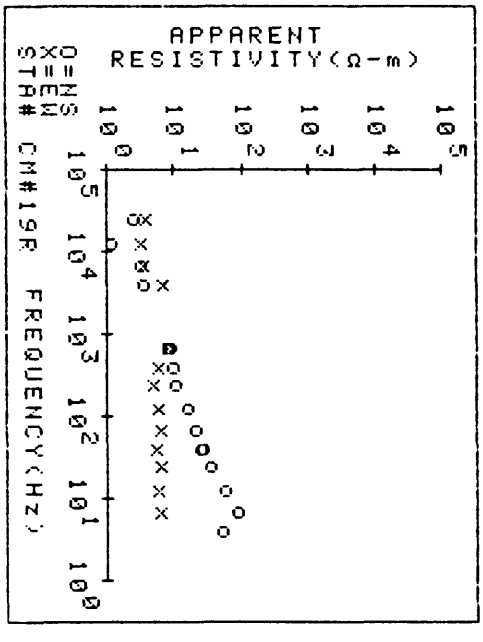

PROJECT=RAHA

STA. ID_CM 29 NS NO FREQ= 16

FREQ	AP-RES	N OBS	STD ERR
4.5	2227.40	3	432.56
7.5	2348.30	6	230.33
14.0	1526.40	6	194.42
27.0	764.54	6	141.51
45.0	662.24	7	86.82
75.0	360.27	3	90.14
140:0	582.58	7	140.84
270.0	254.06	5	14.40
450.0	134.43	5	10.62
750.0	185.78	6	45.70
1400.0	175.16	5	20.65
2700.0	170.00	3	8.18
4500.0	60.76	6	2.89
7500.0	23.64	6	2.00
14000.0	17.70	5	.73
27000.0	16.97	4	1.56

STA ID_CM 29 EW NO FREQ= 16

FREQ	AP-RES	N OBS	STD ERR
4.5	2960.90	4	179.55
7.5	2610.10	9	497.91
14.0	2500.00	5	.06
27.0	1214.30	6	79.22
45.0	1071.10	5	156.90
75.0	722.27	6	64.23
140.0	525.98	6	41.38
270.0	707.10	5	96.60
450.0	399.73	6	21.55
750.0	240.16	6	40.84
1400.0	321.27	4	21.51
2700.0	300.00	4	12.92
4500.0	134.37	7	10.96
7500.0	50.82	6	4.17
14000.0	48.95	4	8.85
27000.0	56.65	6	8.21

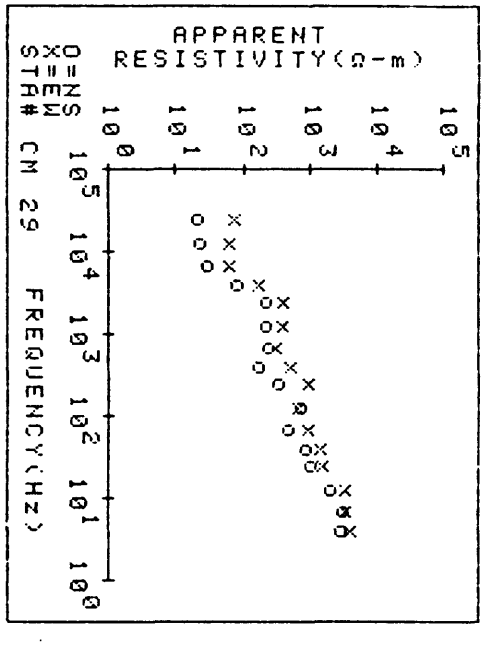

PROJECT=SILSILAH 11/84

STA. ID_CM#23 NS NO FREQ= 14

FREQ	AP-RES	N OBS	STD ERR
4.5	714.64	5	200.22
14.0	251.72	4	22.96
27.0	173.01	4	29.26
45.0	150.49	5	16.27
75.0	167.29	5	17.34
140.0	184.50	6	6.25
270.0	143.87	5	14.52
450.0	91.76	5	17.11
750.0	104.68	7	17.11
1400.0	79.65	4	12.13
2700.0	25.09	5	4.97
4500.0	45.14	6	3.27
7500.0	13.74	6	.57
27000.0	6.14	6	.60

STA. ID_CM#23 EW NO FREQ= 14

FREQ	AP-RES	N OBS	STD ERR
4.5	282.42	6	19.62
14.0	120.93	5	17.07
27.0	66.64	6	10.50
45.0	88.91	6	9.23
75.0	70.52	4	6.31
140.0	84.48	6	8.28
270.0	128.29	6	26.26
450.0	66.97	6	7.53
750.0	38.53	6	2.77
1400.0	37.71	5	2.70
2700.0	42.59	5	5.05
4500.0	47.32	6	1.40
7500.0	14.72	6	2.11
14000.0	16.63	6	.87

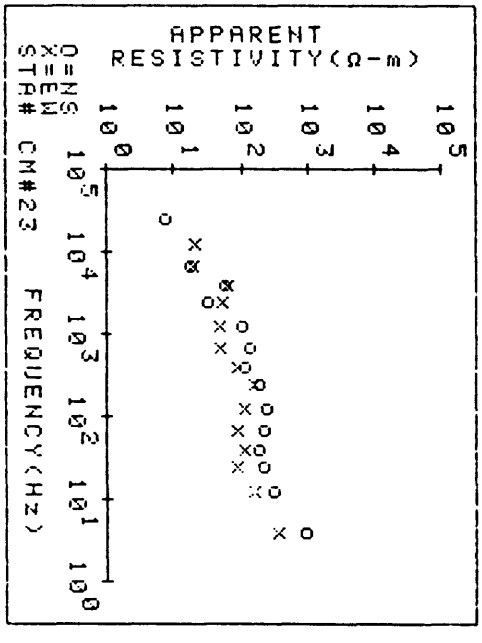

PROJECT=SILSILAH 11/84

STA. ID_CM#24 NS NO FREQ= 12

FREQ	AP-RES	N OBS	STD ERR
4.5	386.58	6	82.97
7.5	162.49	4	25.25
14.0	86.83	4	16.66
27.0	80.28	8	6.84
45.0	65.26	8	8.42
75.0	53.83	11	4.45
270.0	31.49	5	1.29
450.0	28.94	7	3.26
750.0	27.55	6	3.32
1400.0	36.55	4	5.37
4500.0	43.94	8	5.38
7500.0	16.84	7	1.29

STA. ID_CM#24 EW NO FREQ= 12

FREQ	AP-RES	N OBS	STD ERR
7.5	374.12	8	34.77
14.0	273.43	5	40.47
27.0	150.05	4	35.01
45.0	128.49	6	13.93
75.0	89.45	5	7.23
140.0	80.38	4	12.14
270.0	68.92	5	2.53
450.0	53.77	5	3.00
750.0	37.94	5	3.99
1400.0	13.85	5	1.45
2700.0	10.07	8	.53
4500.0	12.03	3	.48

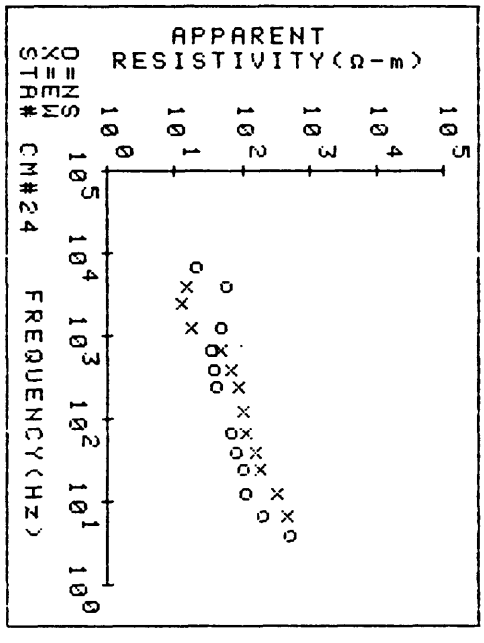

PROJECT=RAHA

STA. ID_CM#30 NS NO FREQ= 14

FREQ	AP-RES	N OBS	STD ERR
4.5	1629.70	5	593.93
7.5	1492.50	3	410.23
14.0	809.60	3	82.00
27.0	628.80	5	96.95
45.0	765.40	7	186.87
75.0	391.61	4	162.37
140.0	932.77	7	140.19
270.0	277.56	4	96.44
450.0	197.55	4	13.80
750.0	80.84	2	25.75
4500.0	55.96	4	7.32
7500.0	21.20	3	2.44
14000.0	20.53	4	1.24
27000.0	15.98	5	2.18

STA. ID_CM#30 EW NO FREQ= 13

FREQ	AP-RES	N OBS	STD ERR
4.513207.00		4	1360.10
7.515051.00		6	2114.90
14.010469.00		7	629.60
27.0 5457.60		4	734.26
45.0 4480.00		7	501.19
75.0 4315.00		6	520.93
140.0 2855.00		6	440.94
270.0 2350.00		5	340.82
450.0	744.18	5	220.64
4500.0	212.88	6	21.29
7500.0	48.07	4	2.03
14000.0	28.31	6	5.03
27000.0	37.78	5	6.17

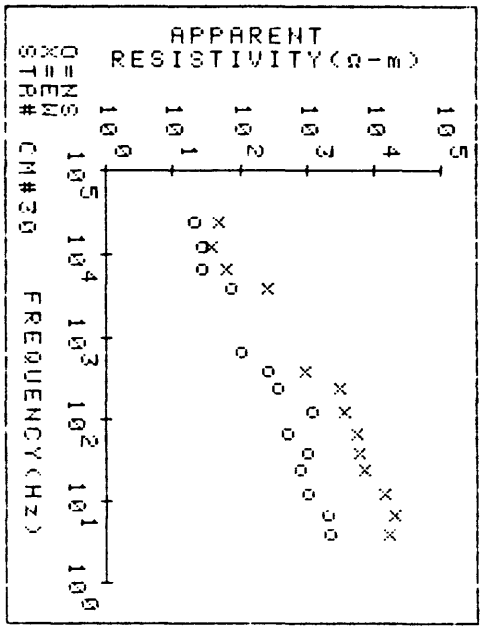

PROJECT=RAHA

STA. ID_CM#31 NS NO FREQ= 14

FREQ	AP-RES	N OBS	STD ERR
4.5	2970.90	3	848.84
7.5	2136.10	4	64.87
14.0	1251.20	5	64.26
27.0	569.37	5	105.64
45.0	675.76	6	89.47
75.0	1445.70	5	413.85
140.0	694.21	7	165.47
270.0	334.20	8	51.75
450.0	206.06	9	28.88
750.0	133.96	2	6.21
4500.0	93.15	10	9.29
7500.0	7.14	8	.32
14000.0	3.68	7	.16
27000.0	5.52	9	.41

STA. ID_CM#31 EW NO FREQ= 13

FREQ	AP-RES	N OBS	STD ERR
4.5	3372.90	4	587.70
7.5	5593.80	10	488.78
14.0	4289.10	9	256.75
27.0	2177.80	8	118.74
45.0	1645.30	8	110.06
75.0	1315.00	7	120.08
140.0	835.67	7	70.00
270.0	535.00	10	31.12
450.0	314.10	7	40.20
4500.0	74.17	6	8.14
7500.0	18.49	5	1.53
14000.0	14.64	4	2.06
27000.0	10.48	10	1.07

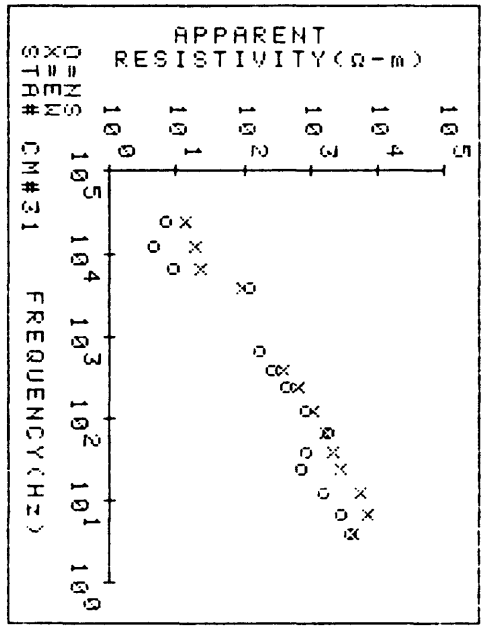

PROJECT=RAHA

STA. ID_CM#32 NS NO FREQ= 14

FREQ	AP-RES	N OBS	STD ERR
4.5	653.32	5	106.70
7.5	519.61	8	23.41
14.0	314.23	7	18.93
27.0	179.99	7	20.16
45.0	137.35	7	9.27
75.0	115.19	7	5.93
140.0	94.94	7	10.94
270.0	53.12	6	8.70
450.0	50.98	4	14.74
750.0	17.80	6	.75
4500.0	8.47	4	1.79
7500.0	5.62	4	1.51
14000.0	5.78	5	.11
27000.0	5.91	5	3.09

STA. ID_CM#32 EW NO FREQ= 13

FREQ	AP-RES	N OBS	STD ERR
4.5	309.07	3	191.68
7.5	135.53	7	15.07
14.0	45.82	6	12.14
27.0	37.00	6	1.68
45.0	29.70	5	6.16
75.0	27.00	5	1.03
140.0	26.70	4	3.12
270.0	25.70	5	.39
450.0	21.00	7	.81
750.0	34.04	4	5.12
7500.0	6.14	6	.27
14000.0	4.53	6	.29
27000.0	4.00	6	1.00

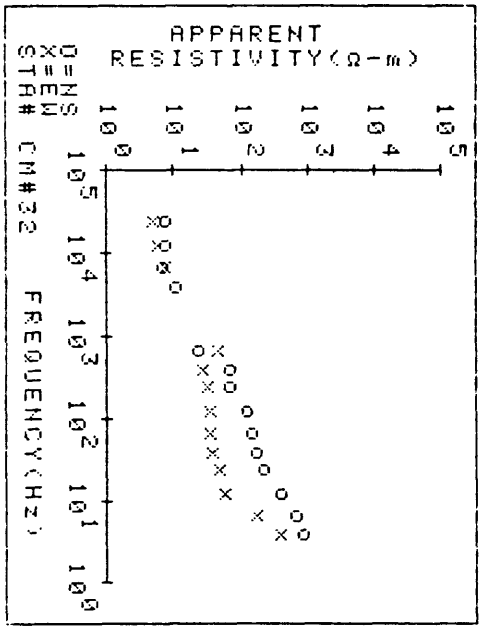

PROJECT=RAHA

STA. ID_CM#32R NS NO FREQ= 15

FREQ	AP-RES	N OBS	STD ERR
4.5	560.45	6	115.77
7.5	543.19	9	27.49
14.0	307.32	7	20.25
27.0	173.30	6	7.12
45.0	127.09	8	7.45
75.0	87.14	7	7.38
140.0	71.96	5	14.92
270.0	32.56	5	2.75
450.0	21.45	5	2.75
750.0	23.05	7	1.85
1400.0	20.85	4	2.00
4500.0	7.77	3	1.56
7500.0	2.92	4	1.34
14000.0	4.02	5	.36
27000.0	5.68	6	.69

STA ID_CM#32R EW NO FREQ= 12

FREQ	AP-RES	N OBS	STD ERR
4.5	98.37	4	10.41
7.5	61.15	4	4.34
14.0	86.62	6	9.88
27.0	41.93	5	9.00
45.0	40.31	6	2.64
75.0	23.35	5	2.20
140.0	17.54	4	.40
270.0	14.69	5	3.98
4500.0	18.57	4	3.77
7500.0	5.74	5	1.08
14000.0	4.41	5	1.08
27000.0	8.99	5	.77

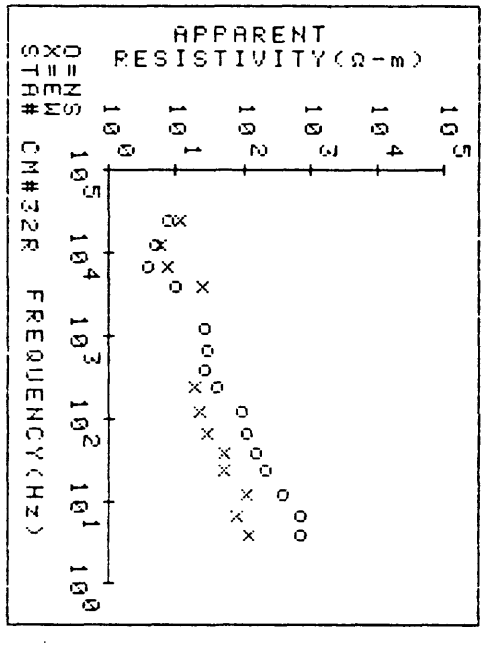

PROJECT=RAHA

STA. ID_CM#33 NS NO FREQ= 15

FREQ	AP-RES	N OBS	STD ERR
4.5	536.36	2	410.94
7.5	979.81	5	69.95
14.0	294.04	6	30.59
27.0	530.74	10	59.11
45.0	986.88	3	280.77
45.0	773.80	2	97.08
75.0	725.36	5	131.45
140.0	619.18	3	87.27
270.0	654.45	6	72.14
450.0	255.92	4	8.68
750.0	279.81	3	42.00
4500.0	250.00	6	4.89
7500.0	135.37	7	13.60
14000.0	77.00	8	2.00
27000.0	74.09	6	6.85

STA. ID_CM#33 EW NO FREQ= 15

FREQ	AP-RES	N OBS	STD ERR
4.5	1363.20	3	392.69
7.5	1123.70	6	105.19
14.0	865.00	9	38.67
27.0	603.88	10	13.76
45.0	481.24	6	45.54
75.0	469.75	4	7.38
140.0	540.99	6	25.07
270.0	491.84	6	29.68
450.0	458.91	10	20.97
750.0	400.00	2	23.85
2700.0	97.00	2	23.85
4500.0	89.00	3	.53
7500.0	86.59	5	5.43
14000.0	51.96	5	4.31
27000.0	31.50	4	2.54

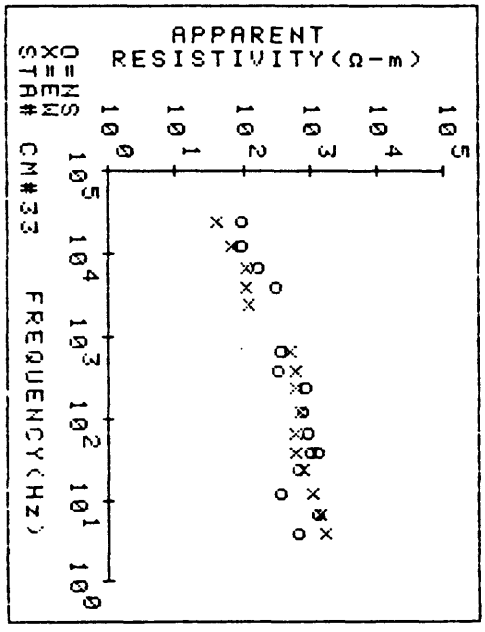

PROJECT=RAHA

STA. ID_CM#34 NS NO FREQ= 15

FREQ	AP-RES	N OBS	STD ERR
4.5	3600.80	2	1234.60
4.5	3600.80	2	1234.60
7.5	1605.70	6	204.13
14.0	977.96	7	92.21
27.0	1544.80	4	339.20
45.0	1461.00	6	87.66
75.0	1124.40	5	298.12
140.0	2100.60	4	184.28
270.0	1274.90	7	199.88
450.0	651.96	6	86.13
750.0	425.05	4	71.51
4500.0	521.64	7	32.00
7500.0	288.86	4	30.60
14000.0	170.00	5	17.39
27000.0	130.13	6	14.27

STA. ID_CM#34 EW NO FREQ= 14

FREQ	AP-RES	N OBS	STD ERR
4.5	1082.60	5	112.44
7.5	481.42	5	55.93
14.0	489.64	6	44.45
27.0	346.68	6	18.27
45.0	256.96	7	18.60
75.0	255.26	5	12.12
140.0	295.41	6	19.88
270.0	327.13	7	17.73
450.0	327.08	6	40.95
750.0	97.00	3	7.63
4500.0	76.15	6	10.01
7500.0	43.33	5	3.73
14000.0	32.85	5	2.26
27000.0	49.14	6	3.29

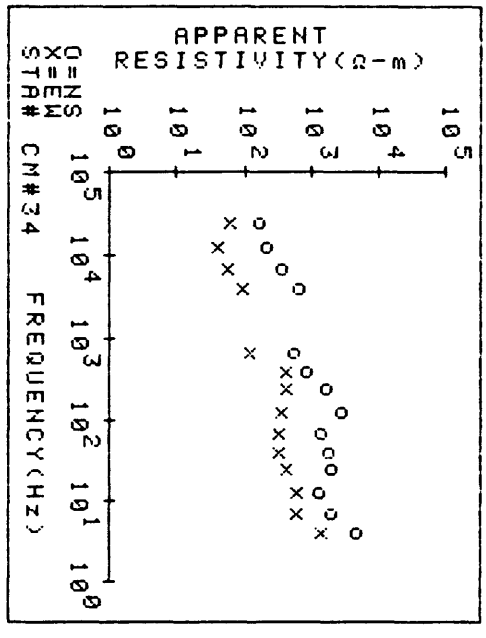

PROJECT=RAHA

STA. ID_CM#35 NS NO FREQ= 14

FREQ	AP-RES	N OBS	STD ERR
4.5	918.00	5	189.86
7.5	816.80	8	71.04
14.0	469.50	7	32.08
27.0	275.69	8	19.60
45.0	236.29	7	20.97
75.0	317.00	10	16.91
140.0	308.62	5	9.55
270.0	203.99	6	18.68
450.0	252.45	4	5.40
750.0	184.17	3	24.09
4500.0	70.00	7	3.39
7500.0	57.29	7	4.96
14000.0	57.20	5	.82
27000.0	57.19	4	4.35

STA. ID_CM#35 EW NO FREQ= 14

FREQ	AP-RES	N OBS	STD ERR
4.5	662.70	5	63.34
7.5	947.78	7	86.69
14.0	631.53	6	14.11
27.0	262.77	5	12.67
45.0	316.29	6	41.26
75.0	301.46	8	25.88
140.0	363.42	7	18.34
270.0	354.47	7	40.12
450.0	324.84	6	30.42
750.0	213.16	4	98.17
4500.0	158.67	3	47.46
7500.0	45.83	5	12.90
14000.0	48.63	4	2.74
27000.0	44.65	4	5.70

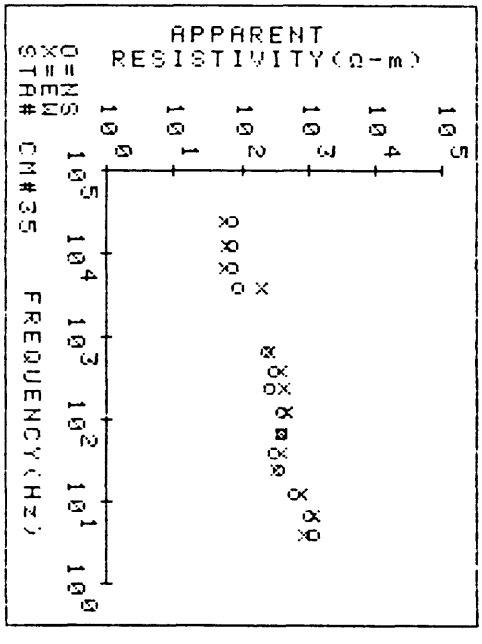

PROJECT=RAHA

STA. ID_CM#36 NS NO FREQ= 16

FREQ	AP-RES	N OBS	STD ERR
4.5	1456.30	2	22.49
7.5	3295.90	6	191.76
14.0	2465.70	4	158.54
27.0	2438.90	6	130.49
45.0	2490.80	6	99.83
75.0	1585.30	6	199.48
140.0	1759.80	6	236.91
270.0	1358.70	5	104.66
450.0	882.21	6	114.90
750.0	558.68	3	86.26
2700.0	500.00	3	7.11
4500.0	740.74	4	85.35
7500.0	351.70	5	12.46
7500.0	338.13	5	6.38
14000.0	63.07	7	2.78
27000.0	296.25	6	13.64

STA ID_CM#36 EW NO FREQ= 12

FREQ	AP-RES	N OBS	STD ERR
4.5	4801.90	8	559.91
7.5	6974.00	6	538.79
14.0	2700.00	5	7.30
27.0	2300.00	5	1.53
45.0	2277.00	6	103.07
75.0	2179.30	6	130.35
140.0	1440.60	5	100.05
270.0	1255.90	6	64.93
450.0	899.83	8	58.62
4500.0	1190.00	7	104.48
14000.0	190.89	6	9.39
27000.0	177.67	7	21.05

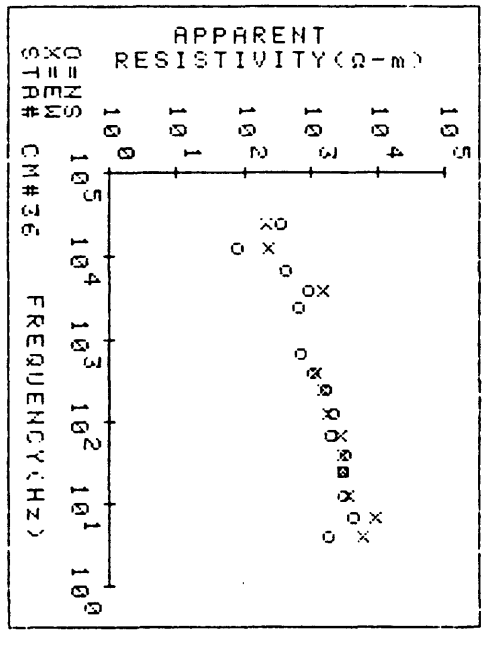

PROJECT=RAHA

NO DATA N-S

STA. ID_36A EW NO FREQ= 9

FREQ	AP-RES	N OBS	STD ERR
7.5	7651.40	4	492.66
14.0	6066.60	6	459.46
27.0	3058.40	6	223.06
45.0	2963.00	5	216.11
75.0	2019.00	4	157.69
140.0	1656.70	5	65.19
270.0	1171.60	5	71.94
450.0	598.53	4	57.61
4500.0	351.75	4	44.08

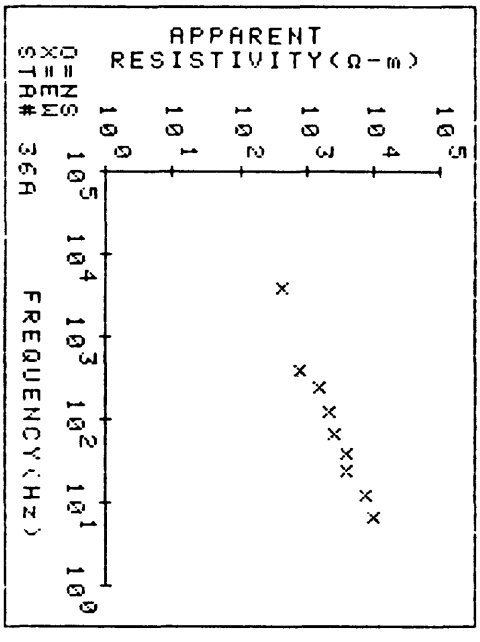

PROJECT=RAHA

STA. ID_CM#37 NS NO FREQ= 11

FREQ	AP-RES	N OBS	STD ERR
7.5	1316.00	4	87.10
14.0	1200.00	3	46.20
27.0	1000.00	3	36.93
75.0	970.48	4	101.30
140.0	808.68	4	104.71
270.0	700.00	3	31.90
450.0	564.91	3	62.30
4500.0	455.84	4	82.71
7500.0	231.63	5	30.85
14000.0	285.10	6	13.64
27000.0	375.00	6	28.69

STA ID_CM#37 EW NO FREQ= 12

FREQ	AP-RES	N OBS	STD ERR
27.020711.00		6	518.83
27.020711.00		6	518.83
45.013358.00		7	592.83
75.011624.00		6	479.73
140.0	8282.90	6	196 20
270.0	6850.50	6	259.34
450.0	4098.30	6	168.91
750.0	1619.70	4	239.22
4500.0	648.41	5	112.67
7500.0	232.07	5	6.64
14000.0	169.98	4	3.76
27000.0	318.39	4	17.93

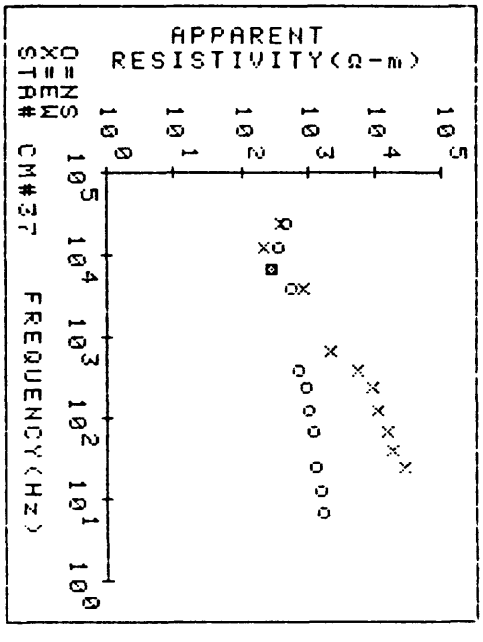

PROJECT=RAHA

STA. ID_CM#38 NS NO FREQ= 10

FREQ	AP-RES	N OBS	STD ERR
14.0	242.26	3	8.74
27.0	161.28	4	17.53
45.0	140.50	5	15.10
75.0	172.55	5	23.90
140.0	89.99	4	3.57
270.0	81.06	5	7.50
450 0	31.01	3	4.19
7500 0	9.64	5	.47
14000.0	1.75	5	.11
27000.0	4.81	4	.41

STA. ID_CM#38 EW NO FREQ= 14

FREQ	AP-RES	N OBS	STD ERR
4.5	658.98	3	99.73
7 5	987.37	6	69.02
14.0	819.69	4	14.63
27.0	344.93	8	17.69
45.0	239.33	7	7.24
75.0	164.65	7	6.17
140.0	164.01	6	5.78
270.0	118.04	5	4.47
450.0	101 01	7	6.45
750 0	21.57	2	2.46
4500 0	8.16	6	.80
7500.0	3.98	5	.25
14000.0	3.61	3	.43
27000.0	5.98	5	.23

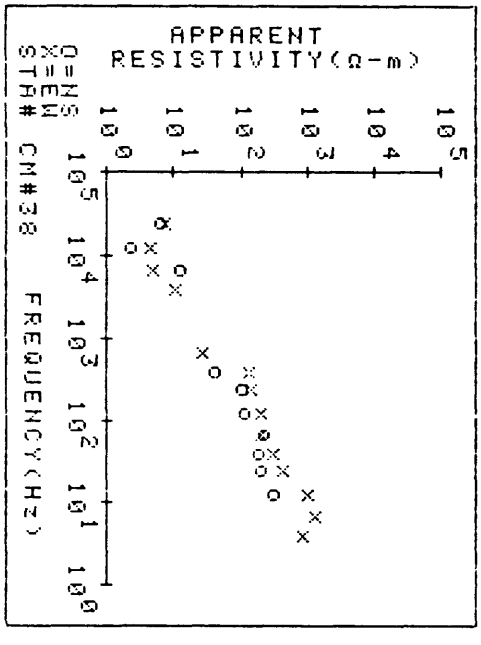

PROJECT=RAHA

STA. ID_CM#39 NS NO FREQ= 16

FREQ	AP-RES	N OBS	STD ERR
4.5	405.41	3	38.81
7.5	480.42	6	58.45
14.0	317.96	6	16.41
27.0	182.69	6	6.05
45.0	127.15	7	9.52
75.0	105.36	6	5.72
140.0	70.17	6	2.19
270.0	40.01	6	2.03
450.0	26.11	7	3.20
750.0	14.74	4	1.35
1400.0	27.00	3	1.29
2700.0	17.00	2	.45
4500.0	15.00	5	.71
7500.0	9.43	5	.71
14000.0	25.00	5	52
27000.0	29.57	6	3.83

STA ID_CM#39 EW NO FREQ= 15

FREQ	AP-RES	N OBS	STD ERR
4.5	119.44	6	15.11
7.5	142.12	4	3.22
14.0	92.55	5	17.68
27.0	87.89	5	5.99
45.0	72.43	5	12.80
75.0	66.35	5	9.15
140.0	50.26	5	2.11
270.0	45.09	6	3.60
450.0	41.16	5	5.18
750.0	24.09	5	2.36
1400.0	37.00	5	6.03
4500.0	34.57	4	4.17
7500.0	24.02	6	1.18
14000.0	20.49	6	1.07
27000.0	40.07	5	1.27

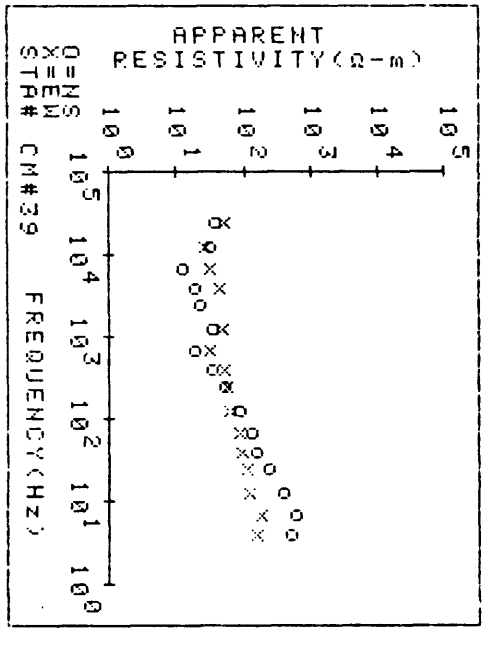

PROJECT=RAHA

STA. ID_CM#40 NS NO FREQ= 11

FREQ	AP-RES	N OBS	STD ERR
7.5	74.29	6	10.34
14.0	63.32	8	4.28
27.0	54.06	8	6.41
45.0	29.48	7	1.81
75.0	33.16	6	4.58
140.0	18.19	5	3.15
450.0	15.37	6	1.38
750.0	16.67	5	1.81
4500.0	17.58	5	.59
7500.0	11.08	3	4.28
27000.0	5.24	6	.71

STA ID_CM#40 EW NO FREQ= 16

FREQ	AP-RES	N OBS	STD ERR
4.5	147.59	3	33.43
7.5	101.91	6	19.69
7.5	111.86	5	19.53
14.0	83.89	5	9.38
27.0	46.84	6	4.76
45.0	41.59	6	3.17
75.0	27.65	5	3.81
140.0	35.38	6	5.96
270.0	17.33	6	2.45
270.0	17.88	5	3.86
450.0	16.01	5	2.88
750.0	13.04	4	1.65
4500.0	32.71	5	5.46
7500.0	12.53	5	2.24
14000.0	19.55	6	1.11
27000.0	7.94	5	1.20

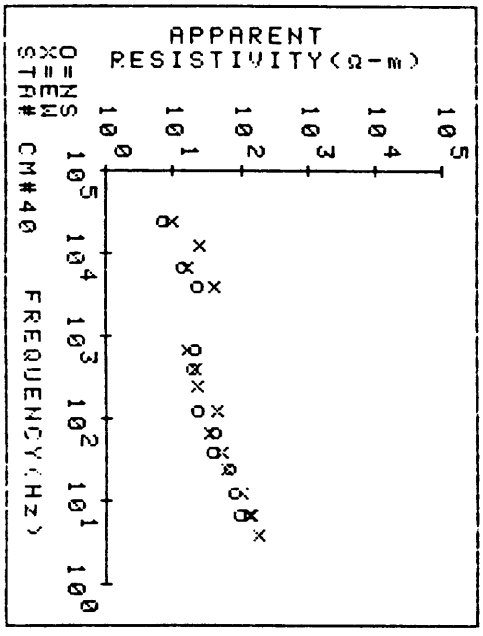

PROJECT=RAHA

STA ID_CM#41 NS NO FREQ= 12

FREQ	AP-RES	N OBS	STD ERR
4.5	59.71	3	17.41
7.5	35.31	10	2.20
14.0	22.57	6	1.80
27.0	14.70	6	1.14
45.0	10.29	4	1.08
75.0	10.89	6	.92
140.0	6.02	6	.37
270.0	6.13	8	1.50
450.0	3.88	6	.26
4500.0	3.55	4	.35
7500.0	1.69	7	.12
27000.0	2.63	5	.50

STA ID_CM#41 EW NO FREQ= 12

FREQ	AP-RES	N OBS	STD ERR
7.5	13.49	4	2.66
14.0	17.97	6	1.51
27.0	11.91	5	1.43
45.0	8.05	4	1.74
75.0	6.38	6	.75
140.0	5.16	4	.61
270.0	6.48	5	.45
450.0	5.88	5	.28
750.0	3.62	5	.46
7500.0	2.81	5	.36
14000.0	3.63	6	.33
27000.0	8.12	3	1.39

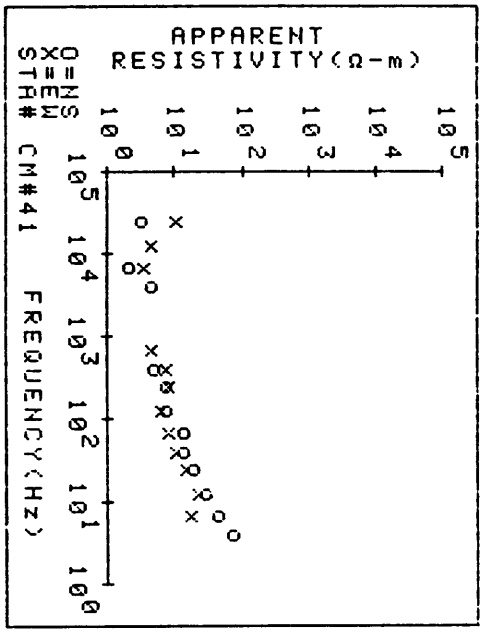

PROJECT=RAHA

STA. ID_CM#42 NS NO FREQ= 11

FREQ	AP-RES	N OBS	STD ERR
4.5	574.38	7	92.66
14.0	164.60	9	7.80
27.0	132.64	10	18.99
45.0	70.88	9	5.09
75.0	67.19	6	5.56
140.0	39.06	10	2.66
270.0	21.73	10	4.27
450.0	16.94	9	1.26
4500.0	4.89	10	.52
7500.0	1.74	7	.19
27000.0	3.57	5	.05

STA. ID_CM#42 EW NO FREQ= 12

FREQ	AP-RES	N OBS	STD ERR
4.5	476.45	4	114.09
7.5	145.14	5	20.49
7.5	301.14	8	11.40
14.0	349.80	6	23.34
27.0	171.71	5	9.36
45.0	87.86	5	3.06
75.0	73.23	6	6.45
140.0	63.68	6	4.66
270.0	29.98	4	3.45
450.0	38.59	5	4.92
4500.0	9.77	3	.51
27000.0	4.95	5	.50

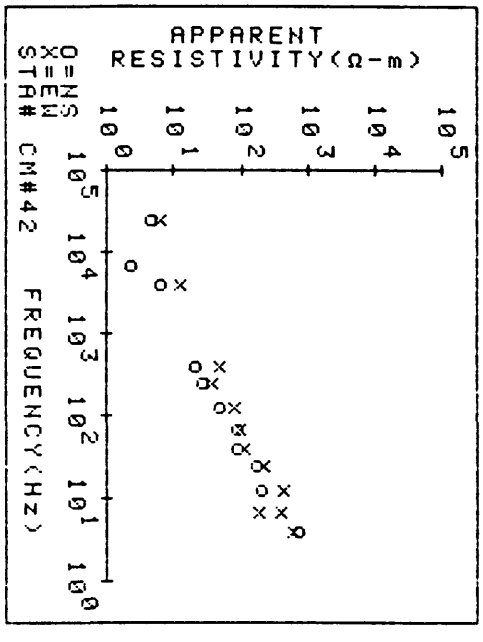

PROJECT=RAHA

STA. ID_CM#43 NS NO FREQ= 12

FREQ	AP-RES	N OBS	STD ERR
4.5	2828.80	4	214.17
14.0	7078.00	3	996.84
27.0	3846.20	7	441.50
45.0	3723.40	7	395.79
75.0	6618.00	5	988.97
140.0	3606.50	6	559.00
270.0	4620.80	5	709.83
450.0	2771.60	4	1105.40
750.0	781.37	3	198.07
4500.0	438.56	5	34.46
7500.0	204.10	5	7.13
27000.0	217.65	5	12.92

STA. ID_CM#43 EW NO FREQ= 12

FREQ	AP-RES	N OBS	STD ERR
4.5	10733.00	4	1597.30
7.5	8991.90	7	1092.10
14.0	7073.00	6	983.34
27.0	6545.60	6	687.40
45.0	6956.60	7	545.88
75.0	6366.00	4	583.62
140.0	6421.30	4	629.44
270.0	5133.90	6	583.50
450.0	3105.40	6	470.29
7500.0	636.30	5	91.53
14000.0	430.93	5	43.83
27000.0	451.89	6	39.46

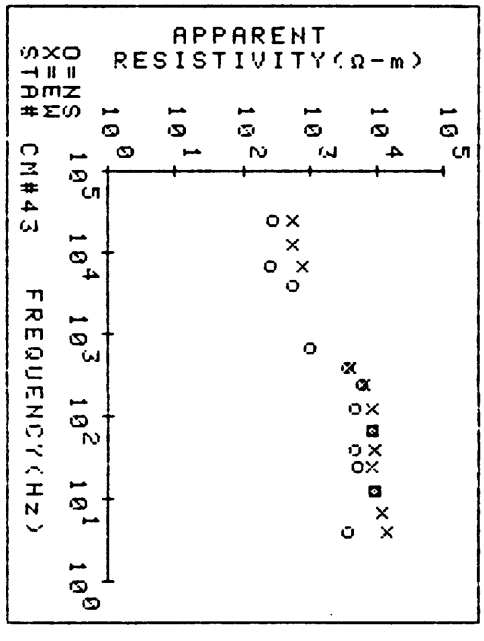

PROJECT=RAHA

STA. ID_CM#44 NS NO FREQ= 12

FREQ	AP-RES	N OBS	STD ERR
4.5	3136.50	6	236.26
7.5	2055.90	8	183.61
14.0	1564.20	5	144.78
27.0	1071.60	6	49.95
45.0	790.35	6	25.18
75.0	735.10	4	143.13
140.0	612.81	5	32.39
270.0	547.39	7	75.40
450.0	249.64	3	12.57
4500.0	137.12	5	18.40
7500.0	91.21	4	5.45
27000.0	61.26	4	8.06

STA. ID_CM#44 EW NO FREQ= 13

FREQ	AP-RES	N OBS	STD ERR
4.5	1060.60	2	170.79
7.5	963.45	6	45.59
14.0	1001.40	6	139.58
27.0	610.71	5	62.20
45.0	457.18	6	24.52
75.0	446.27	6	35.03
140.0	393.95	6	15.07
270.0	474.62	5	14.56
450.0	260.76	6	35.46
4500.0	58.44	5	7.47
7500.0	39.17	4	7.72
14000.0	35.19	5	.85
27000.0	35.17	5	3.05

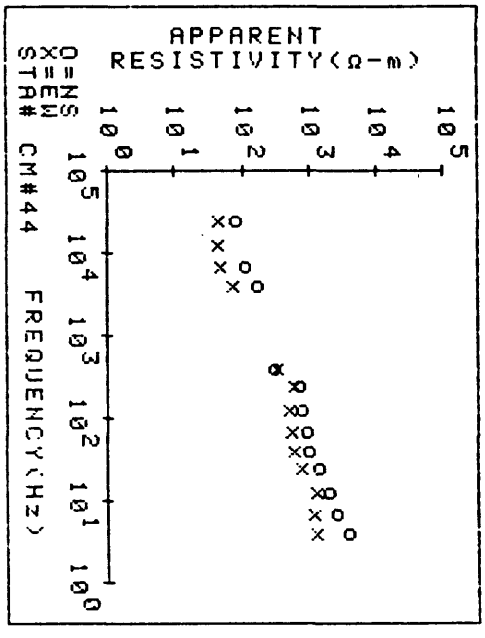

PROJECT=RAHA

STA. ID_CM#45 NS NO FREQ= 11

FREQ	AP-RES	N OBS	STD ERR
4.5	203.03	4	11.09
7.5	244.25	5	20.76
14.0	201.65	5	7.86
27.0	146.18	7	9.44
45.0	106.62	7	9.55
75.0	93.22	7	3.71
140.0	88.85	6	4.77
270.0	100.15	4	16.13
4500.0	114.98	6	10.24
7500.0	70.02	4	1.95
27000.0	59.19	4	3.12

STA. ID_CM#45 EW NO FREQ= 12

FREQ	AP-RES	N OBS	STD ERR
4.5	2280.70	3	568.20
7.5	2466.90	7	162.94
14.0	1729.40	5	182.56
27.0	992.66	3	57.82
45.0	657.39	6	31.95
75.0	570.81	6	59.30
140.0	492.62	7	42.82
270.0	401.48	6	24.83
450.0	163.78	5	53.08
7500.0	78.19	5	11.36
14000.0	110.08	6	15.73
27000.0	111.17	4	9.86

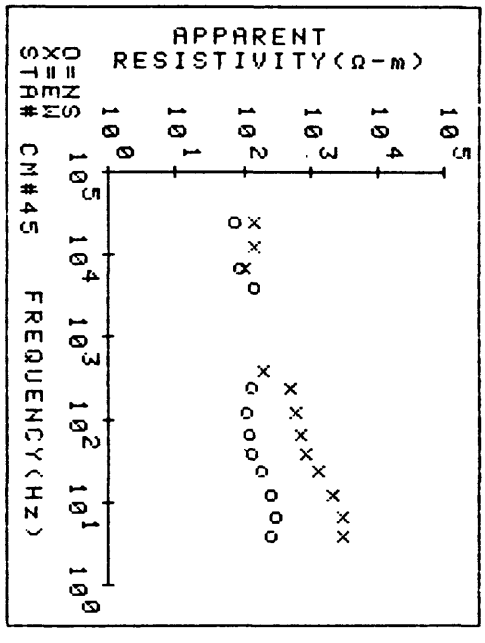

PROJECT=RAHA

STA. ID_CM#47 NS NO FREQ= 12

FREQ	AP-RES	N OBS	STD ERR
4.5	849.65	5	241.91
7.5	864.31	7	83.21
14.0	430.47	4	133.64
27.0	490.26	6	58.32
45.0	456.62	7	28.80
75.0	436.64	6	20.28
140.0	478.59	6	20.63
270 0	475.41	6	66.88
450.0	209.03	5	26.36
4500.0	192.08	4	21.93
14000.0	152.02	4	15.38
27000.0	110.75	4	10.65

STA. ID_CM#47 EW NO FREQ= 14

FREQ	AP-RES	N OBS	STD ERR
4.5	584.06	6	83.28
7.5	506.62	4	60.22
14.0	471.30	7	28.43
27.0	352.04	5	12.04
45.0	252.81	6	25.22
75.0	240.07	5	15.28
140.0	222.96	7	28.68
270.0	264.30	6	40.96
450.0	268.18	3	32.22
750.0	59.14	3	7.22
4500.0	45.80	3	7.86
7500.0	51.26	5	5.68
14000.0	41.17	5	2.56
27000.0	36.23	5	1.81

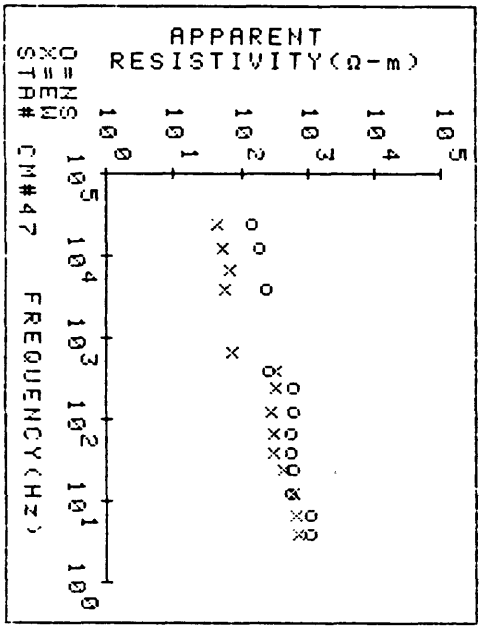

PROJECT=RAHA

STA. ID_CM#48 NS NO FREQ= 12

FREQ	AP-RES	N OBS	STD ERR
4.5	1404.30	5	272.82
7.5	1011.70	5	122.80
14.0	1105.90	4	406.27
27.0	754.37	6	137.54
45.0	758.78	5	147.27
75.0	1013.10	6	66.39
140.0	700.00	7	14.48
270.0	534.10	3	181.60
450.0	184.85	2	49.25
7500.0	134.39	5	50.84
14000.0	77.00	4	.97
27000.0	69.23	4	10.45

STA. ID_CM#48 EW NO FREQ= 14

FREQ	AP-RES	N OBS	STD ERR
4.5	600.14	6	56.30
7.5	450.19	5	29.07
14.0	286.05	8	10.32
27.0	202.06	5	3.79
45.0	132.04	6	6.18
75.0	129.62	6	15.68
140.0	162.61	7	5.48
270.0	173.97	6	5.63
450.0	164.11	5	16.73
750.0	84.38	3	14.76
4500.0	198.55	7	10.37
7500.0	62.07	7	2.27
14000.0	40.85	6	.87
27000.0	61.21	5	1.08

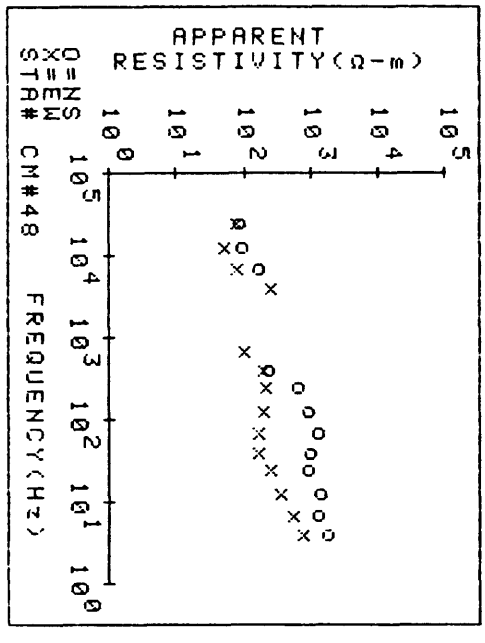

PROJECT=RAHA

STA. ID_CM#49 NS NO FREQ= 12

FREQ	AP-RES	N OBS	STD ERR
4.5	3946.20	3	802.91
7.5	4385.10	7	79.35
14.0	1849.80	8	235.11
27.0	1363.40	5	82.48
45.0	712.93	5	19.78
75.0	815.90	8	89.27
140.0	588.52	8	31.18
270.0	400.00	5	7.51
4500.0	59.16	4	5.86
7500.0	12.34	3	1.81
14000.0	4.31	5	.47
27000.0	7.47	5	2.97

STA. ID_CM#49 EW NO FREQ= 13

FREQ	AP-RES	N OBS	STD ERR
4.5	1700.00	4	128.01
7.5	1544.50	6	108.20
14.0	973.40	8	65.85
27.0	666.49	11	50.58
45.0	615.98	4	11.85
75.0	650.38	6	68.39
140.0	576.88	5	22.69
270.0	180.16	4	18.38
450.0	218.33	4	6.35
4500.0	47.56	3	2.61
7500.0	27.96	8	.76
14000.0	16.77	7	1.33
27000.0	8.83	4	.62

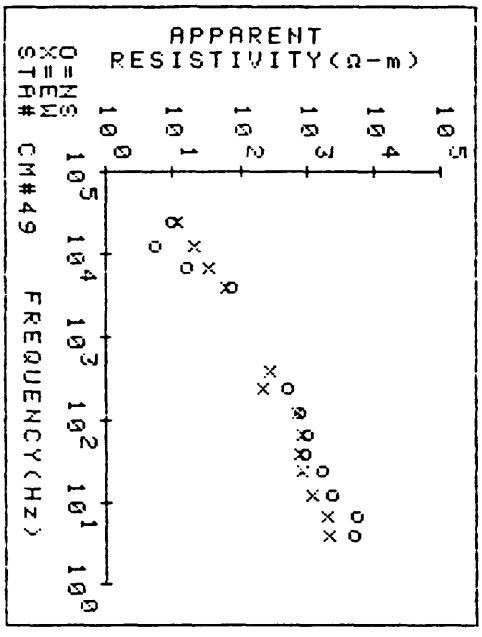

PROJECT=RAHA

STA ID_CM$52 NS NO FREQ= 11

FREQ	AP-RES	N OBS	STD ERR
7.5	242.74	4	37.99
14.0	148.82	6	11.55
27.0	127.87	6	5.48
45.0	47.63	4	8.45
75.0	40.92	3	5.18
140.0	30.52	6	6.62
270.0	33.23	5	5.77
450.0	12.58	5	2.14
4500.0	9.02	4	.33
7500.0	5.80	7	.34
27000.0	7.40	7	.52

STA ID_CM$52 EW NO FREQ= 12

FREQ	AP-RES	N OBS	STD ERR
4.5	73.48	2	8.18
7.5	36.80	3	1.64
14.0	31.23	6	1.74
27.0	23.43	5	1.04
45.0	21.82	7	.72
75.0	24.82	6	1.92
140.0	31.48	7	2.23
270.0	30.91	7	1.51
450.0	37.92	6	1.44
7500.0	13.62	5	2.25
14000.0	18.37	5	1.57
27000.0	35.46	3	3.45

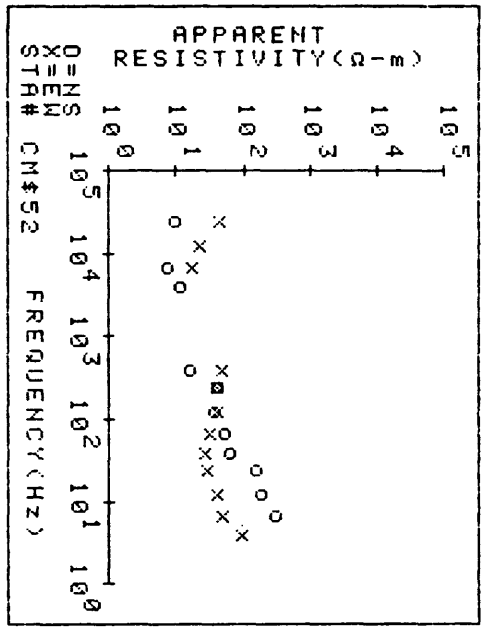

PROJECT=RAHA

STA. ID_CM#50 NS NO FREQ= 14

FREQ	AP-RES	N OBS	STD ERR
4.5	110.00	5	11.00
7.5	125.00	6	11.00
14.0	131.15	6	13.01
27.0	145.57	3	12.56
45.0	128.85	4	23.89
75.0	126.86	6	15.29
140.0	94.18	6	6.88
270.0	97.73	6	10.25
450.0	89.57	3	10.00
750.0	89.28	3	11.10
4500.0	36.97	3	5.69
7500.0	17.31	7	2.78
14000.0	10.00	5	.50
27000.0	8.65	7	.74

STA ID_CM#50 EW NO FREQ= 13

FREQ	AP-RES	N OBS	STD ERR
4.5	877.29	2	6.64
7.5	905.86	8	81.53
14.0	797.19	8	39.89
27.0	530.00	6	50.00
45.0	405.81	7	15.60
75.0	444.88	8	35.82
140.0	327.39	4	12.99
270.0	307.26	5	41.16
450.0	162.43	9	19.09
4500.0	59.05	5	5.84
7500.0	11.24	5	1.45
14000.0	14.59	5	3.95
27000.0	11.31	5	.48

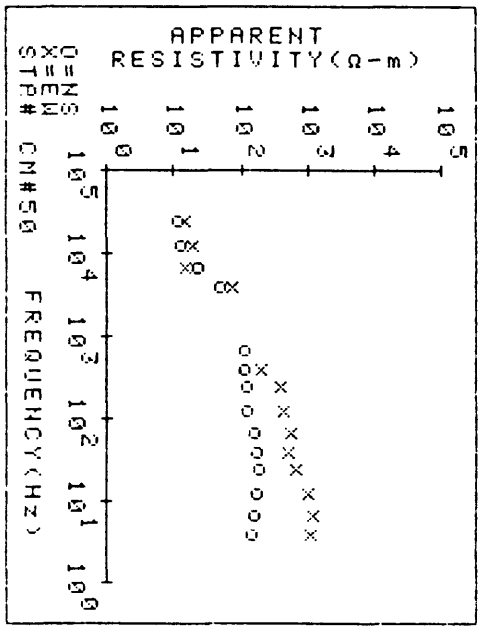

PROJECT=RAHA

STA. ID_CM#51 NS NO FREQ= 13

FREQ	AP-RES	N OBS	STD ERR
4.5	4899.60	4	929.82
7.5	2901.40	5	131.64
14.0	2803.70	4	259.86
27.0	1823.40	7	77.96
75.0	860.00	7	15.49
140.0	400.00	6	11.55
270.0	280.60	6	58.54
450.0	246.22	4	56.96
750.0	220.00	7	15.70
4500.0	70.98	3	11.83
7500.0	51.90	4	1.03
14000.0	31.20	3	3.66
27000.0	23.02	3	2.41

STA ID_CM#51 EW NO FREQ= 13

FREQ	AP-RES	N OBS	STD ERR
4.5	165.75	2	35.20
7.5	170.26	8	17.15
14.0	154.28	8	7.78
27.0	70.23	7	9.17
45.0	65.59	8	3.60
75.0	59.86	8	5.86
140.0	44.33	9	2.40
270.0	40.23	8	2.94
450.0	28.80	4	2.93
4500.0	63.93	3	9.86
7500.0	20.71	5	1.22
14000.0	15.01	6	.78
27000.0	9.73	6	.97

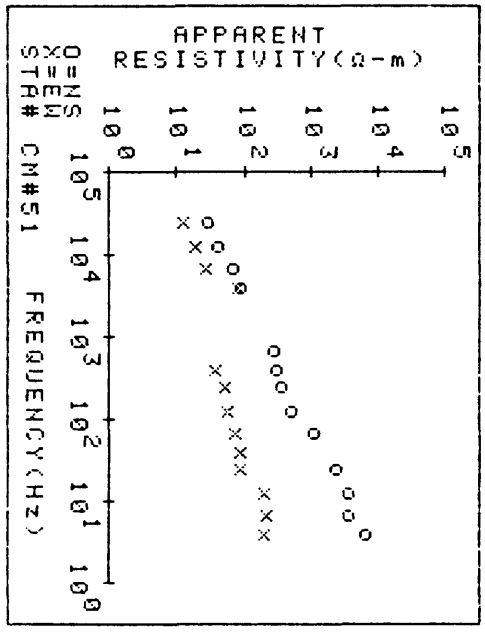

PROJECT=RAHA

STA ID_CM 60 NS NO FREQ= 12

FREQ	AP-RES	N OBS	STD ERR
14.0	344.57	3	65.21
27.0	517.75	3	65.21
45.0	555.16	5	179.11
75.0	319.38	5	45.81
140.0	329.76	4	35.56
270.0	377.82	4	30.59
450.0	433.58	5	81.35
750.0	292.51	3	68.54
4500.0	339.22	3	18.85
7500.0	149.29	4	15.28
14000.0	175.80	3	1.71
27000.0	205.58	7	14.77

STA ID_CM 60 EW NO FREQ= 12

FREQ	AP-RES	N OBS	STD ERR
7.5	4341.80	5	305.60
14.0	3177.60	7	199.89
27.0	1600.80	3	45.88
45.0	1076.20	7	81.54
75.0	757.22	6	24.36
140.0	694.08	6	41.86
270.0	534.60	6	61.81
450.0	283.42	5	31.51
4500.0	239.47	3	98.84
7500.0	197.90	3	7.69
14000.0	167.92	4	9.27
27000.0	304.71	7	27.07

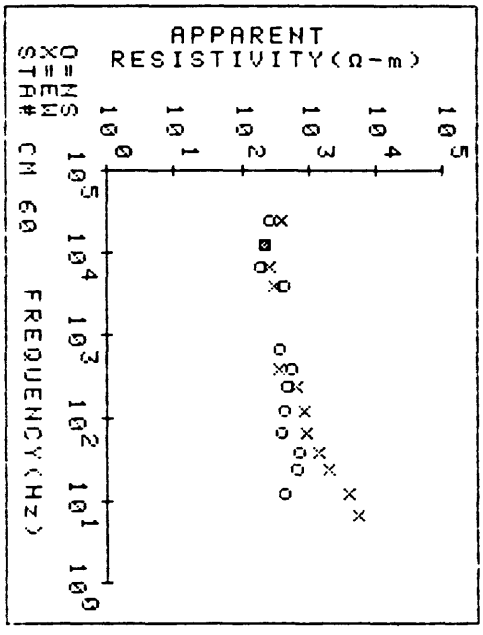

PROJECT=RAHA

STA ID_CM 61 NS NO FREQ= 6

FREQ	AP-RES	N OBS	STD ERR
14.0	6022.90	5	485.58
27.0	1222.50	4	252.77
45.0	537.70	5	85.81
75.0	1088.60	7	230.61
140.0	842.28	5	66.05
270.0	576.10	5	57.90

STA ID_CM 61 EW NO FREQ= 11

FREQ	AP-RES	N OBS	STD ERR
7.5	3775.60	6	330.65
14.0	1811.70	6	54.22
27.0	918.53	7	39.99
45.0	511.14	6	28.42
75.0	428.22	5	15.93
140.0	371.58	8	33.17
270.0	288.12	4	14.06
4500.0	102.10	4	5.44
7500.0	73.20	4	2.47
14000.0	63.98	5	2.43
27000.0	89.57	5	4.94

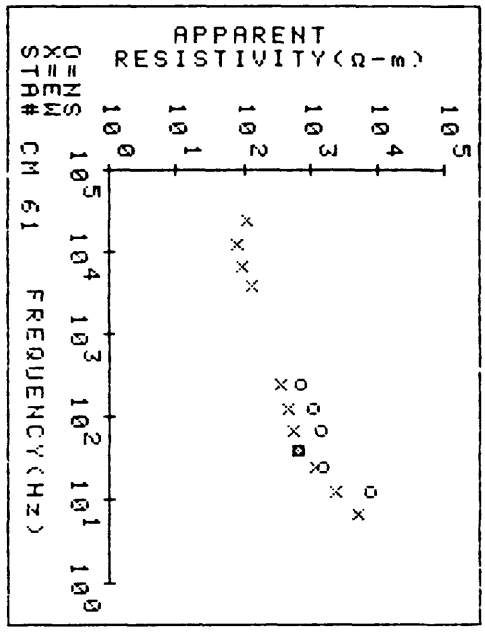

PROJECT=RAHA

STA ID_CM 63 NS NO FREQ= 12

FREQ	AP-RES	N OBS	STD ERR
7.5	5199.30	5	215.24
14.0	3650.20	5	245.39
27.0	1740.20	4	53.68
45.0	992.36	6	97.53
75.0	791.72	7	54.06
140.0	483.74	5	6.47
270.0	193.28	7	39.98
270.0	161.08	5	59.12
450.0	91.96	2	.99
4500.0	19.30	4	.41
14000.0	4.48	5	.01
27000.0	2.57	4	.26

STA. ID_CM 63 EW NO FREQ= 11

FREQ	AP-RES	N OBS	STD ERR
7.5	1066.60	6	128.77
14.0	932.72	5	44.65
27.0	345.21	6	8.17
45.0	221.10	6	9.21
75.0	182.39	6	13.87
140.0	99.18	6	4.53
270.0	90.90	4	32.60
450.0	70.40	4	.78
4500.0	15.20	4	.58
7500.0	6.19	4	.49
14000.0	8.76	4	.78

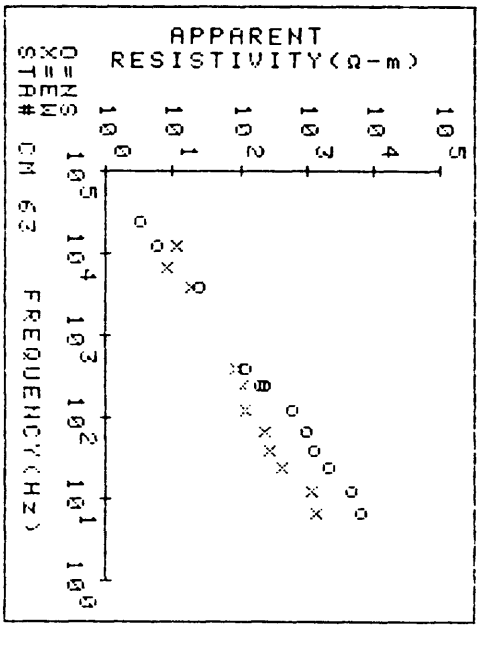

PROJECT=RAHA

STA ID_CM 64 NS NO FREQ= 11

FREQ	AP-RES	N OBS	STD ERR
27.0	9035.80	4	1366.80
45.0	4903.70	4	622.18
75.0	4522.60	3	156.00
140.0	1349.60	4	176.50
270.0	706.33	3	191.85
450.0	221.89	4	55.42
750.0	88.00	3	.57
4500.0	83.08	4	4.23
7500.0	23.33	5	3.04
14000.0	5.06	5	1.61
27000.0	4.65	3	.27

STA. ID_CM 64 EW NO FREQ= 12

FREQ	AP-RES	N OBS	STD ERR
7.5	3905.70	3	815.40
14.0	1572.20	3	149.26
27.0	345.02	6	12.42
45.0	219.49	4	8.95
75.0	183.68	5	12.25
140.0	144.04	3	6.59
270.0	43.73	4	5.97
450.0	47.62	4	2.40
4500.0	8.12	4	3.69
7500.0	5.58	3	1.18
14000.0	3.29	4	1.59
27000.0	6.10	4	1.17

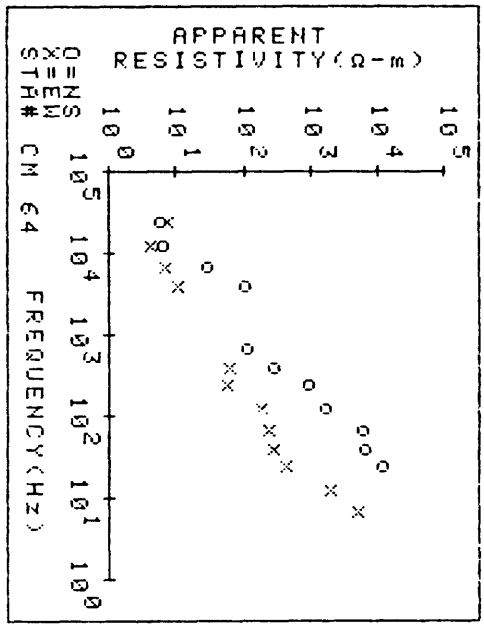

PROJECT=RAHA

STA. ID_CM 65 NS NO FREQ= 9

FREQ	AP-RES	N OBS	STD ERR
14.0	22511.00	6	1123.40
27.0	15404.00	4	428.45
45.0	8206.50	6	543.96
75.0	7012.00	6	639.82
140.0	6016.60	9	287.85
270.0	5785.20	6	313.00
450.0	5000.00	4	178.15
7500.0	753.12	3	14.00
14000.0	267.80	5	.34

STA. ID_CM 65 EW NO FREQ= 8

FREQ	AP-RES	N OBS	STD ERR
7.5	2340.60	7	152.54
14.0	1333.90	7	132.23
27.0	772.56	5	55.16
45.0	839.25	5	136.54
75.0	632.70	5	21.71
140.0	874.40	4	114.41
270.0	430.88	3	7.70
450.0	354.00	3	5.60

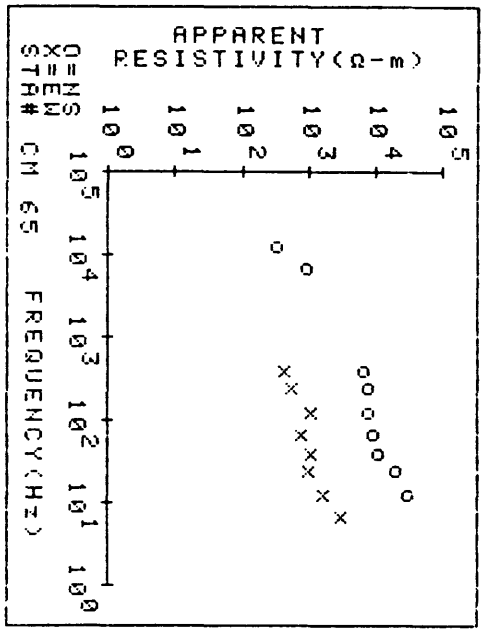

PROJECT=RAHA

STA ID_CM 66 NS NO FREQ= 8

FREQ	AP-RES	N OBS	STD ERR
7.5	16815.00	3	3529.20
14.0	11582.00	4	431.89
27.0	3070.60	3	582.77
45.0	3060.60	5	432.00
75.0	2037.80	7	239.82
140.0	1608.90	10	92.57
270.0	1600.00	3	34.00
14000.0	42.70	4	.63

STA. ID_CM 66 EW NO FREQ= 9

FREQ	AP-RES	N OBS	STD ERR
7.5	2773.30	4	139.62
14.0	1522.70	7	89.59
27.0	782.41	6	90.20
45.0	469.79	4	21.60
75.0	369.80	5	25.50
140.0	256.82	5	42.37
270.0	157.31	5	15.60
14000.0	40.70	5	12.00
27000.0	37.70	3	5.70

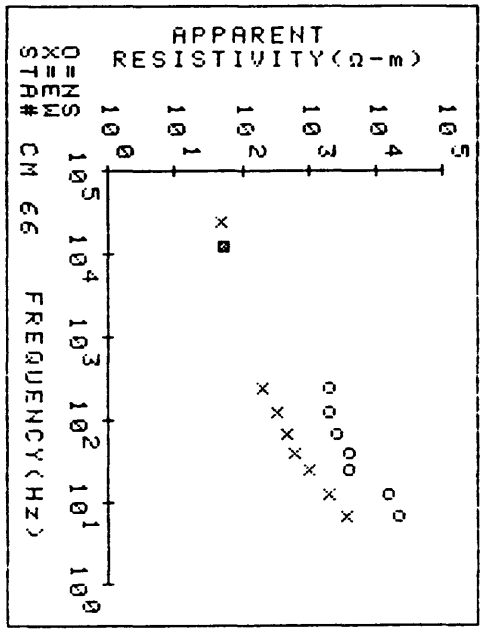

PROJECT=RAHA

STA. ID_CM 67 NS NO FREQ= 8

FREQ	AP-RES	N OBS	STD ERR
14.0	1476.90	6	181.42
27.0	947.07	4	138.25
45.0	758.40	4	81.30
75.0	725.71	4	64.99
140.0	685.82	6	99.80
270.0	709.98	7	67.52
450.0	1013.60	4	203.54
14000.0	.43	5	.01

STA ID_CM 67 EW NO FREQ= 7

FREQ	AP-RES	N OBS	STD ERR
7.5	8455.80	4	472.69
14.0	3446.20	4	143.08
27.0	1779.20	4	20.26
45.0	1089.10	7	71.03
75.0	849.85	4	26.62
140.0	557.52	6	100.12
270.0	331.80	4	24.60

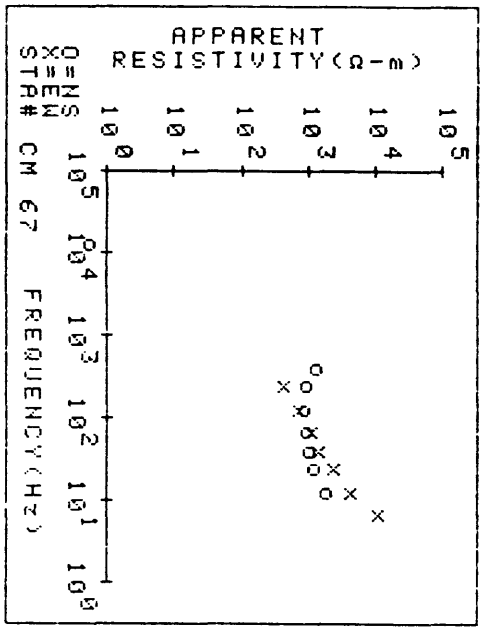

PROJECT=RAHA

STA. ID_CM 68 NS NO FREQ= 12

FREQ	AP-RES	N OBS	STD ERR
7.5	8612.40	2	474.41
14.0	4838.00	4	2957.70
27.0	4509.00	3	115.00
45.0	3550.80	5	17.00
75.0	745.22	5	43.86
140.0	616.57	7	91.47
270.0	197.22	6	48.32
450.0	122.04	4	8.93
4500.0	13.07	5	25.00
7500.0	7.81	3	13.00
14000.0	5.30	6	1.20
27000.0	4.69	2	.10

STA. ID_CM 68 EW NO FREQ= 5

FREQ	AP-RES	N OBS	STD ERR
14.0	1053.50	6	62.97
27.0	566.17	7	34.42
45.0	321.47	7	16.22
75.0	192.08	4	19.34
140.0	56.00	3	1.00

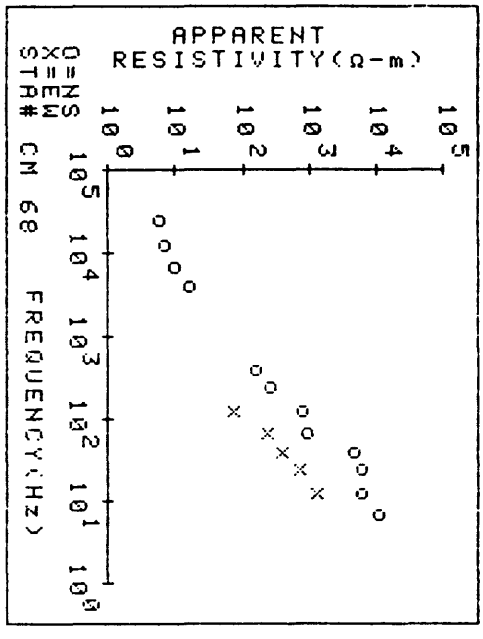

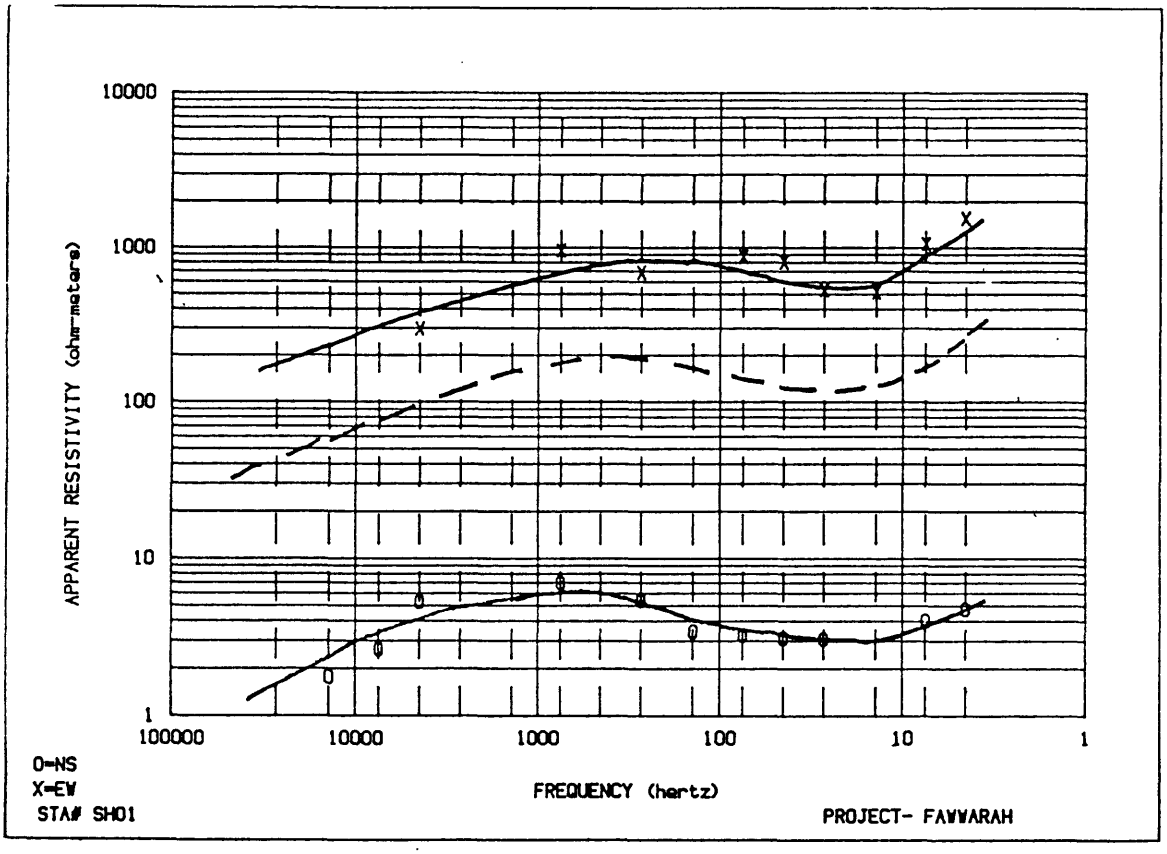
10000
1000
100
10
1
APPARENT RESISTIVITY (ohm-meters)
100000
10000
1000
100
10
1
O=NS
X=EW
STA# SH01
FREQUENCY (hertz)
PROJECT- FAWWARAH

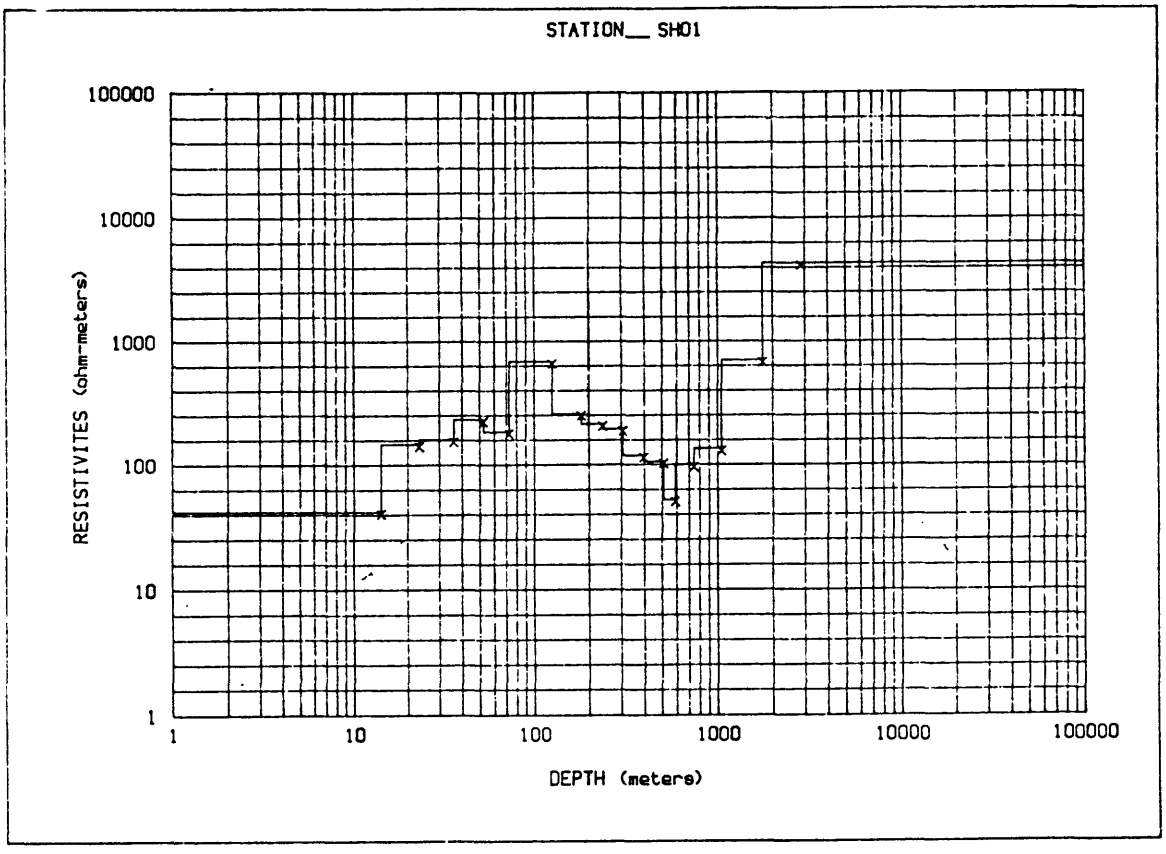
STATION__ SH01
100000
10000
1000
100
10
1
RESISTIVITES (ohm-meters)
1
10
100
1000
10000
100000
DEPTH (meters)

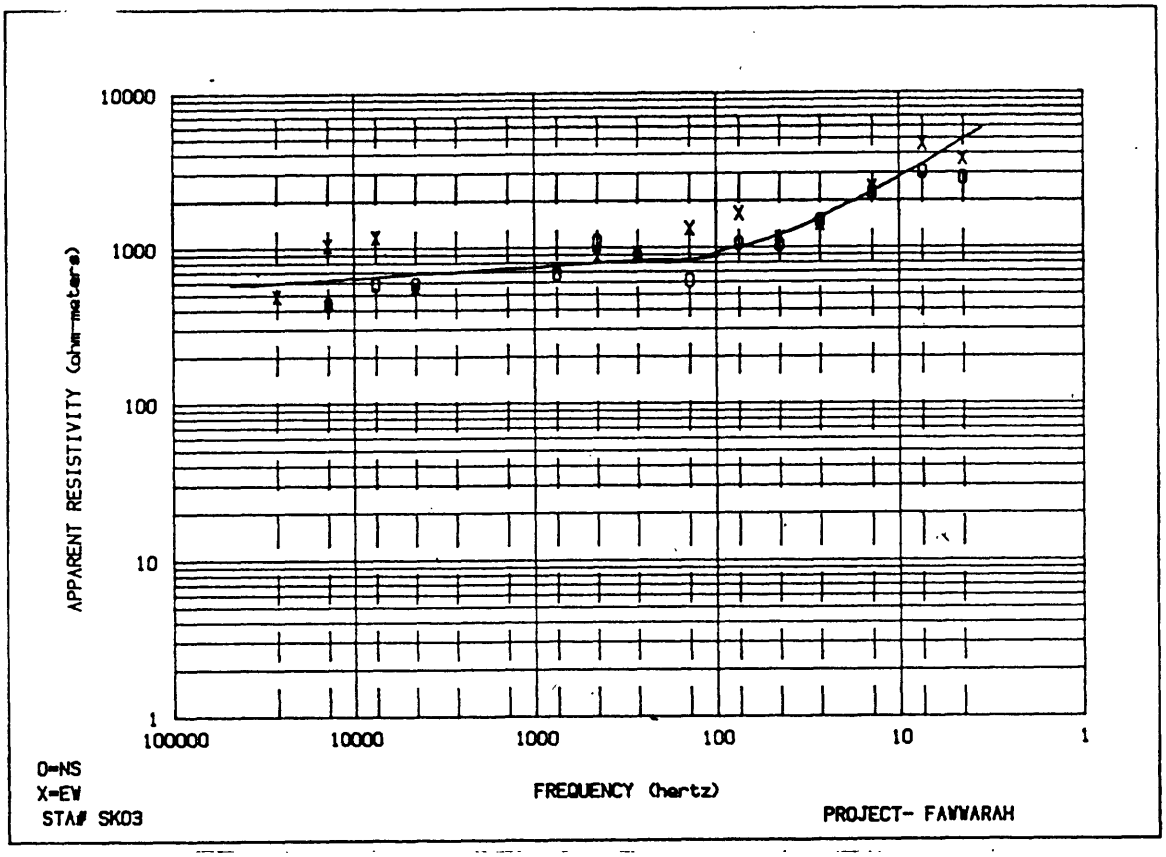
10000
1000
100
10
1
APPARENT RESISTIVITY (ohm-meters)
100000
10000
1000
100
10
1
FREQUENCY (hertz)
O=NS
X=EW
STA# SK03
PROJECT- FAWWARAH

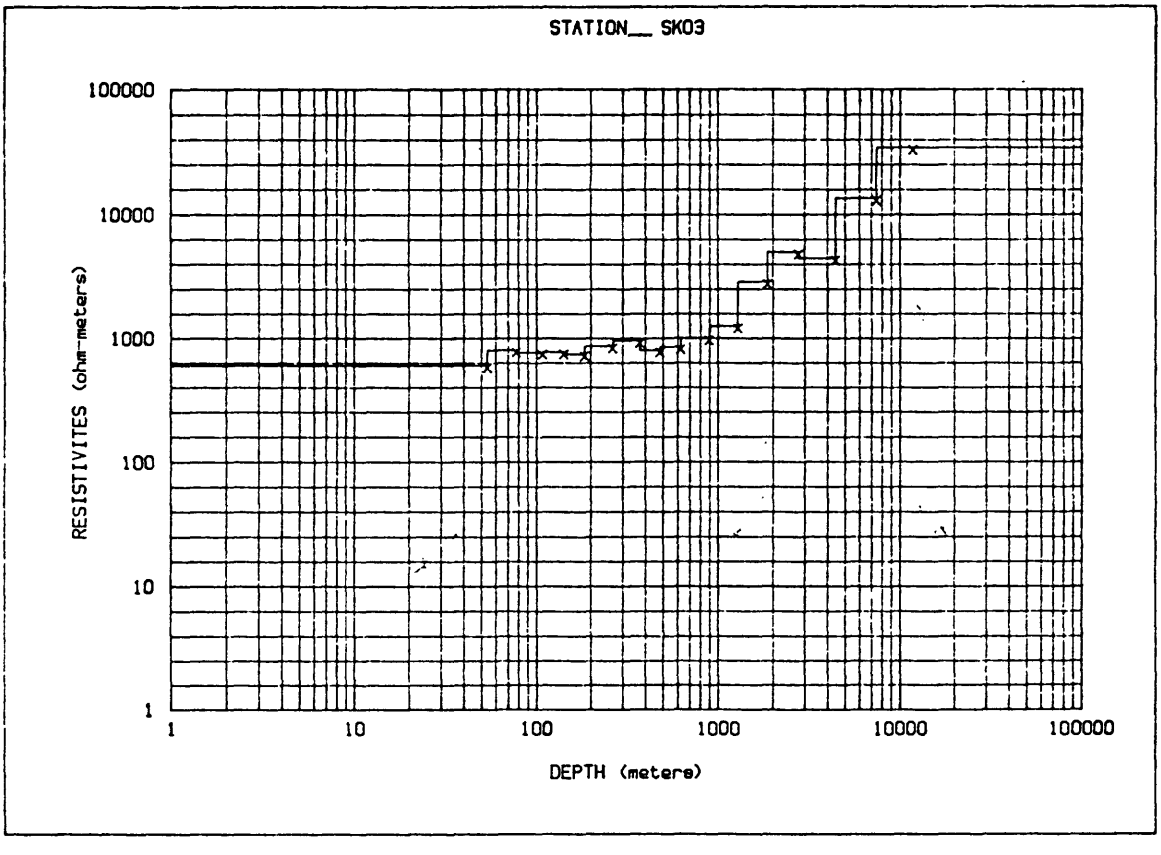
STATION__ SK03
100000
10000
1000
100
10
1
RESISTIVITES (ohm-meters)
1
10
100
1000
10000
100000
DEPTH (meters)

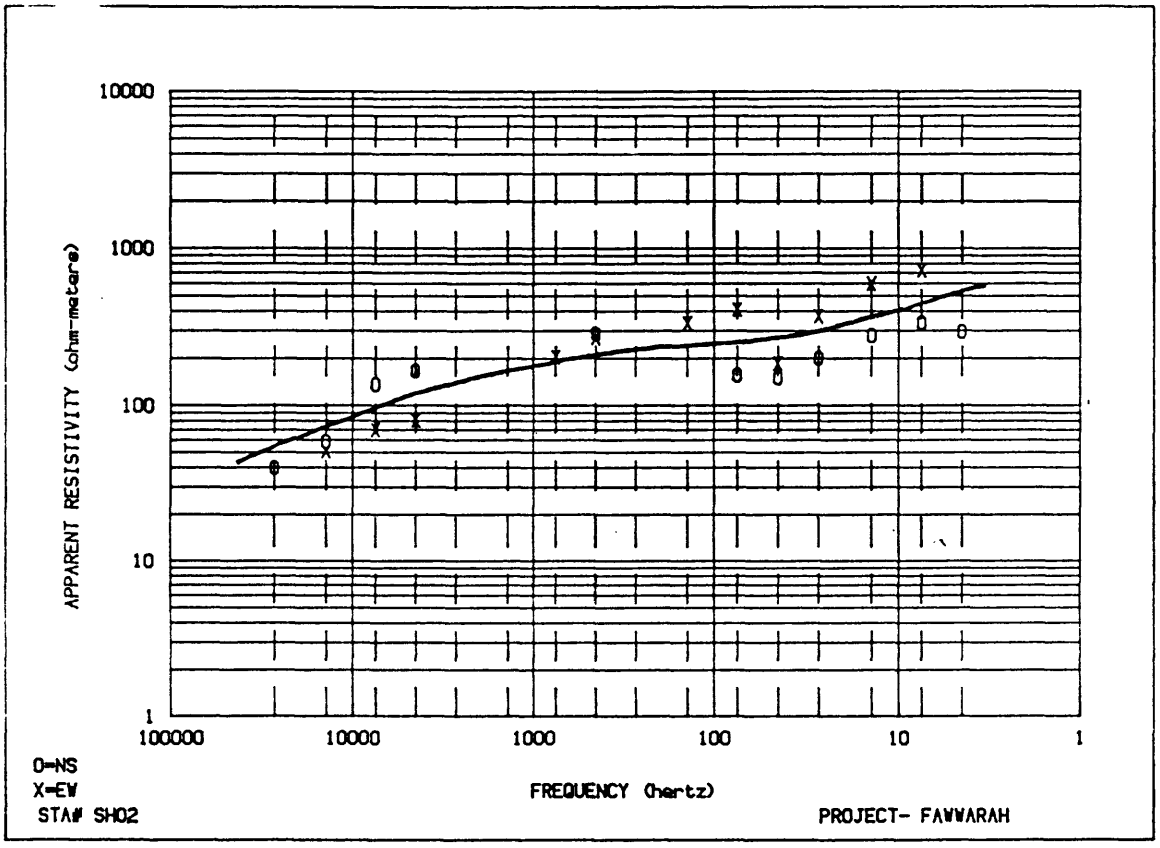
10000
1000
100
10
1
APPARENT RESISTIVITY (ohm-meters)
100000
10000
1000
100
10
1
FREQUENCY (hertz)
O=NS
X=EW
STA# SH02
PROJECT- FAWWARAH

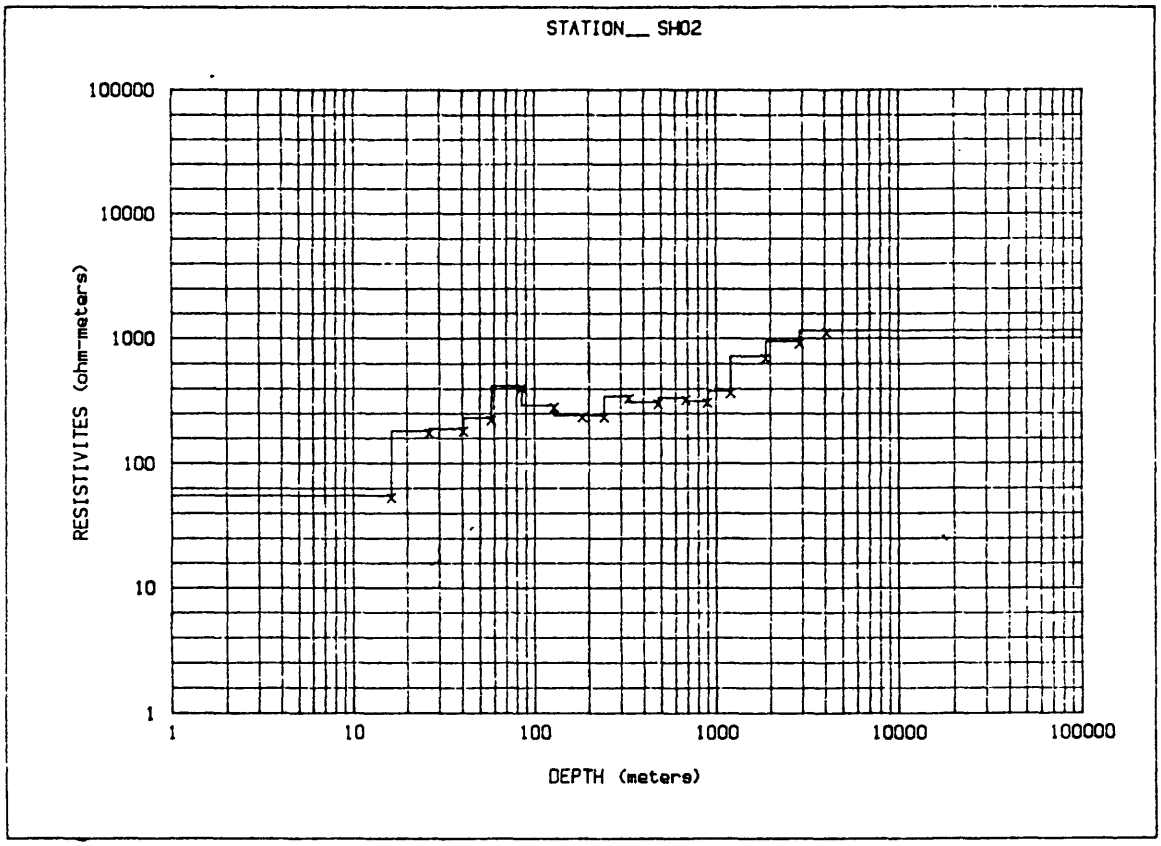
STATION__ SH02
100000
10000
1000
100
10
1
RESISTIVITES (ohm-meters)
1
10
100
1000
10000
100000
DEPTH (meters)

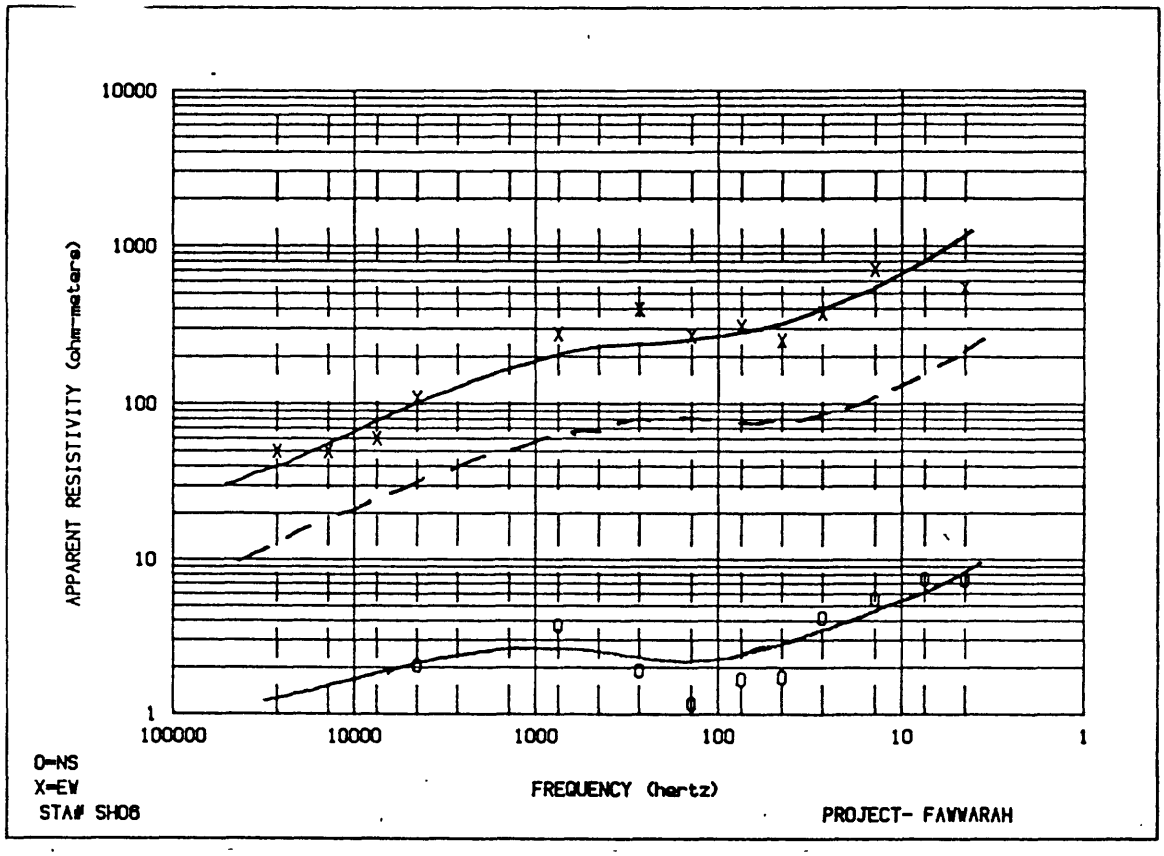
10000
1000
100
10
1
APPARENT RESISTIVITY (ohm-meters)
100000
10000
1000
100
10
1
FREQUENCY (hertz)
O=NS
X=EW
STA# SH06
PROJECT- FAWWARAH

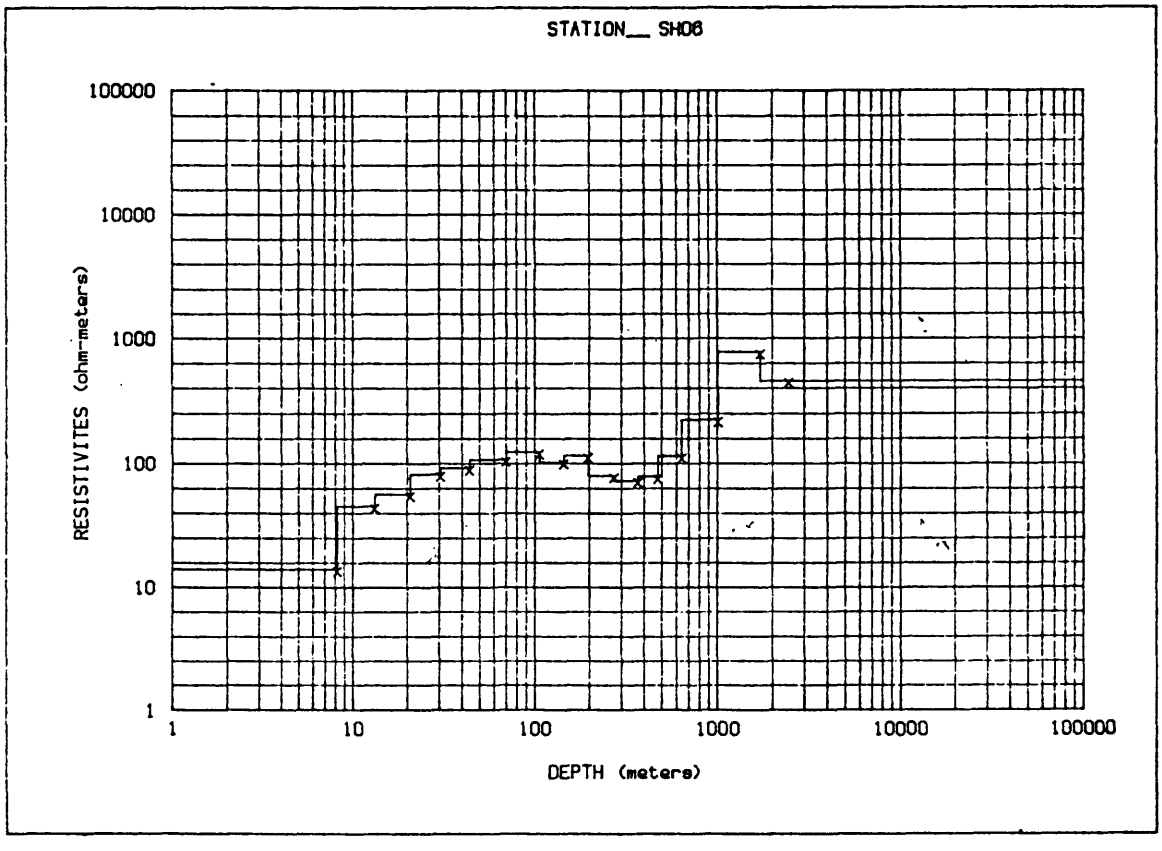
STATION__ SH06
100000
10000
1000
100
10
1
RESISTIVITES (ohm-meters)
1
10
100
1000
10000
100000
DEPTH (meters)

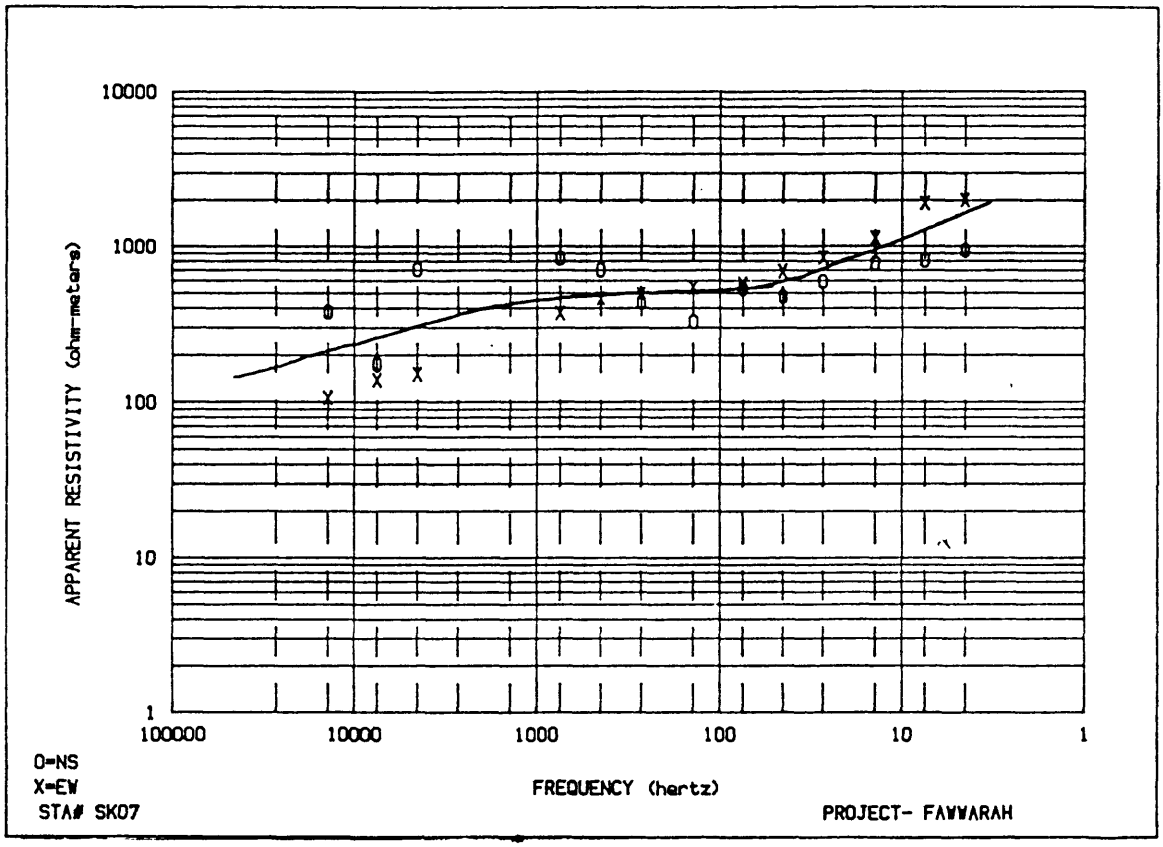
10000
1000
100
10
1
APPARENT RESISTIVITY (ohm-meters)
100000
10000
1000
100
10
1
FREQUENCY (hertz)
O=NS
X=EW
STA# SK07
PROJECT- FAWWARAH

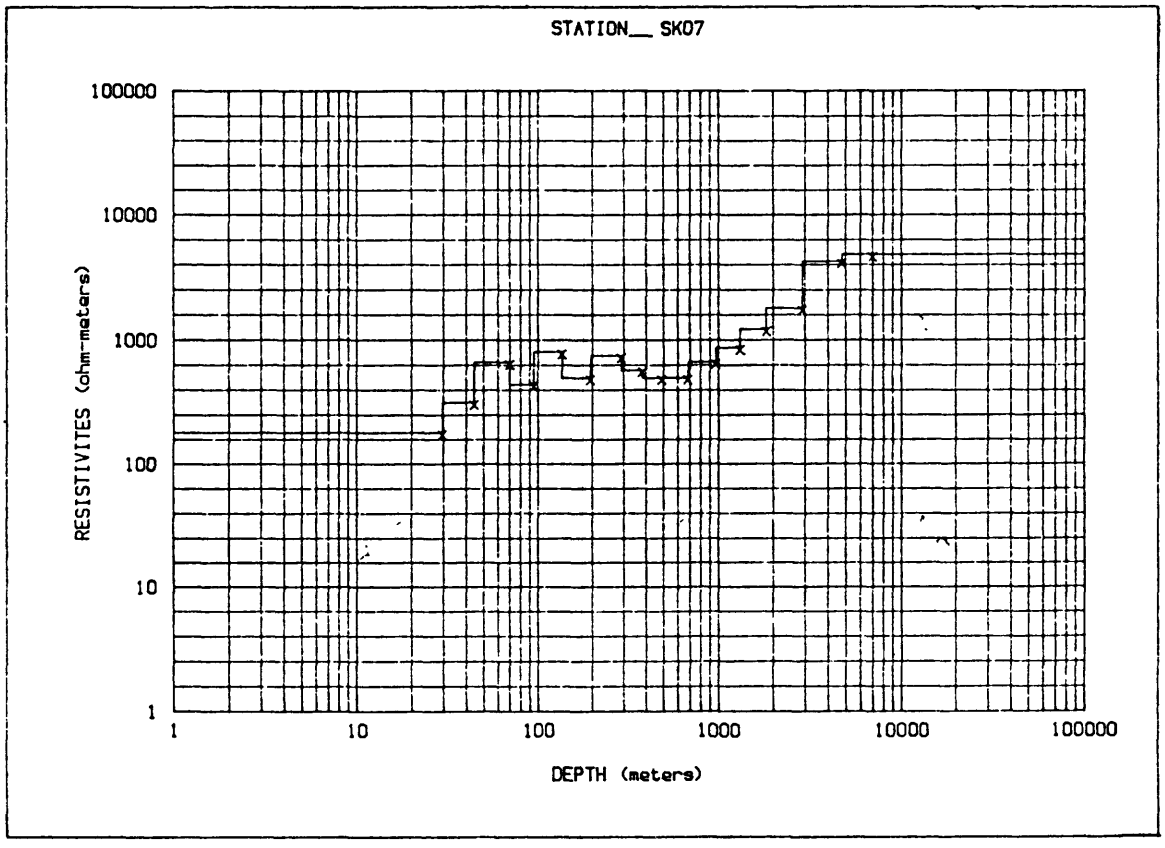
STATION__ SK07
100000
10000
1000
100
10
1
RESISTIVITES (ohm-meters)
1
10
100
1000
10000
100000
DEPTH (meters)

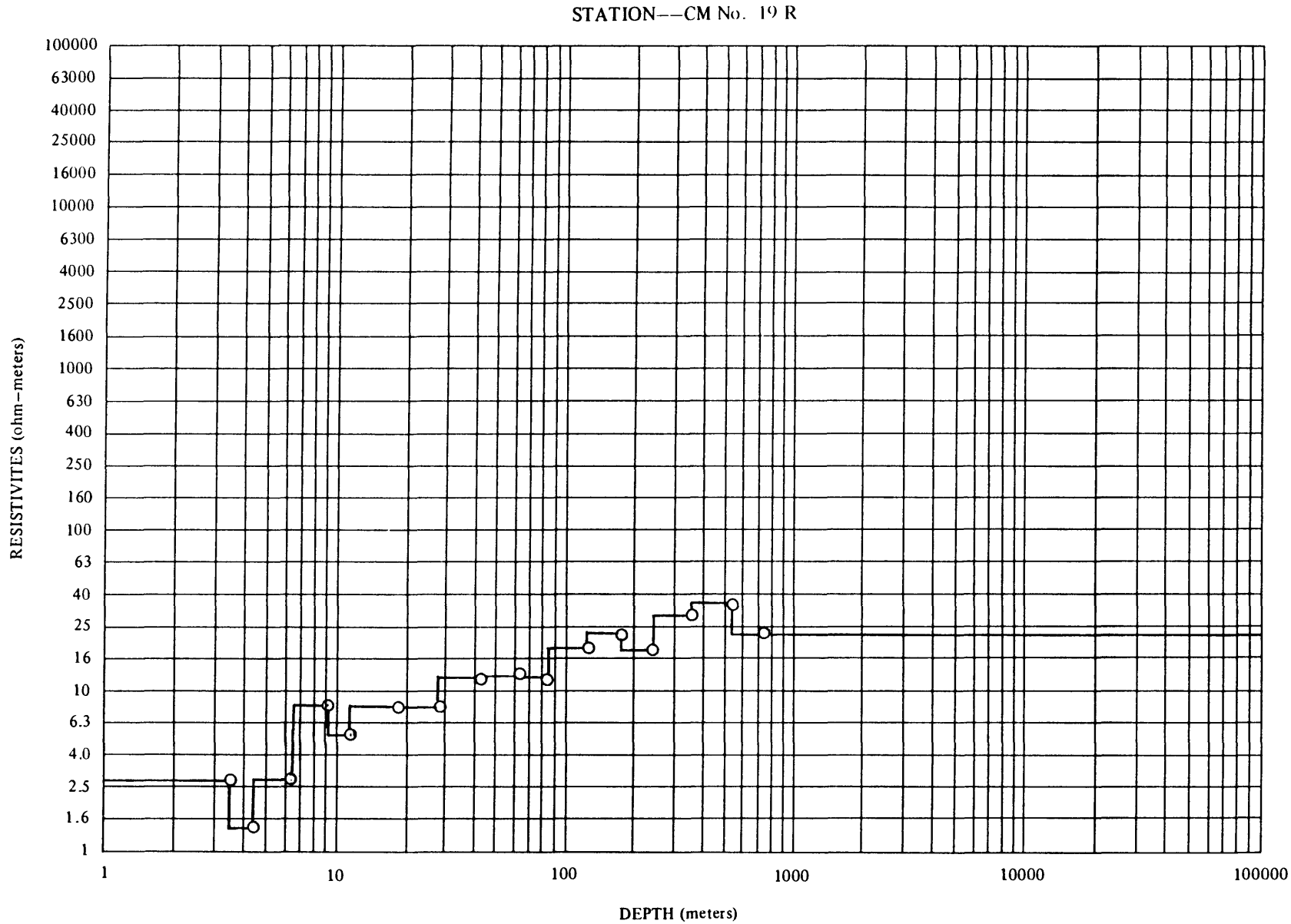
STATION--CM No. 19 R
RESISTIVITES (ohm-meters)
100000
63000
40000
25000
16000
10000
6300
4000
2500
1600
1000
630
400
250
160
100
63
40
25
16
10
6.3
4.0
2.5
1.6
1
1
10
100
1000
10000
100000
DEPTH (meters)

STATION—CM No 22

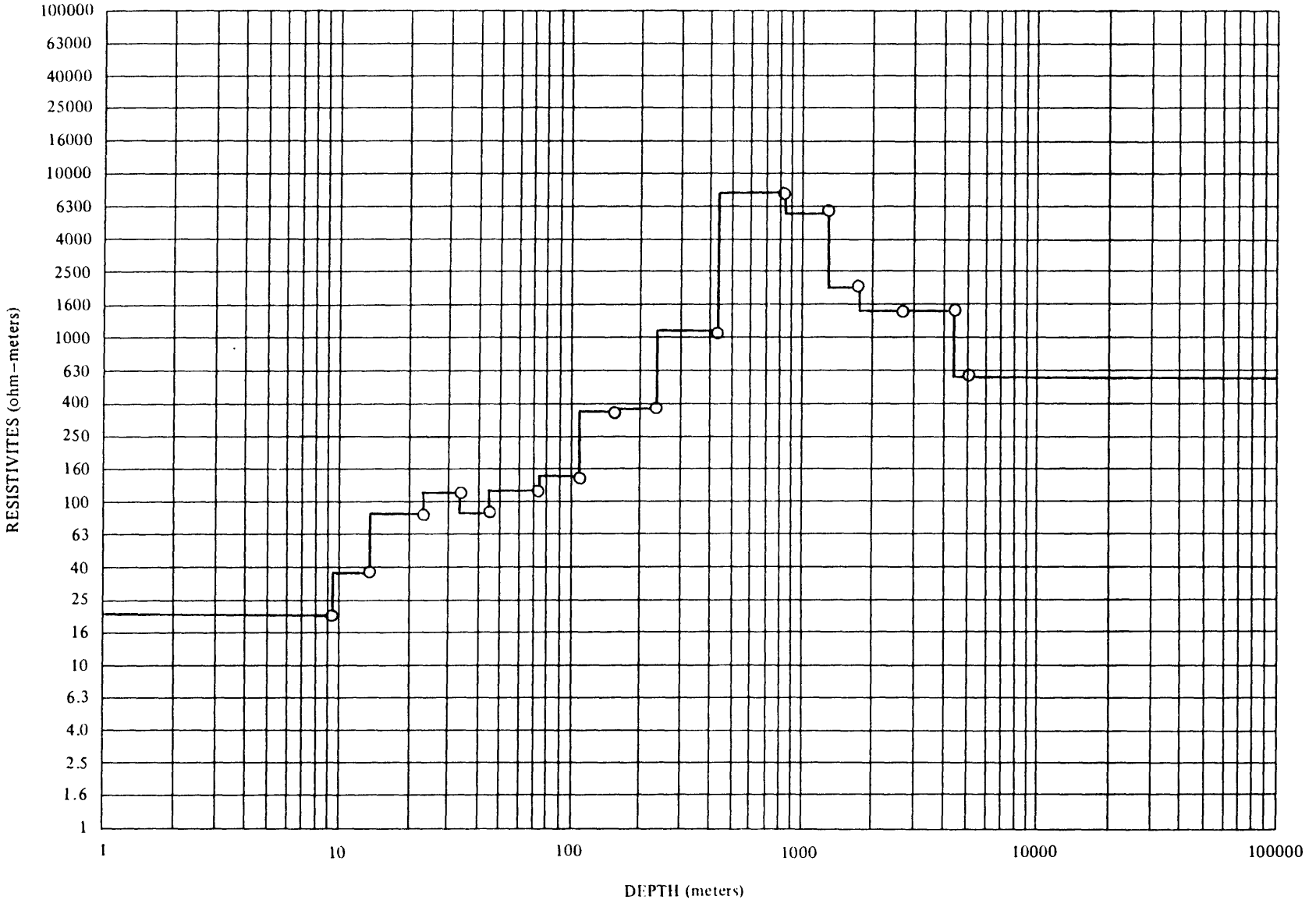

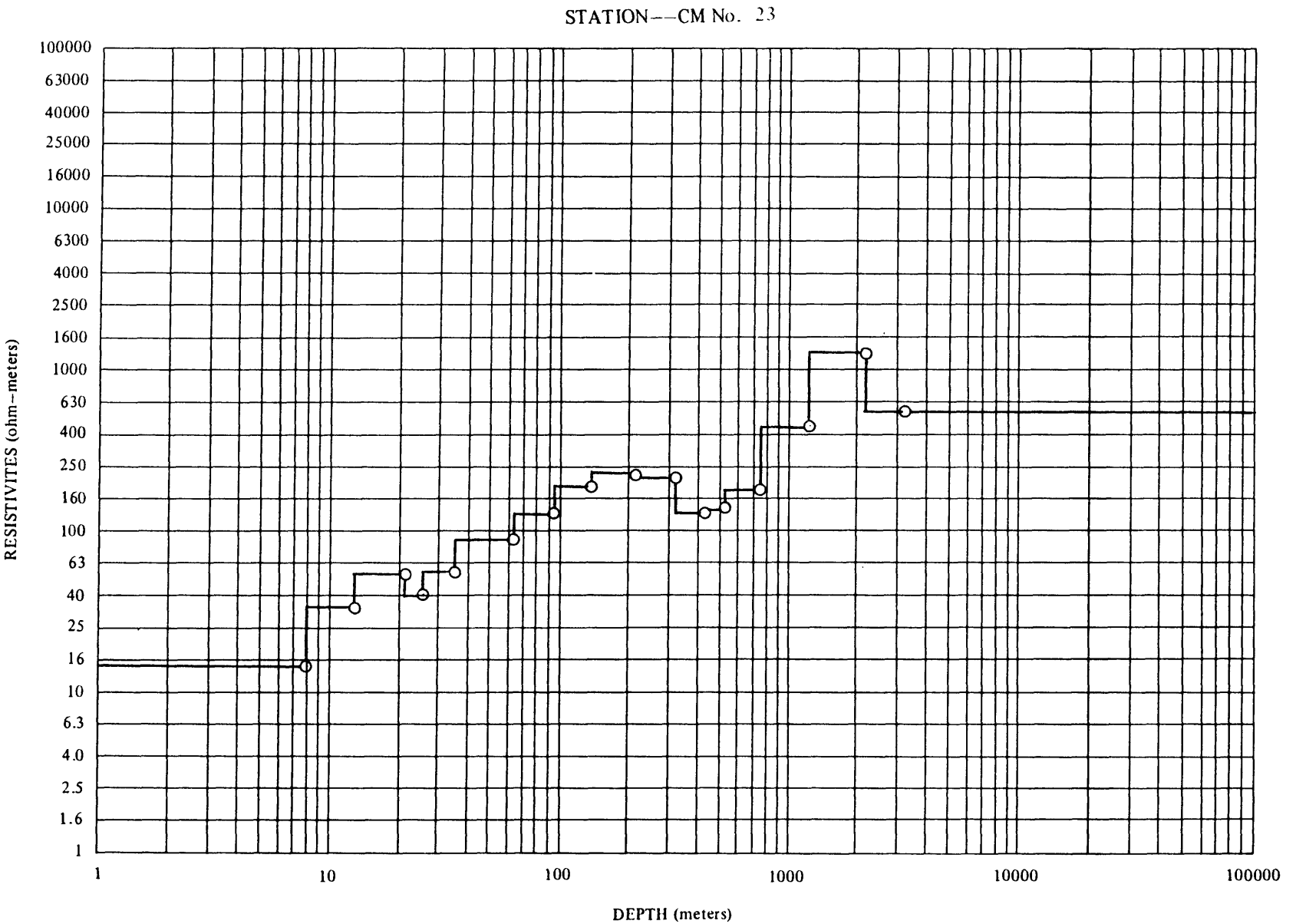
STATION--CM No. 23
RESISTIVITES (ohm-meters)
100000
63000
40000
25000
16000
10000
6300
4000
2500
1600
1000
630
400
250
160
100
63
40
25
16
10
6.3
4.0
2.5
1.6
1
1
10
100
1000
10000
100000
DEPTH (meters)

STATION--CM No. 24

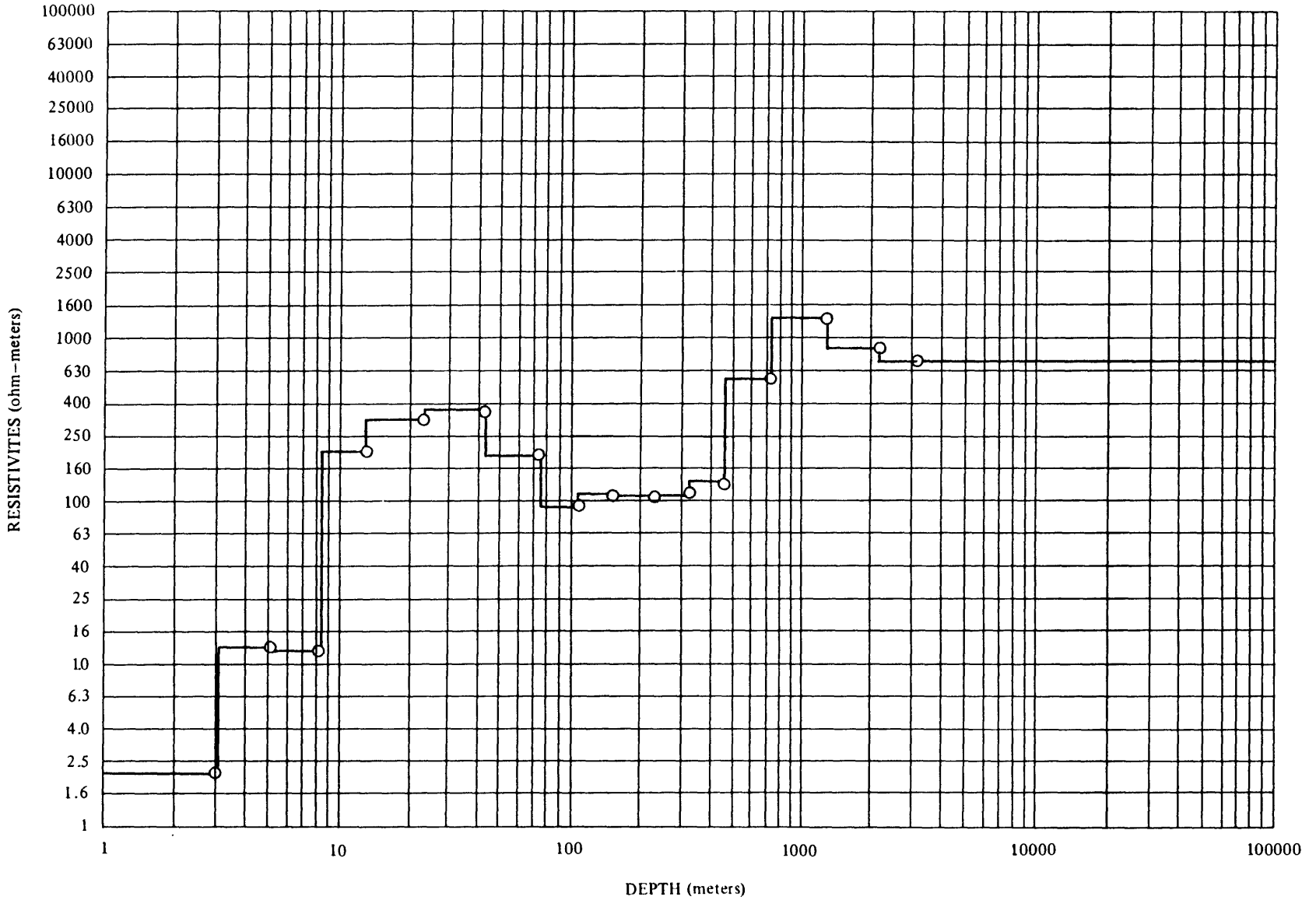

STATION—CM No. 29

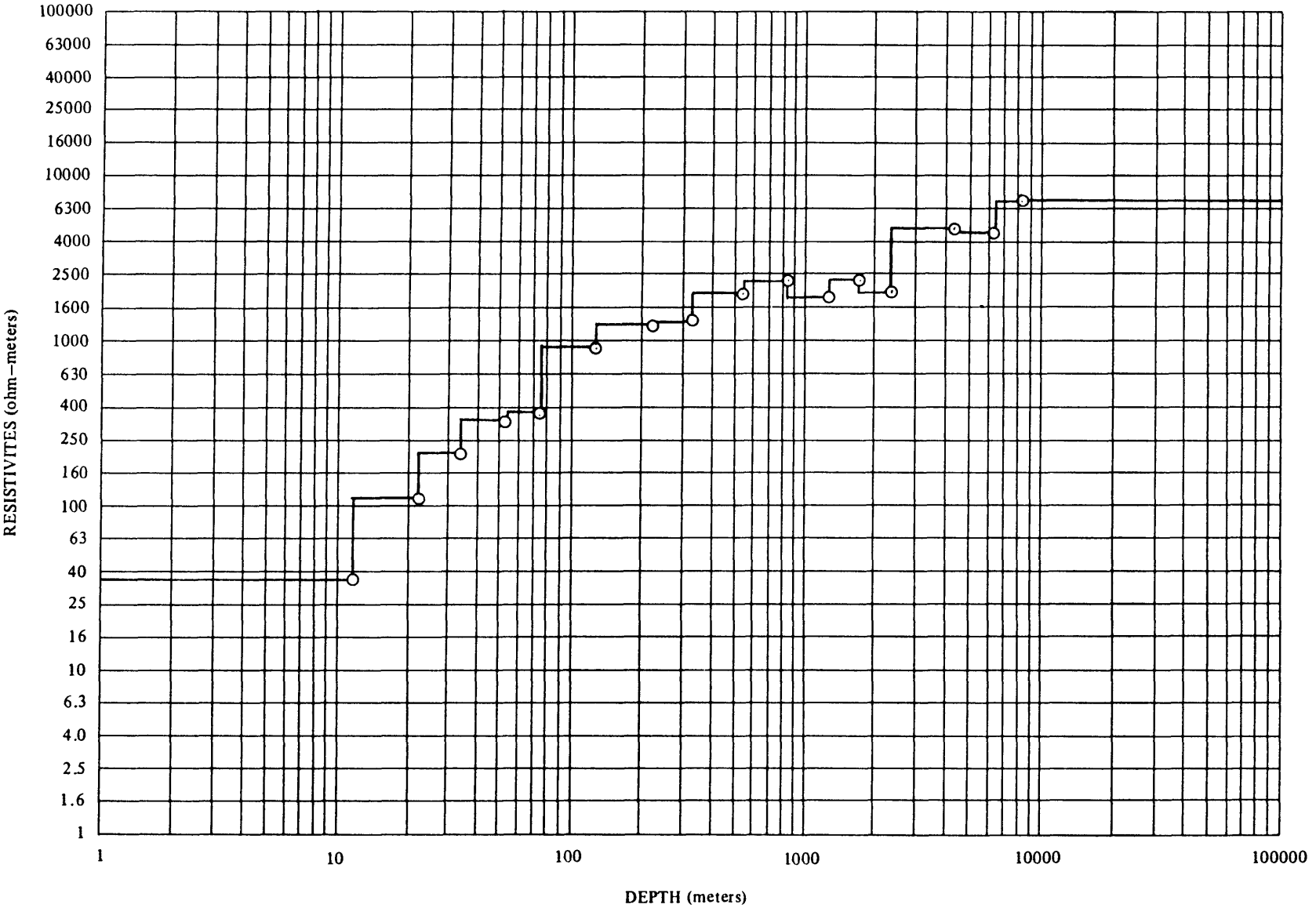

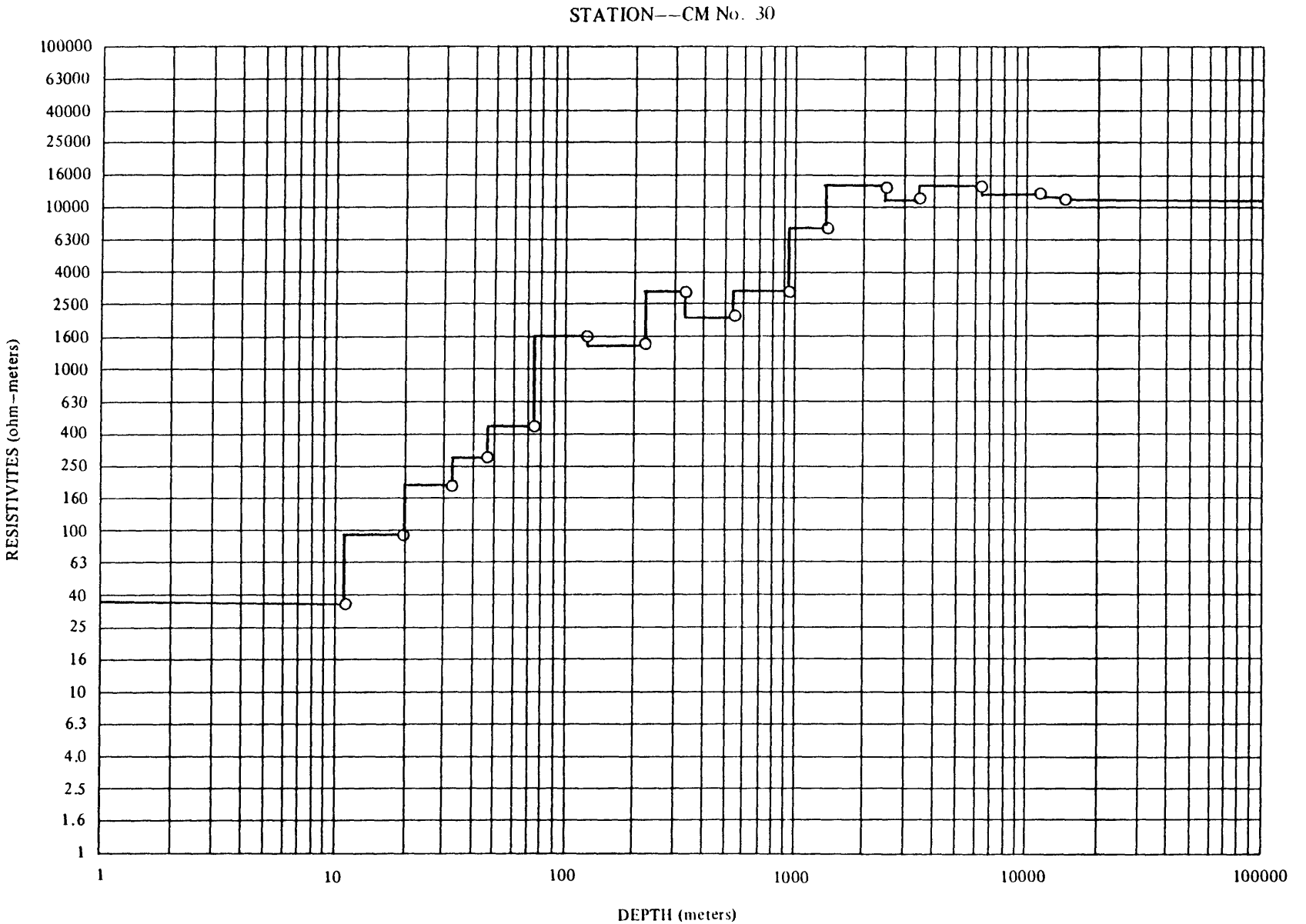
STATION--CM No. 30
RESISTIVITES (ohm-meters)
100000
63000
40000
25000
16000
10000
6300
4000
2500
1600
1000
630
400
250
160
100
63
40
25
16
10
6.3
4.0
2.5
1.6
1
1
10
100
1000
10000
100000
DEPTH (meters)

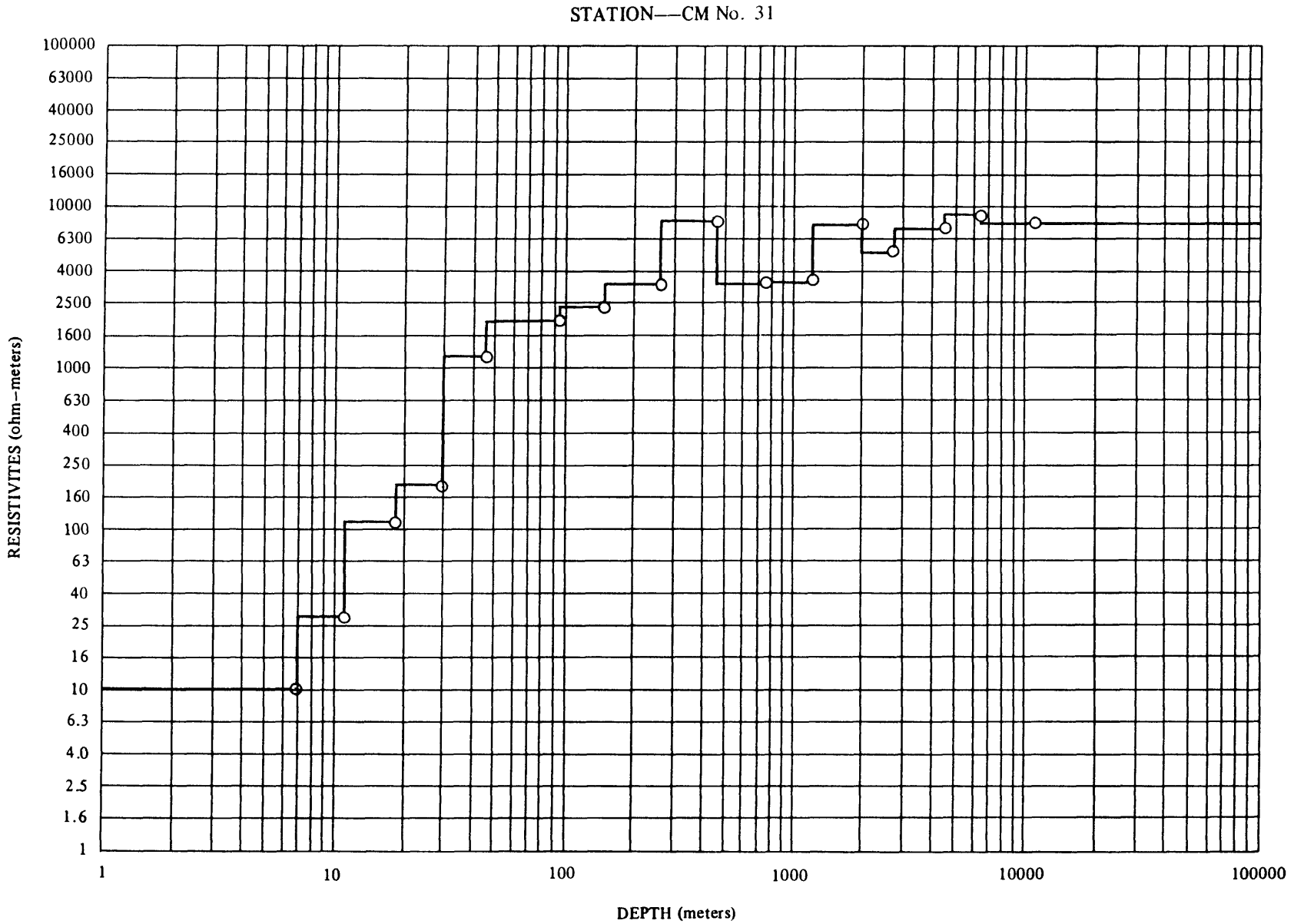
STATION—CM No. 31
RESISTIVITES (ohm-meters)
100000
63000
40000
25000
16000
10000
6300
4000
2500
1600
1000
630
400
250
160
100
63
40
25
16
10
6.3
4.0
2.5
1.6
1
1
10
100
1000
10000
100000
DEPTH (meters)

STATION---CM No 32

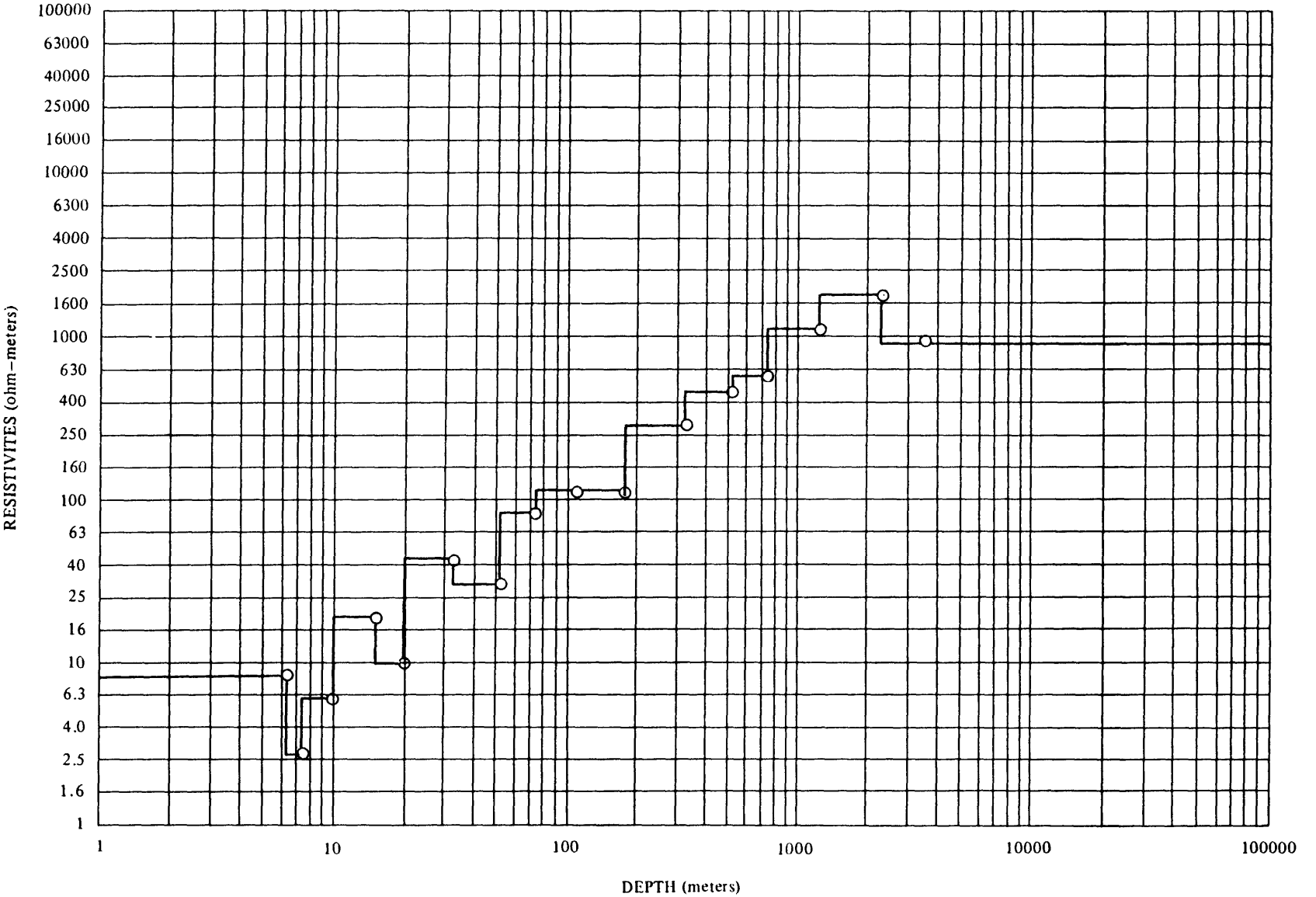

STATION—CM No. 33

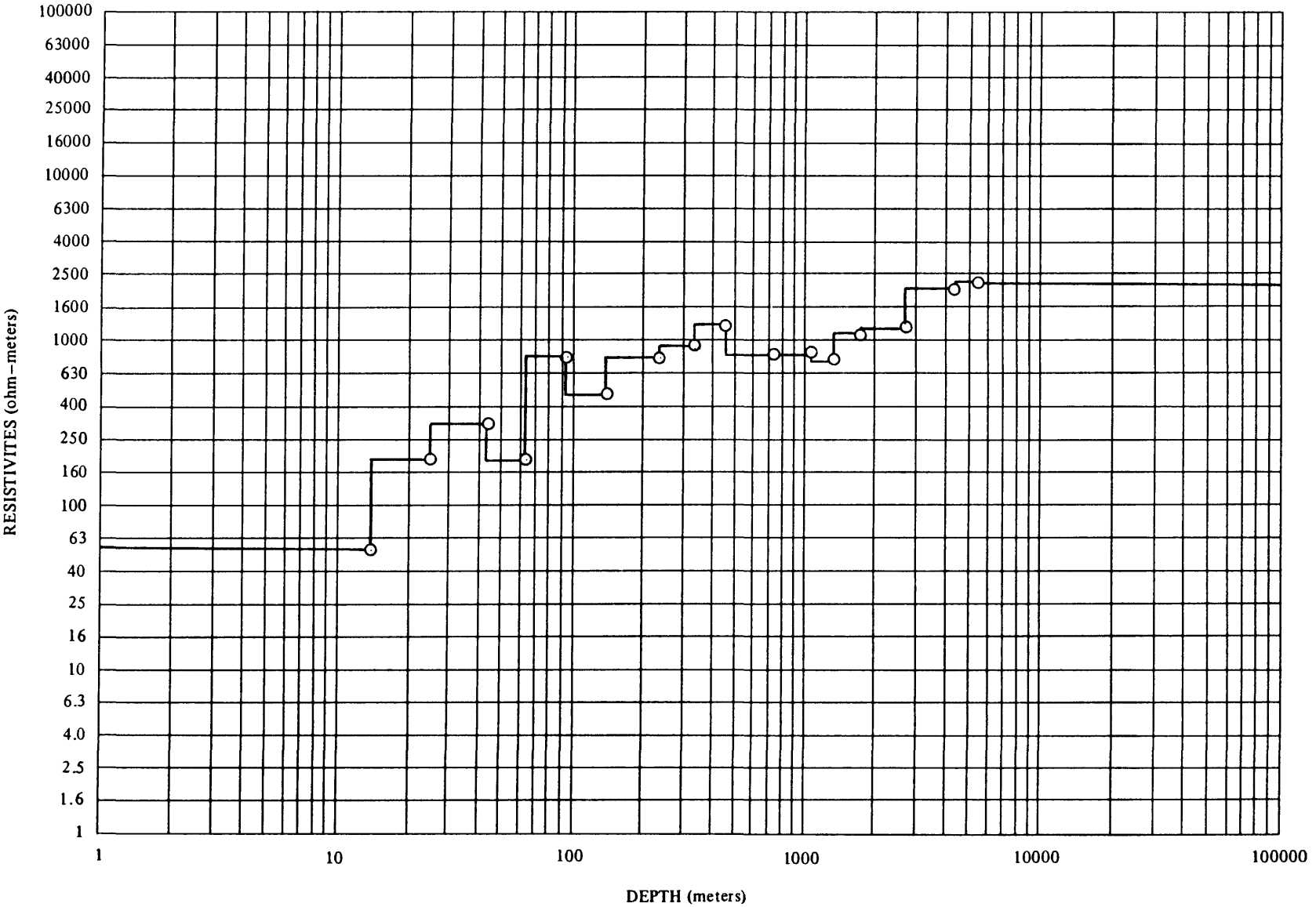

STATION---CM No. 34

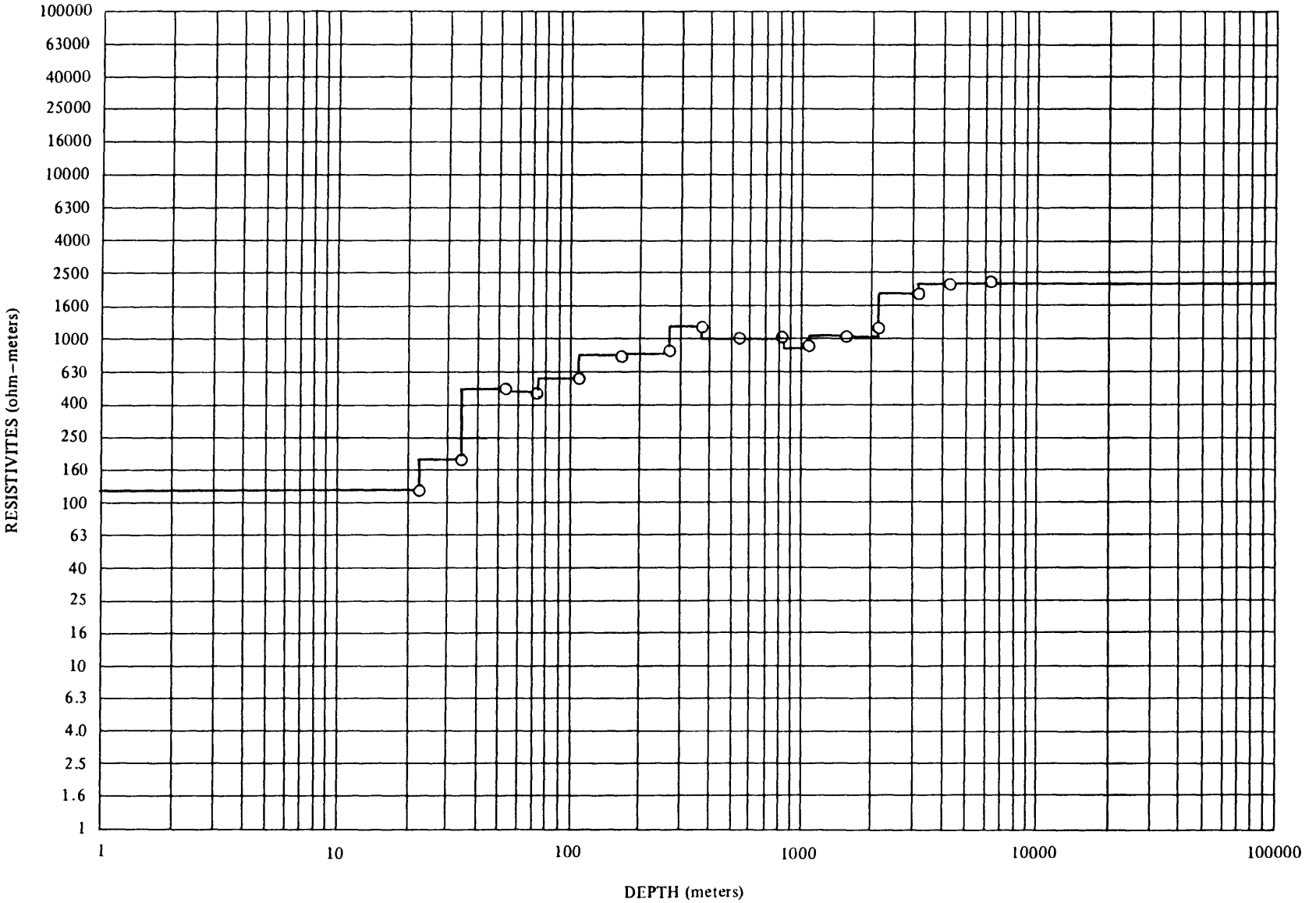

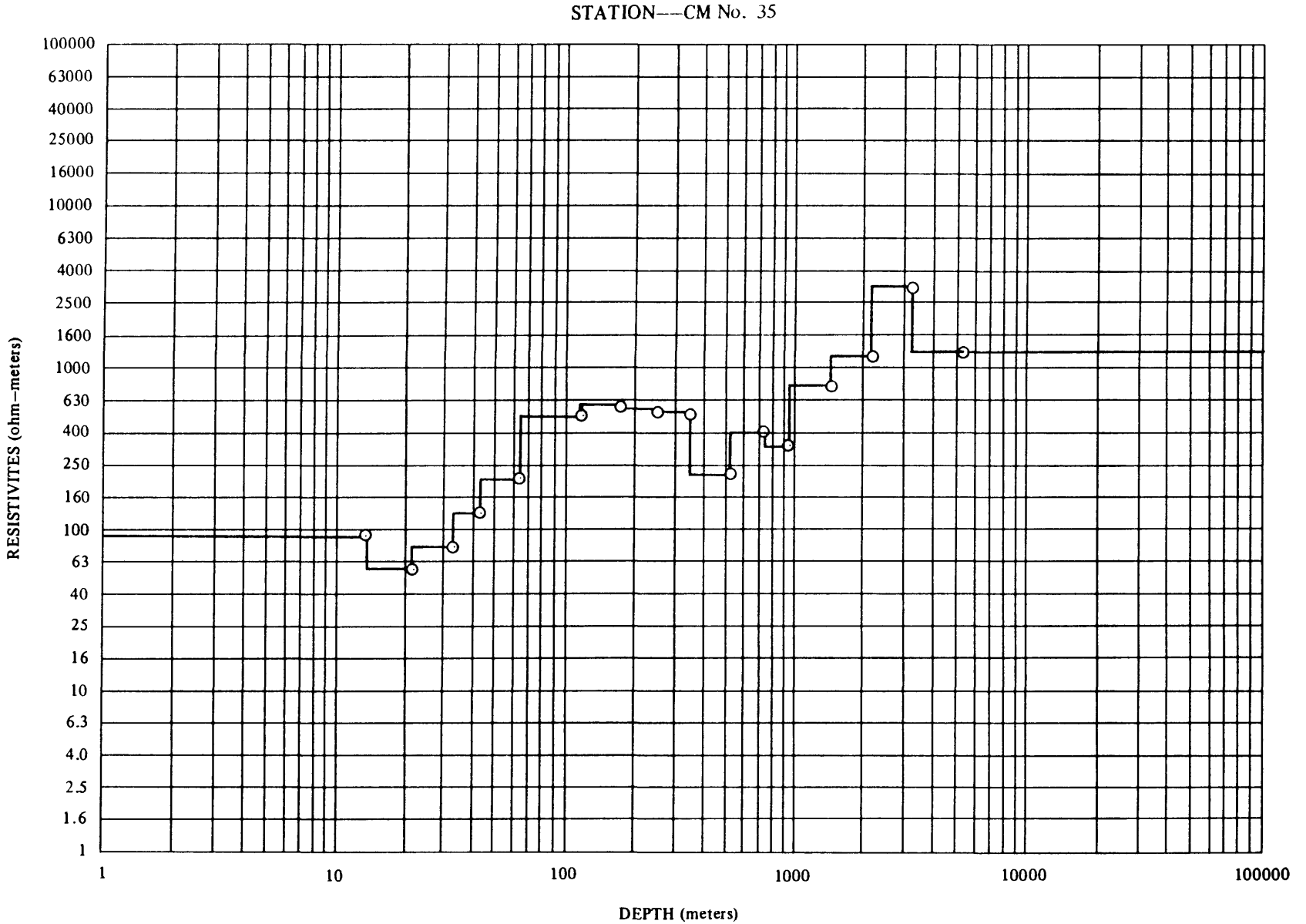
STATION---CM No. 35
RESISTIVITES (ohm-meters)
100000
63000
40000
25000
16000
10000
6300
4000
2500
1600
1000
630
400
250
160
100
63
40
25
16
10
6.3
4.0
2.5
1.6
1
1
10
100
1000
10000
100000
DEPTH (meters)

STATION---CM No. 36

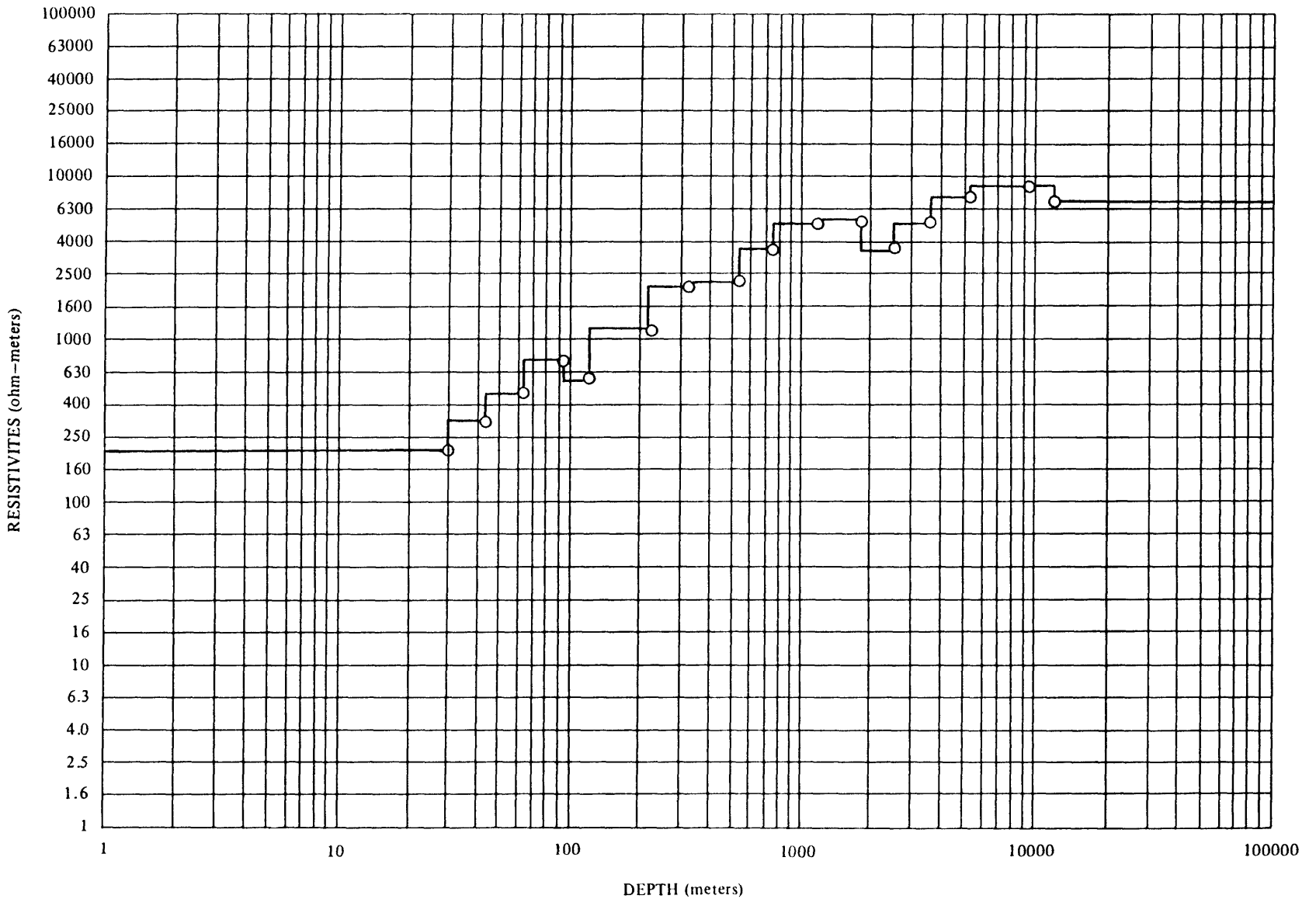

STATION—CM No. 36 A

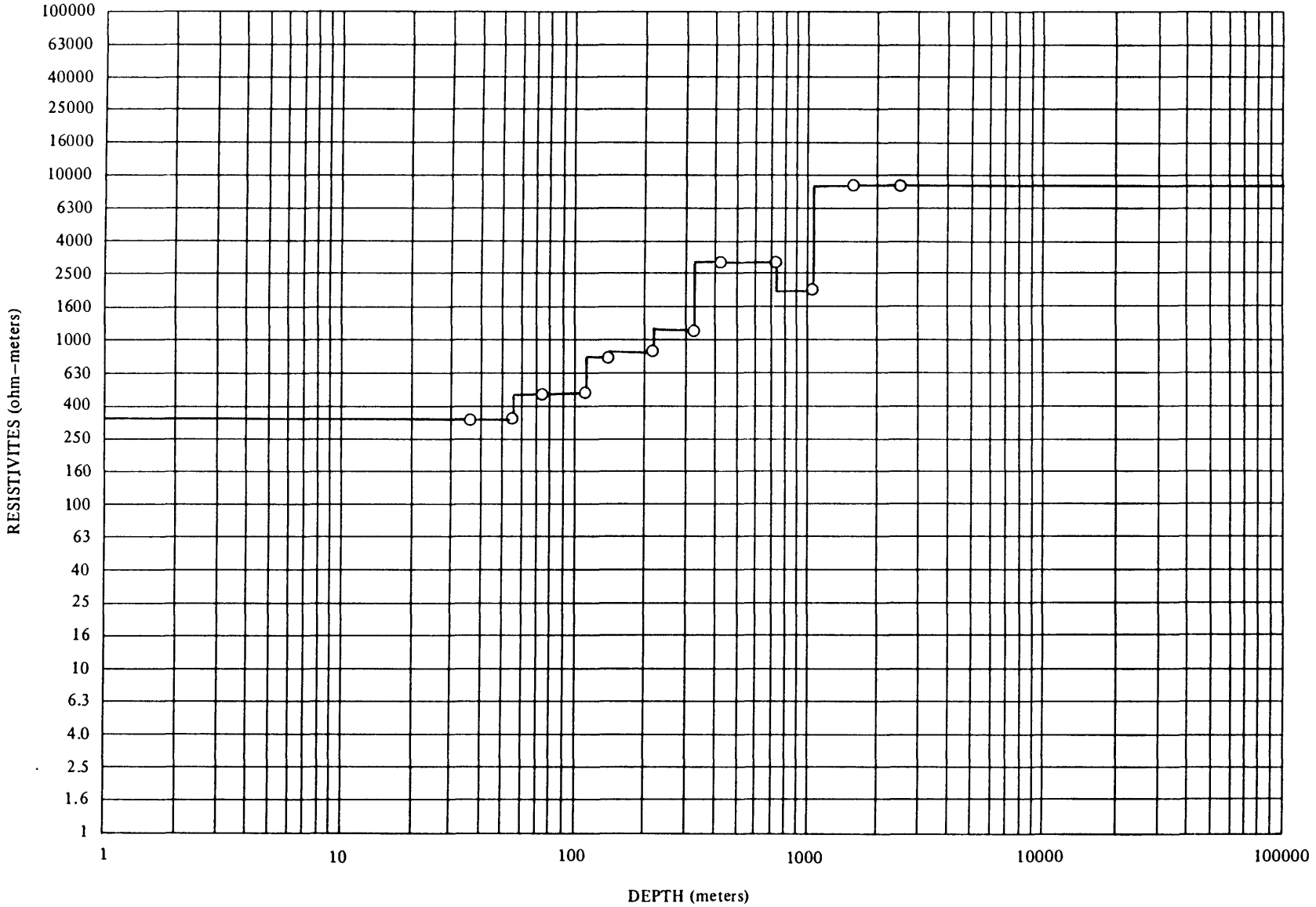

STATION—CM No 37

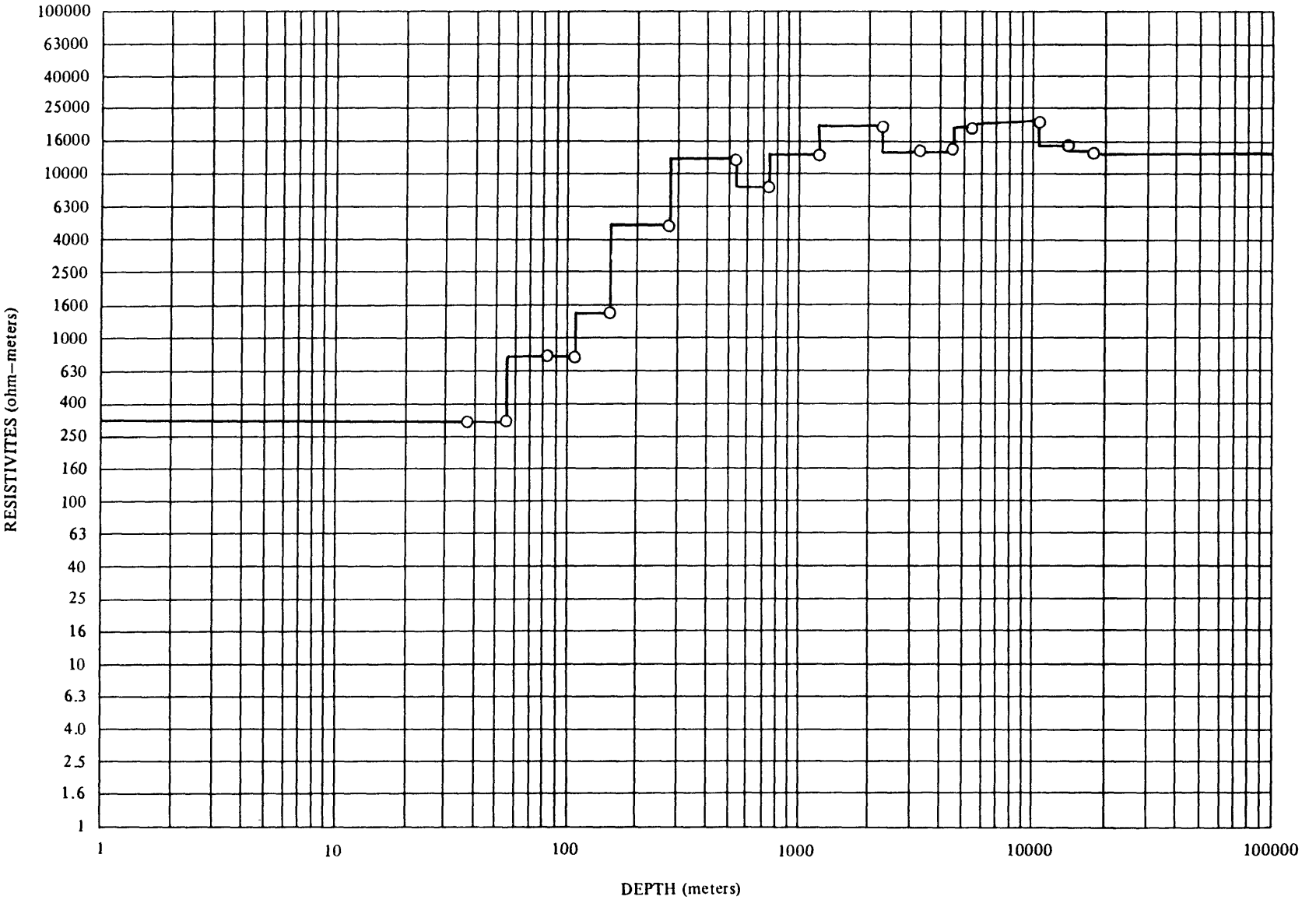

STATION—CM No. 38

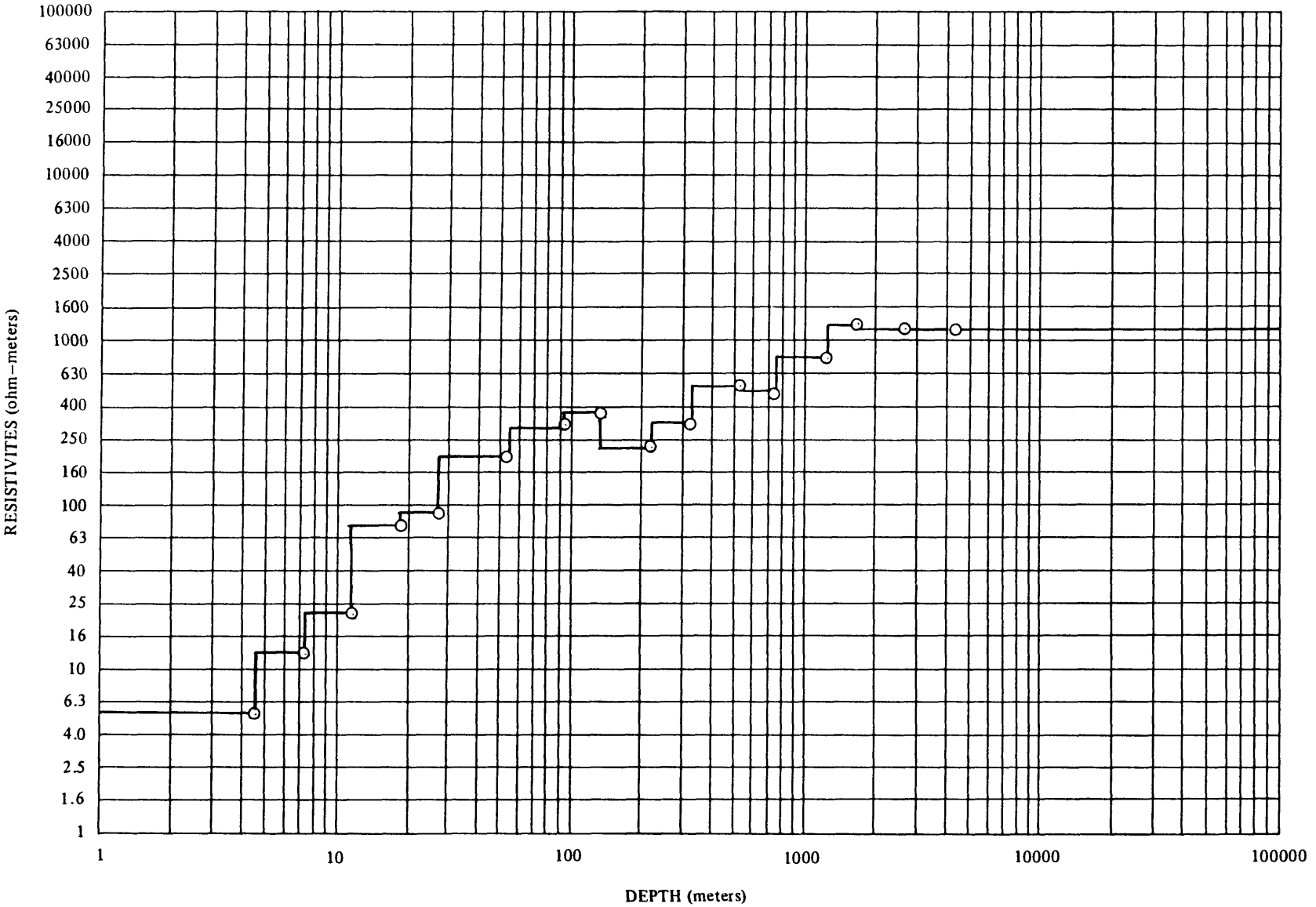

STATION—CM No 39

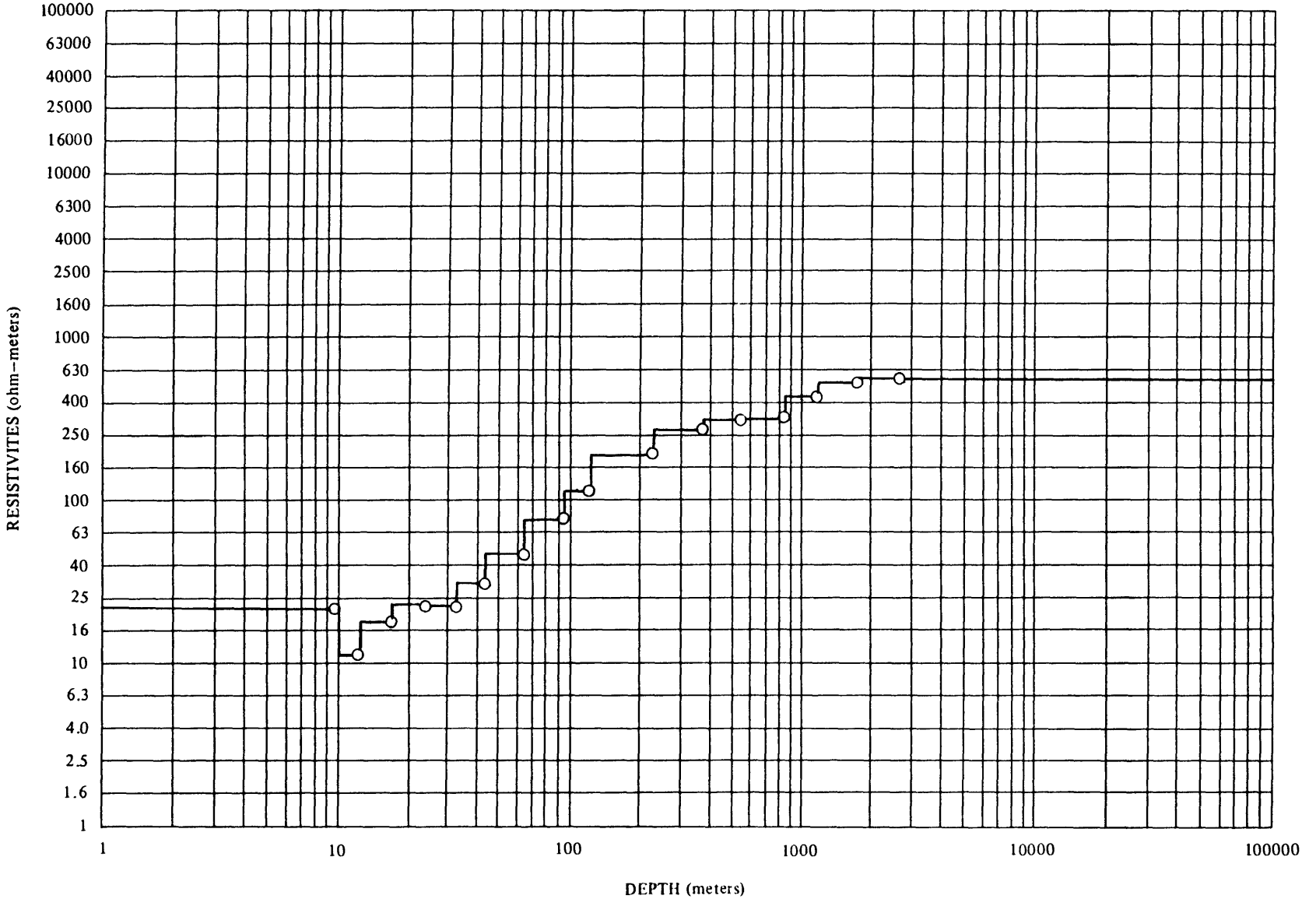

STATION—CM No. 40

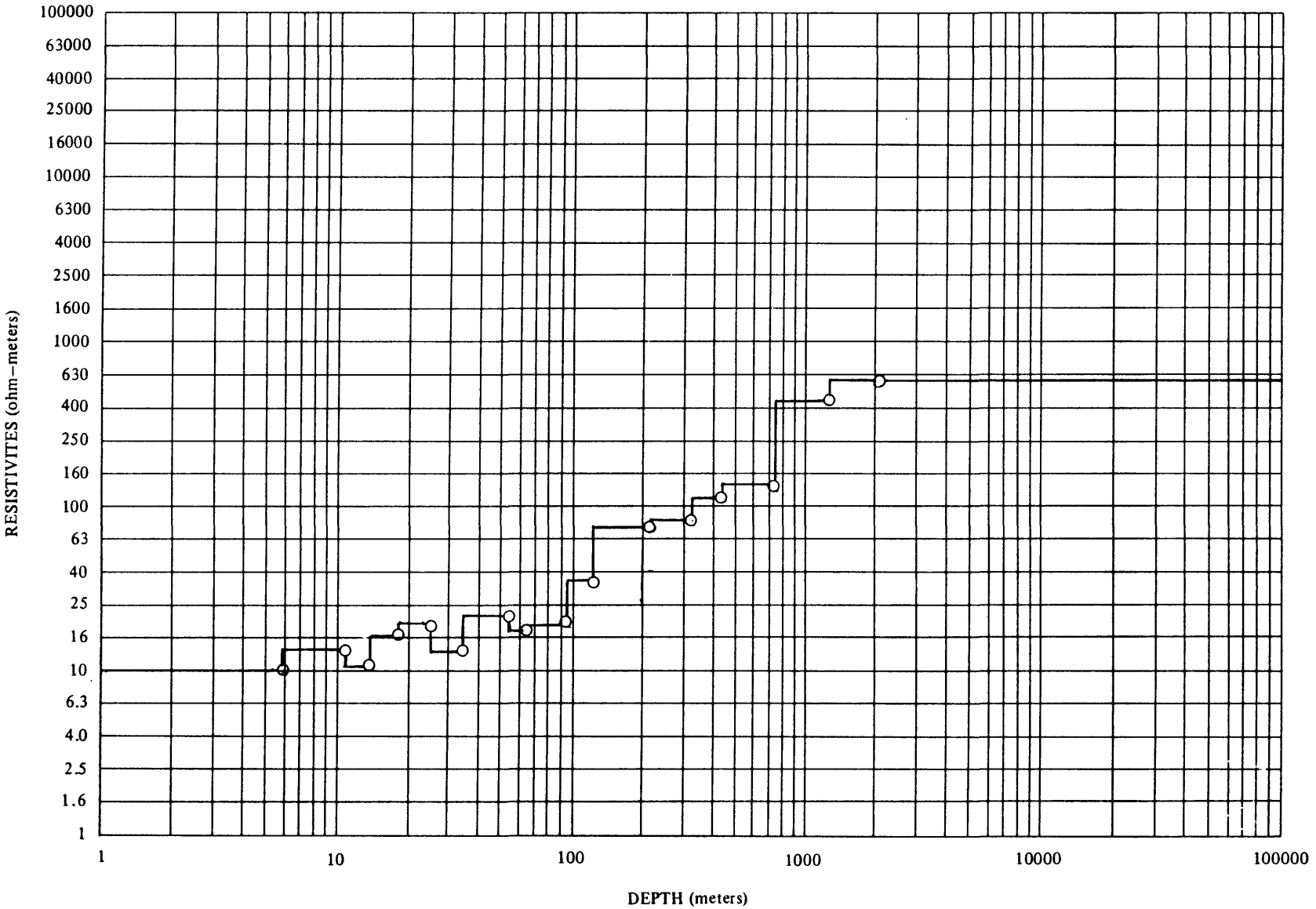

STATION--CM No. 41

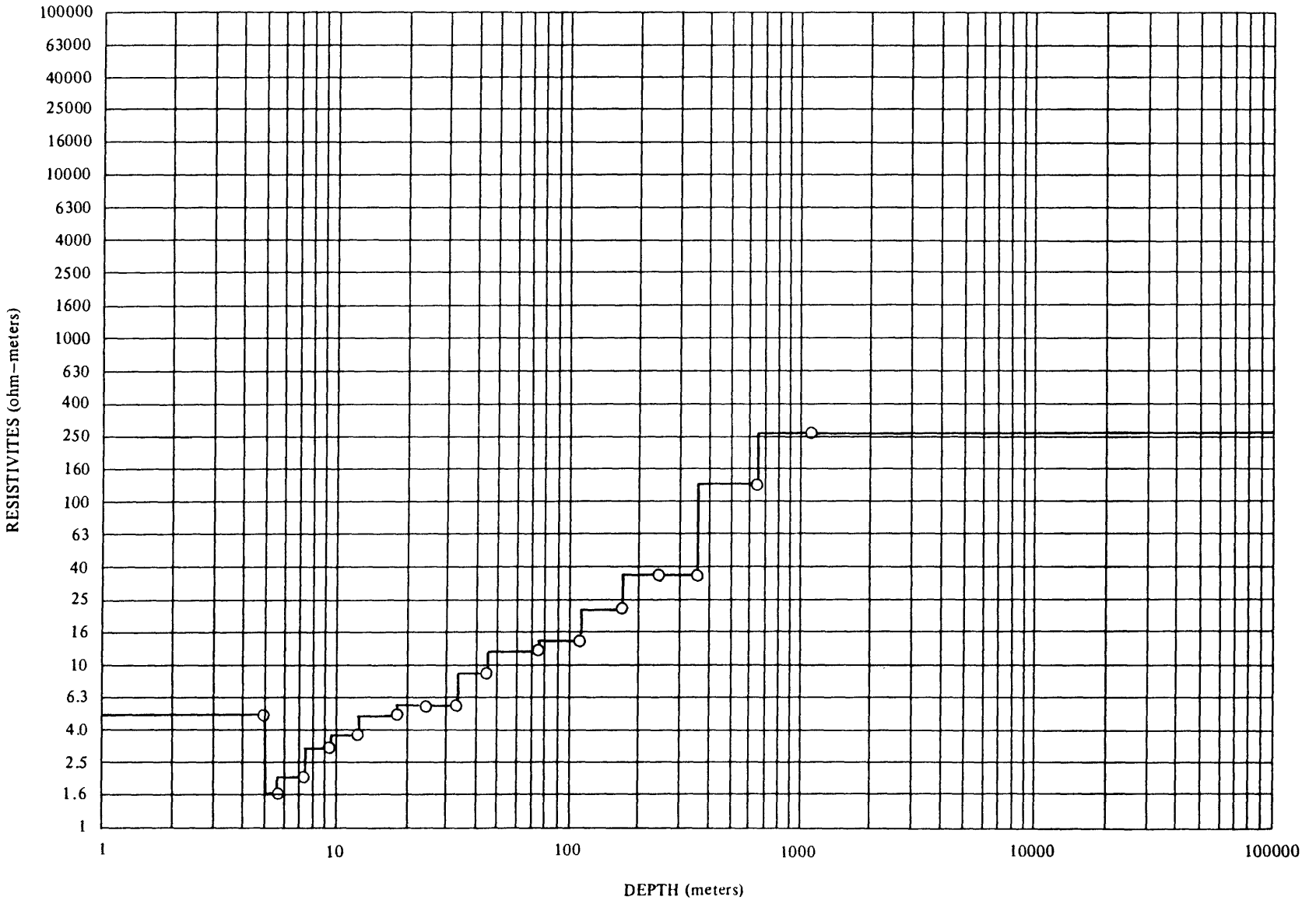

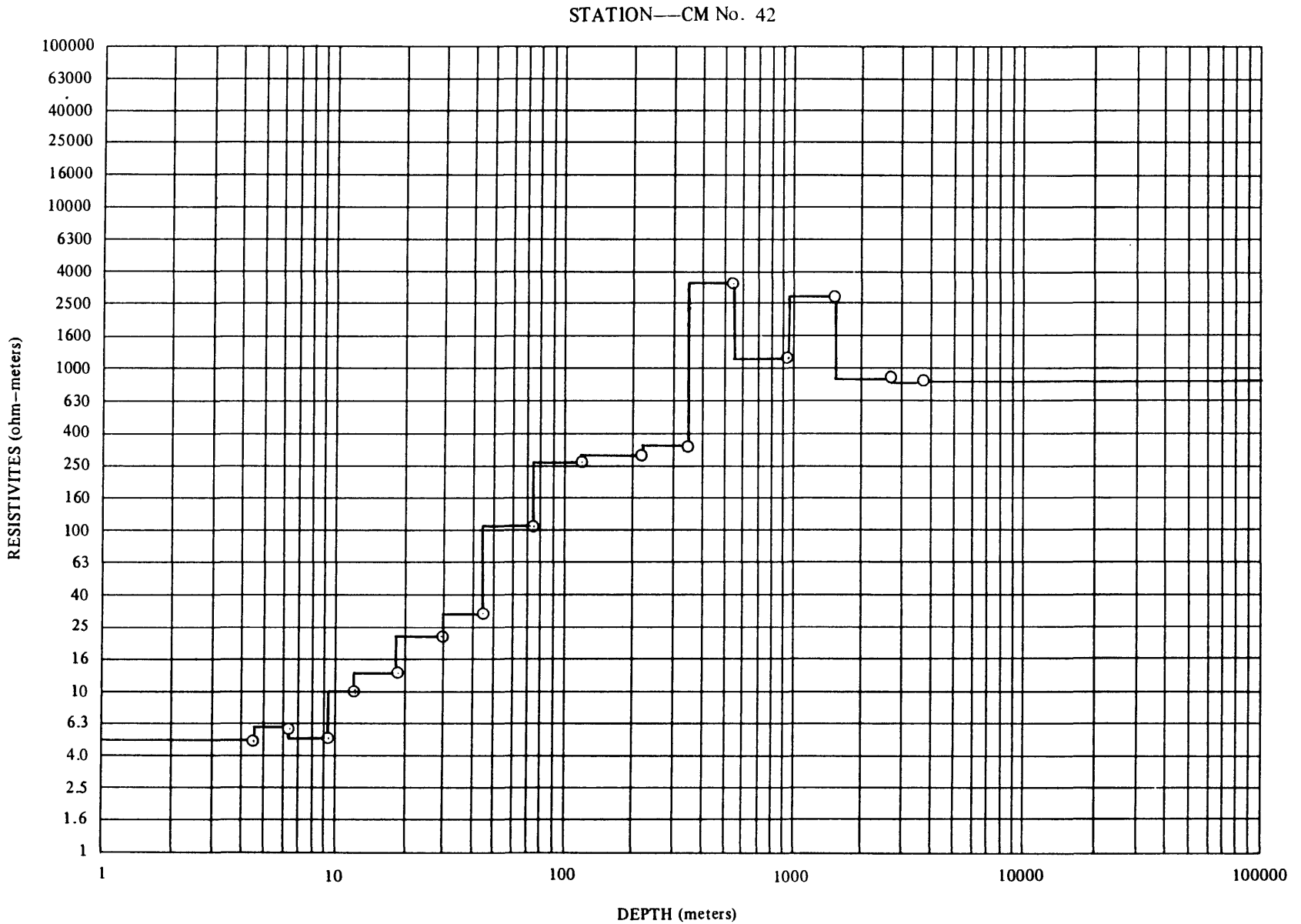
STATION—CM No. 42
RESISTIVITES (ohm-meters)
100000
63000
40000
25000
16000
10000
6300
4000
2500
1600
1000
630
400
250
160
100
63
40
25
16
10
6.3
4.0
2.5
1.6
1
1
10
100
1000
10000
100000
DEPTH (meters)

STATION—CM No. 43

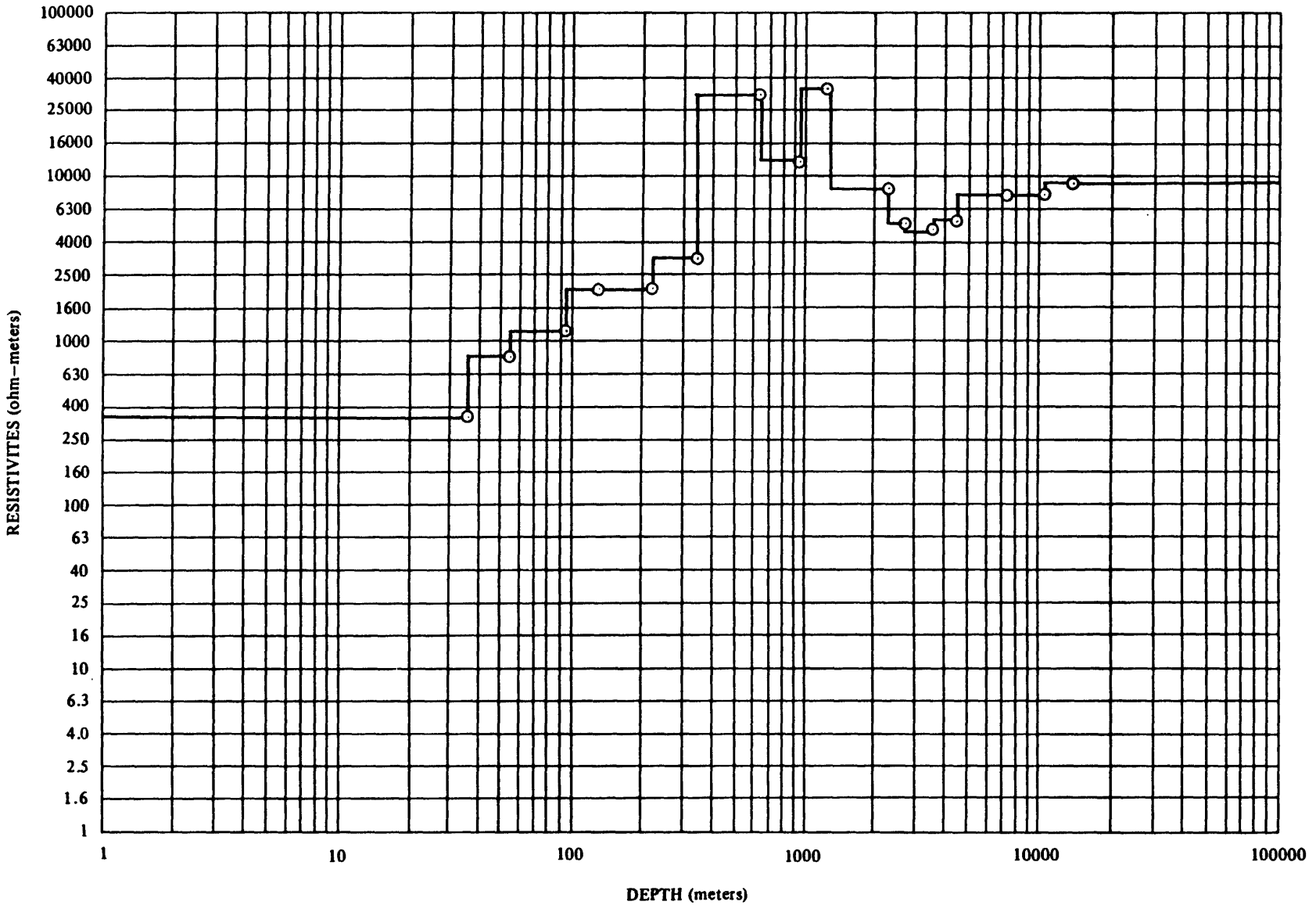

STATION---CM No. 44

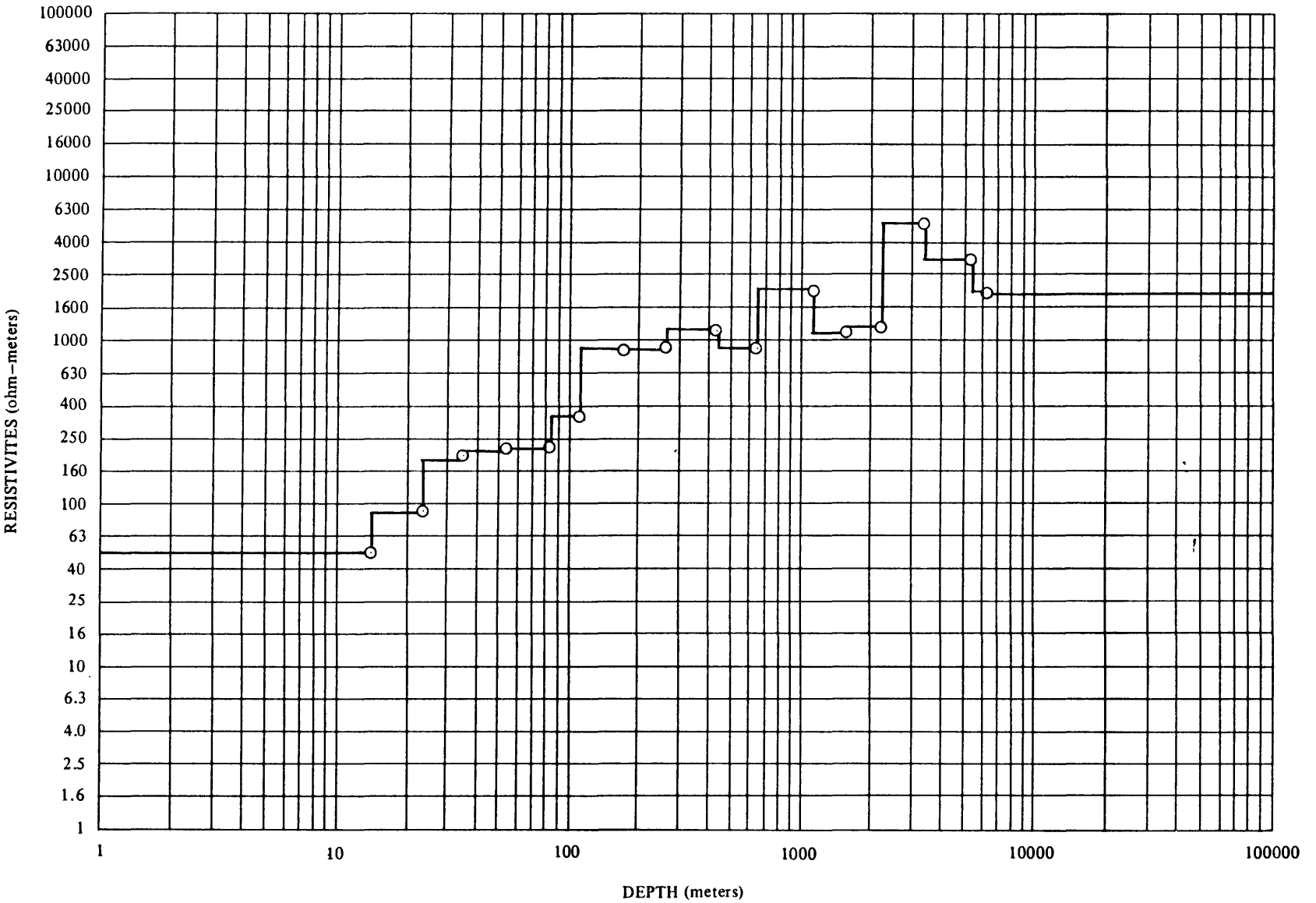

STATION—CM No. 45

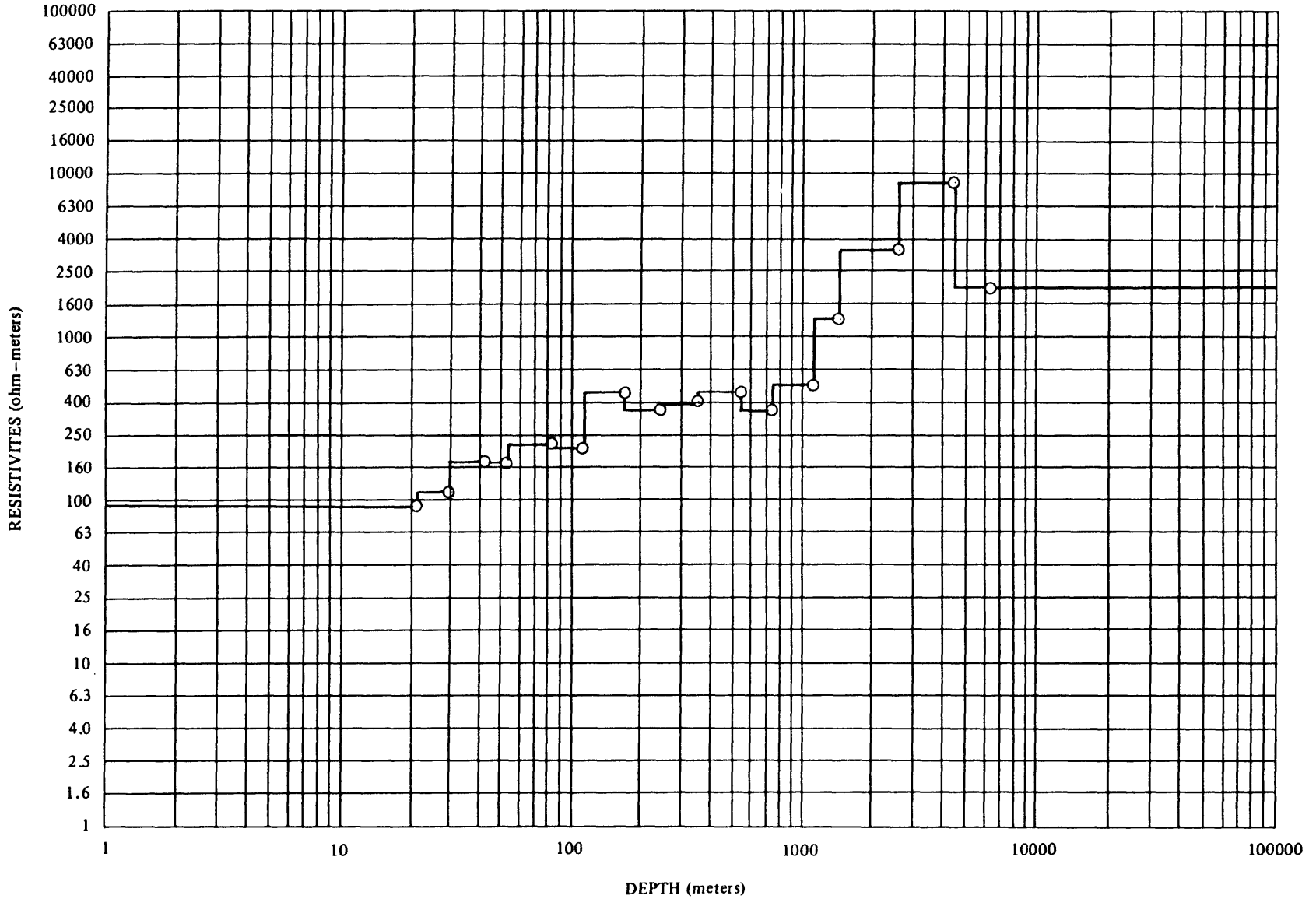

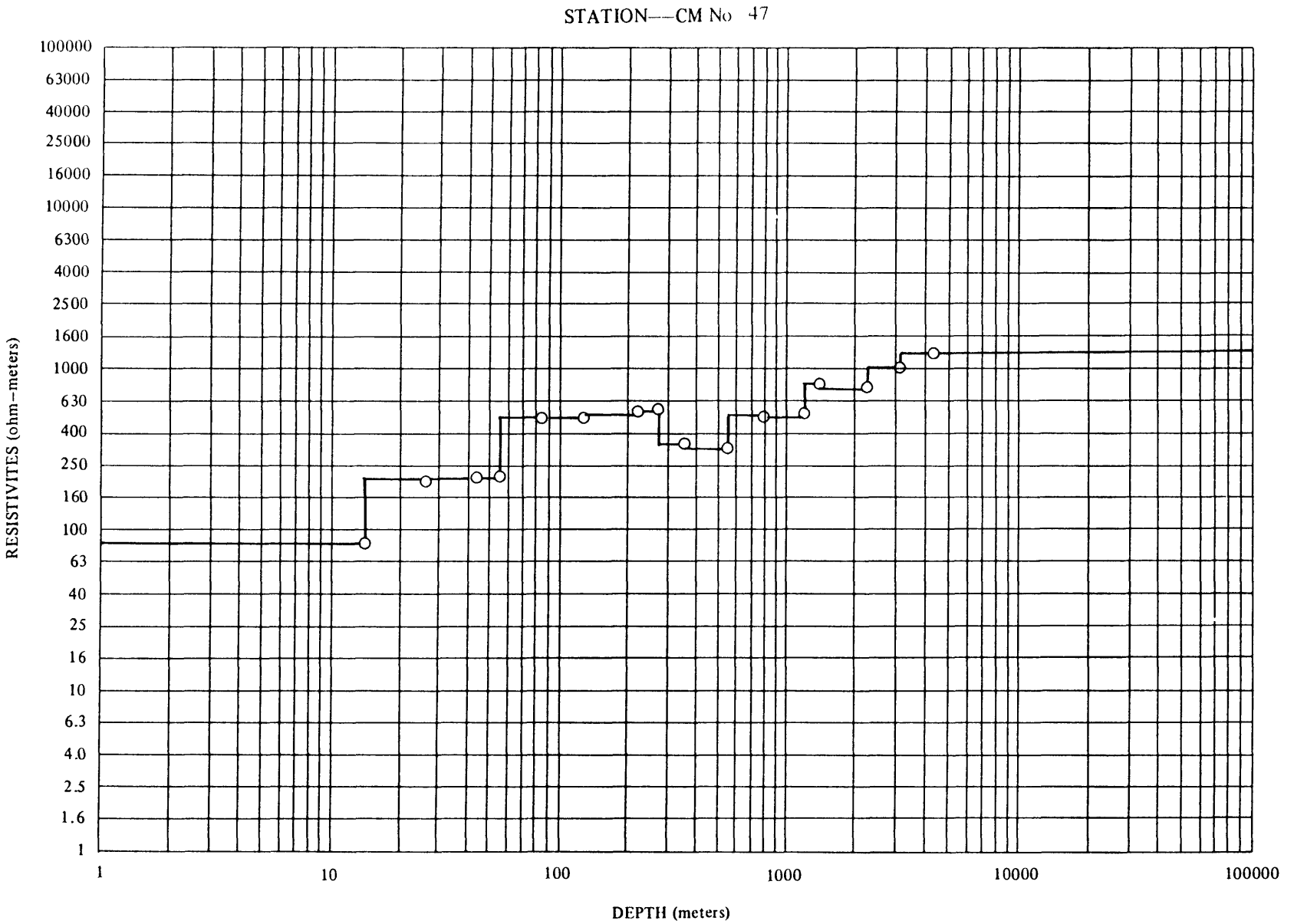
STATION—CM No 47
RESISTIVITES (ohm-meters)
100000
63000
40000
25000
16000
10000
6300
4000
2500
1600
1000
630
400
250
160
100
63
40
25
16
10
6.3
4.0
2.5
1.6
1
1
10
100
1000
10000
100000
DEPTH (meters)

STATION—CM No. 48

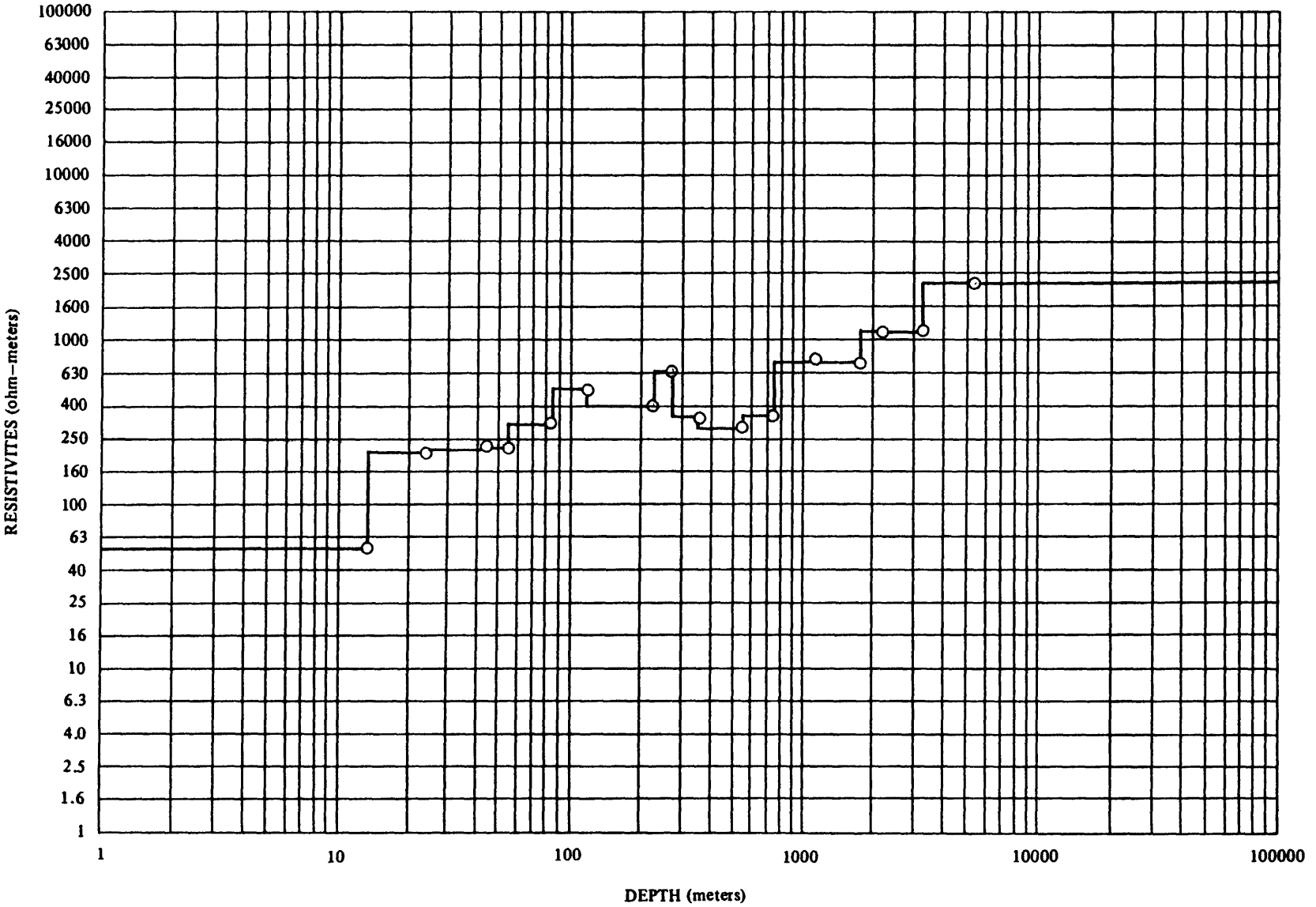

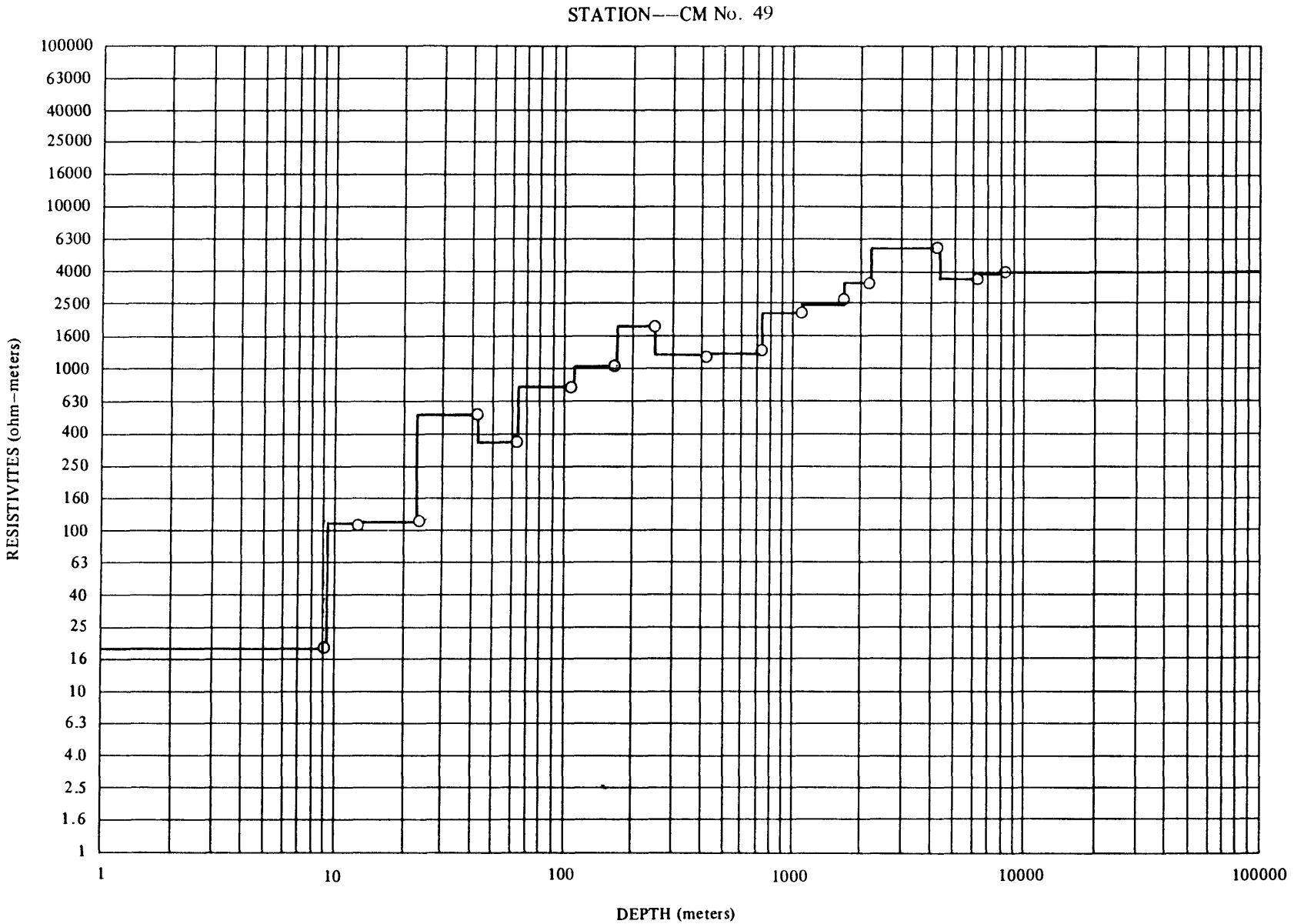
STATION—CM No. 49
RESISTIVITES (ohm-meters)
100000
63000
40000
25000
16000
10000
6300
4000
2500
1600
1000
630
400
250
160
100
63
40
25
16
10
6.3
4.0
2.5
1.6
1
1
10
100
1000
10000
100000
DEPTH (meters)

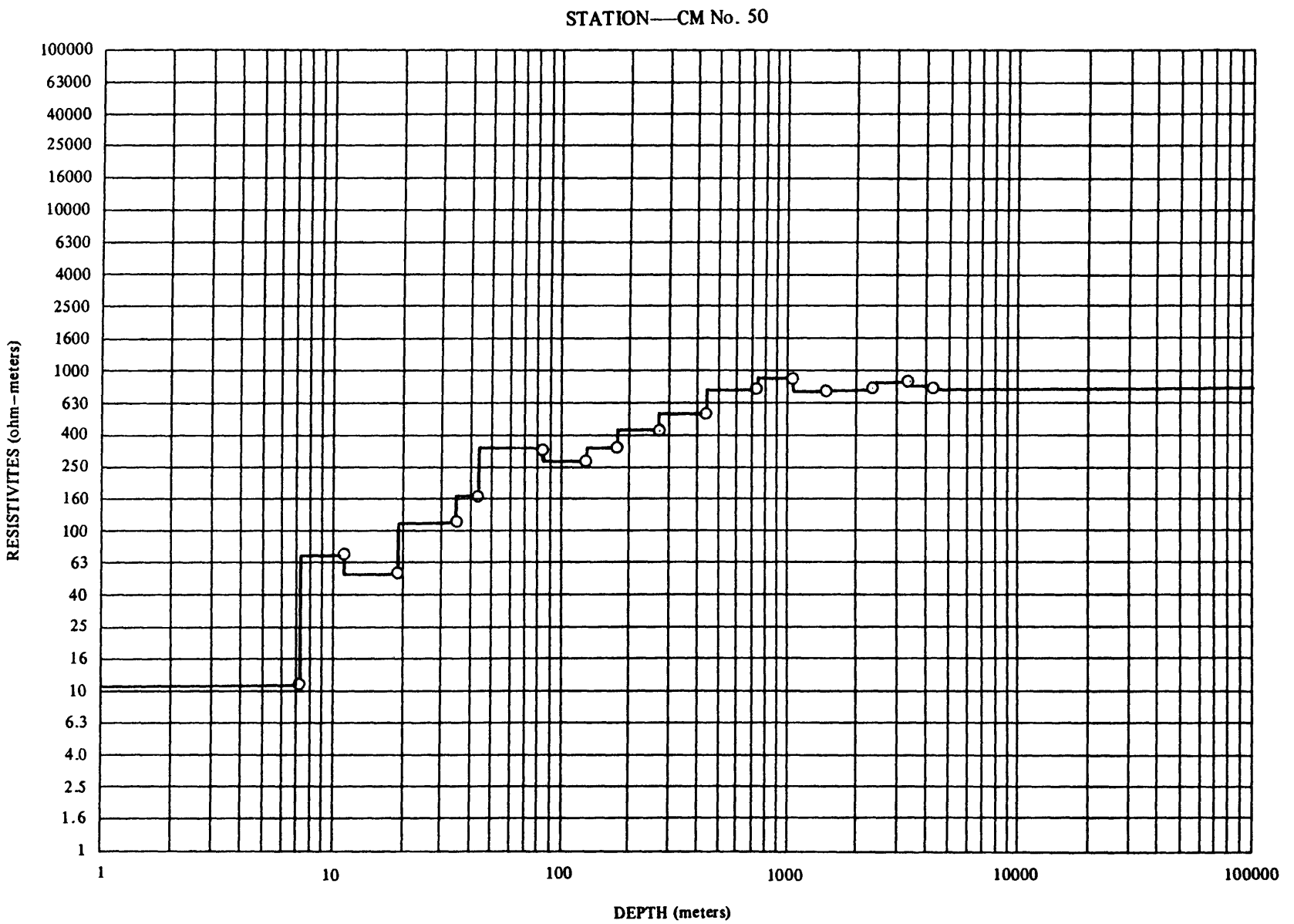
STATION—CM No. 50
RESISTIVITES (ohm-meters)
100000
63000
40000
25000
16000
10000
6300
4000
2500
1600
1000
630
400
250
160
100
63
40
25
16
10
6.3
4.0
2.5
1.6
1
1
10
100
1000
10000
100000
DEPTH (meters)

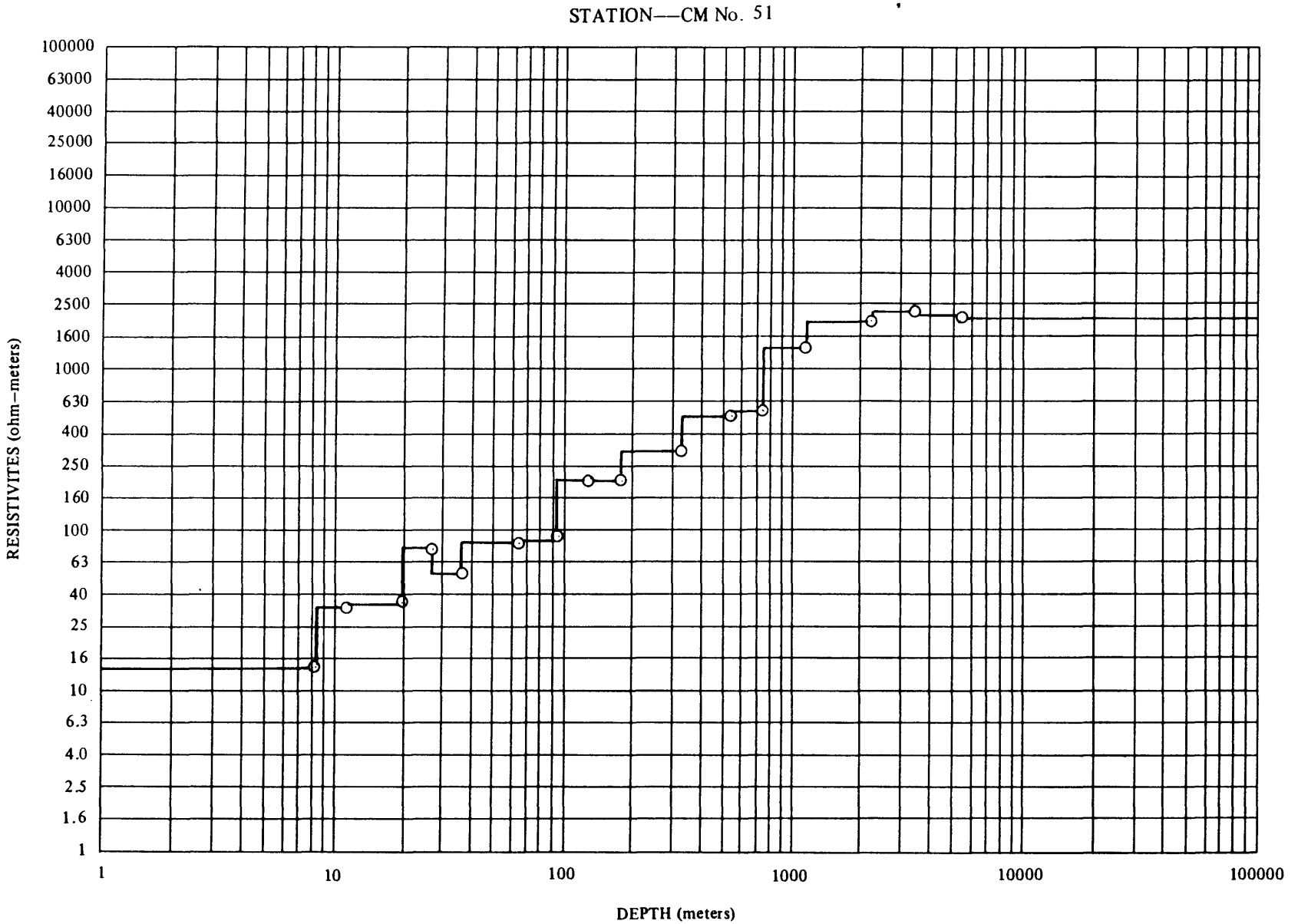
STATION—CM No. 51
RESISTIVITES (ohm–meters)
100000
63000
40000
25000
16000
10000
6300
4000
2500
1600
1000
630
400
250
160
100
63
40
25
16
10
6.3
4.0
2.5
1.6
1
1
10
100
1000
10000
100000
DEPTH (meters)

STATION—CM No. 52

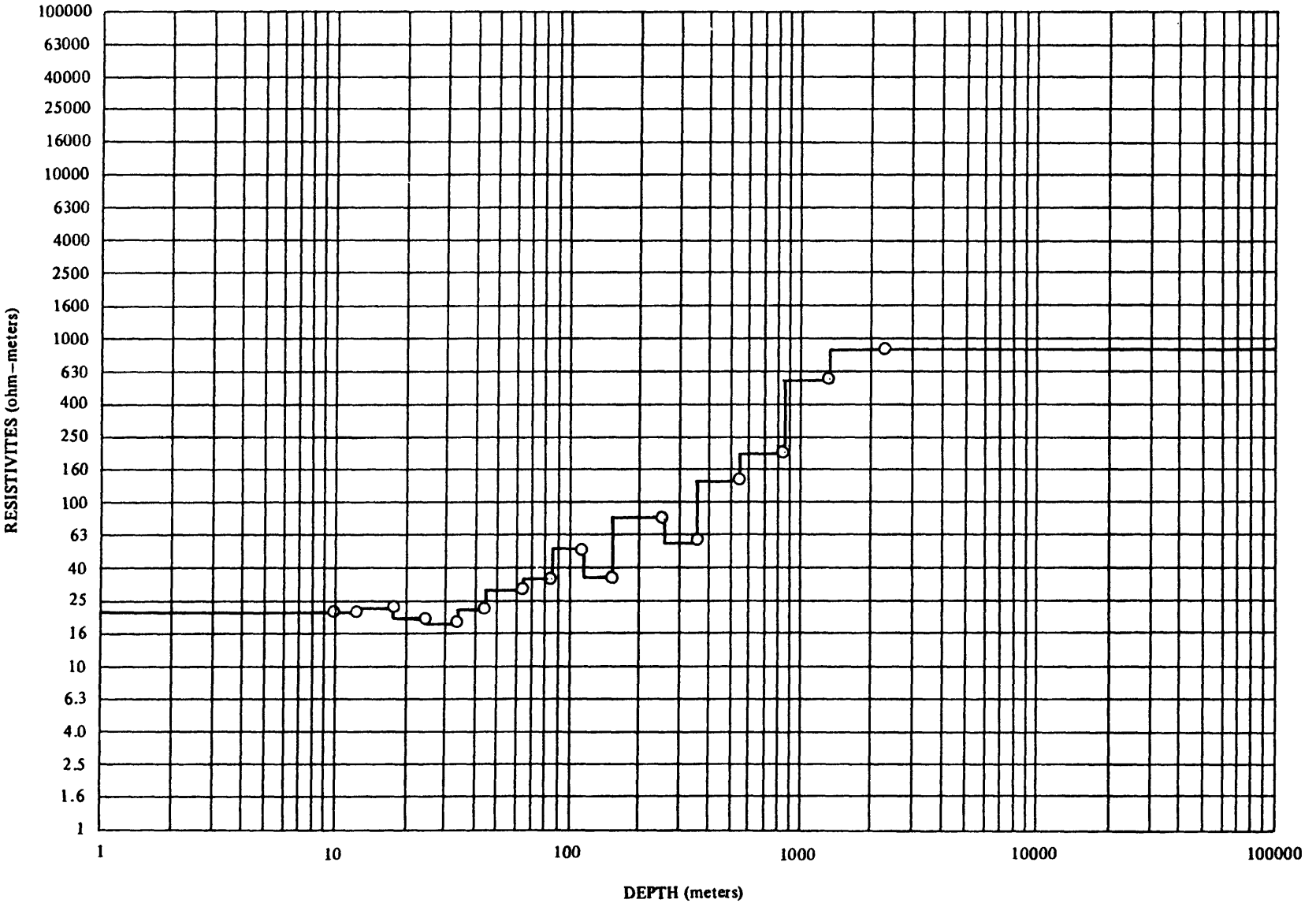

STATION—CM No. 60

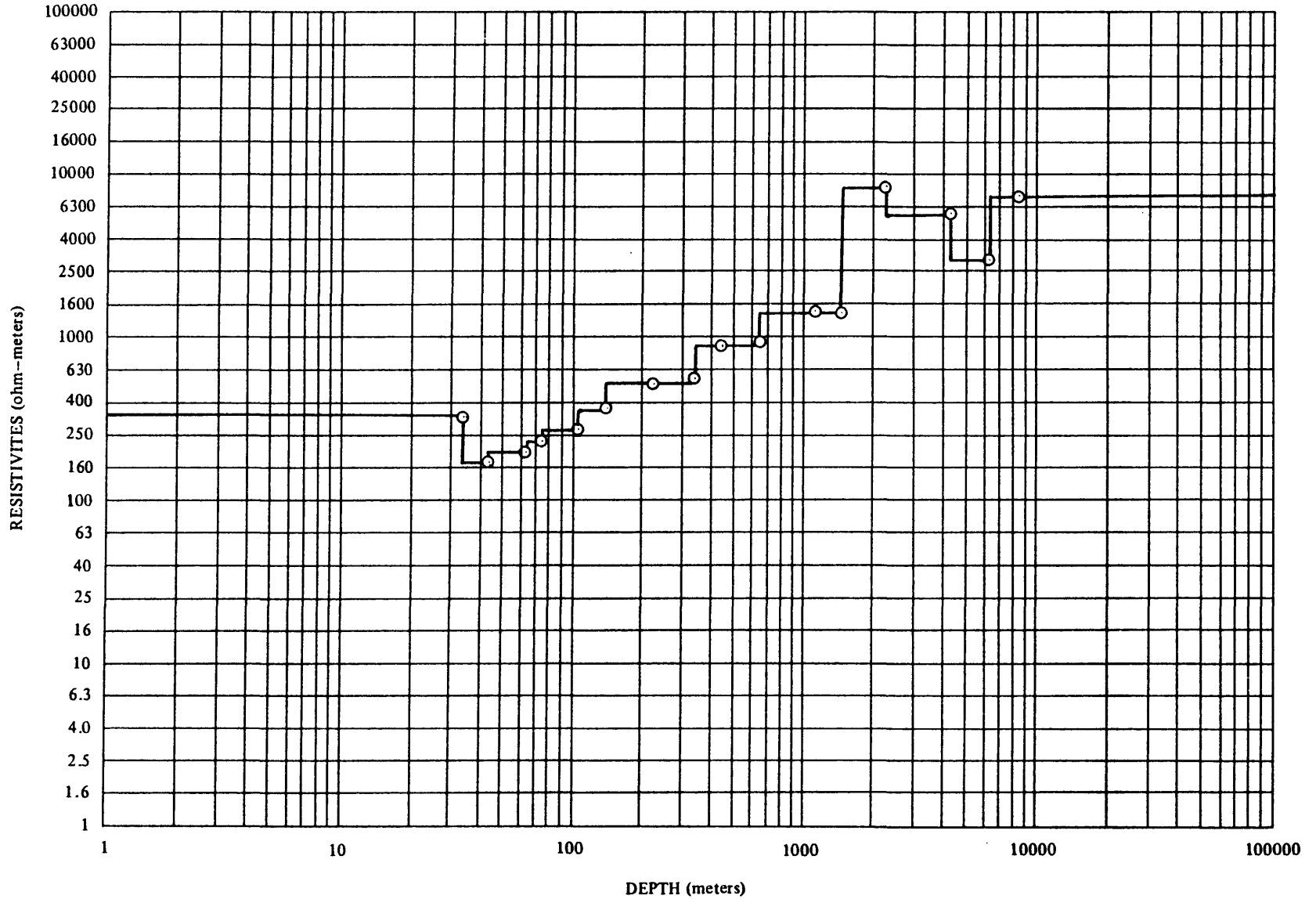

STATION—CM No. 61

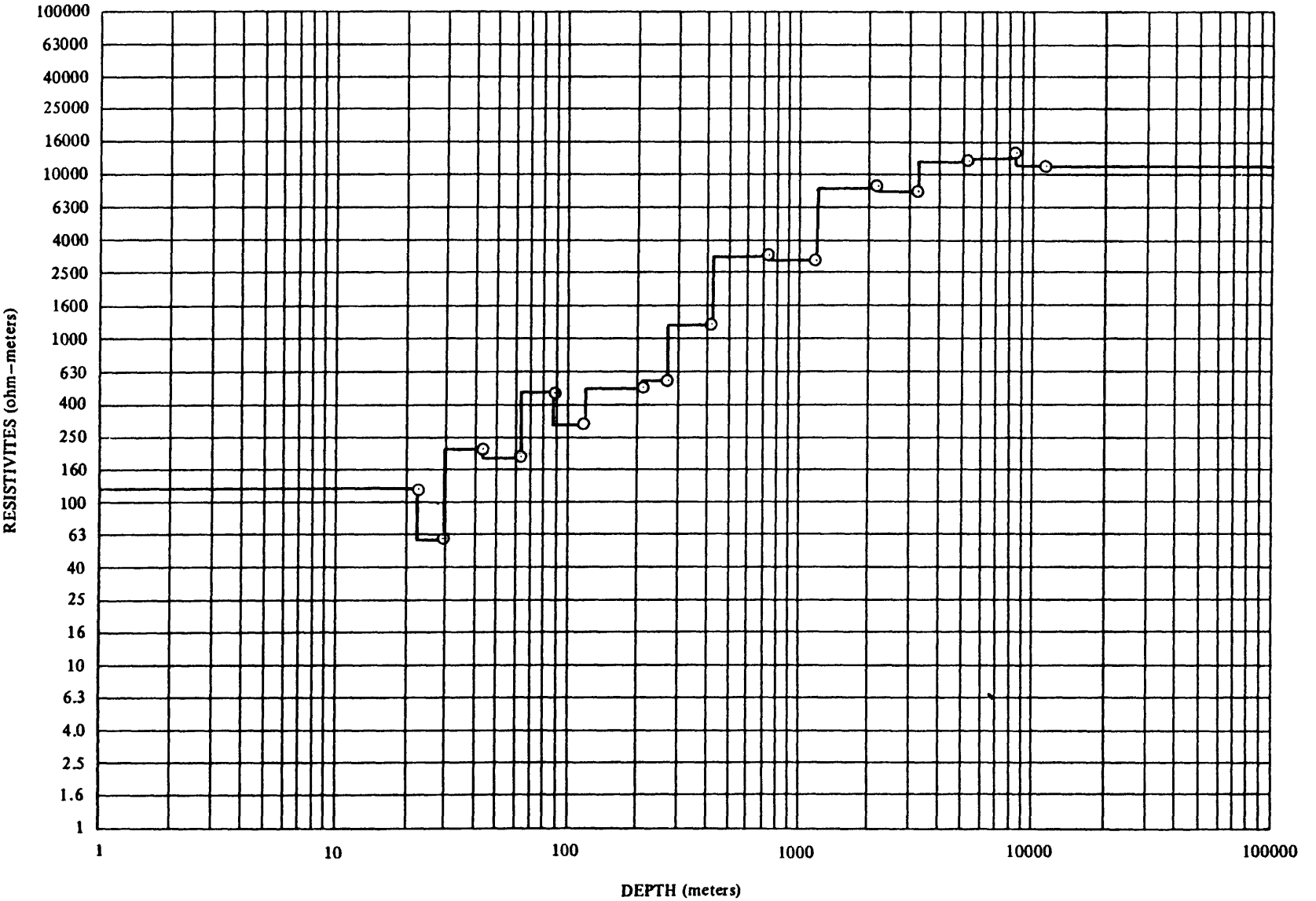

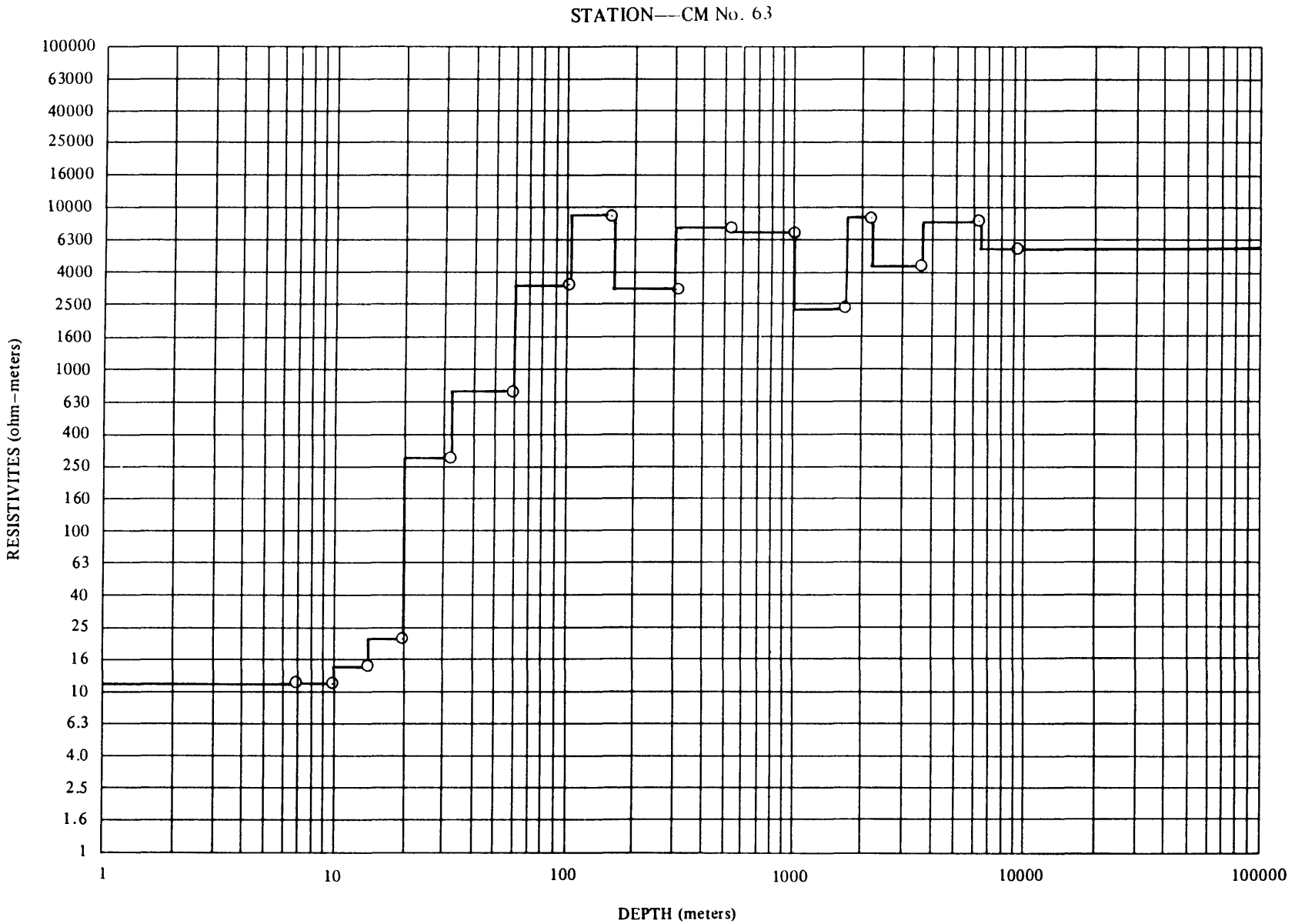
STATION—CM No. 63
RESISTIVITES (ohm-meters)
100000
63000
40000
25000
16000
10000
6300
4000
2500
1600
1000
630
400
250
160
100
63
40
25
16
10
6.3
4.0
2.5
1.6
1
1
10
100
1000
10000
100000
DEPTH (meters)

STATION—CM No. 64

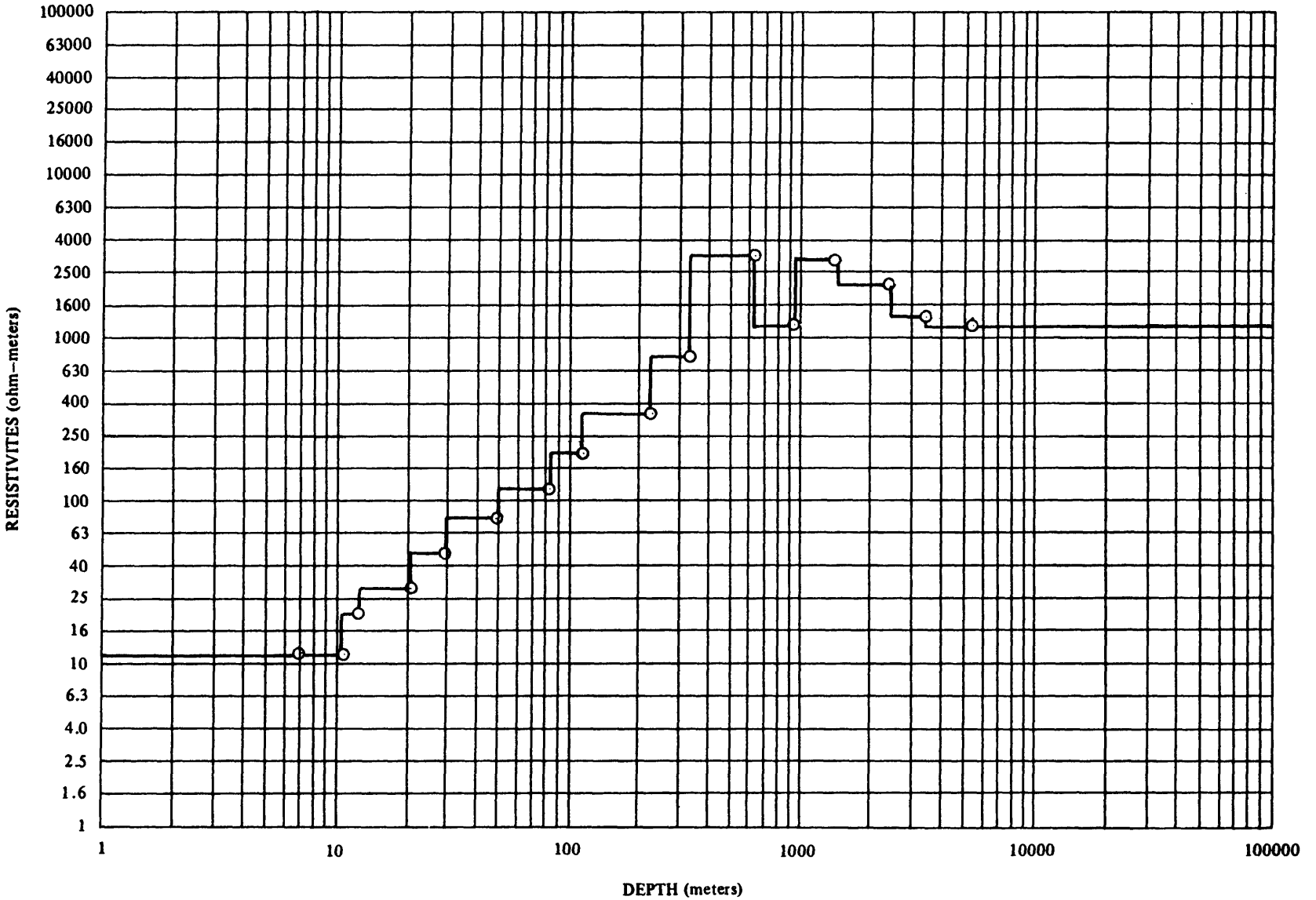

STATION---CM No. 65

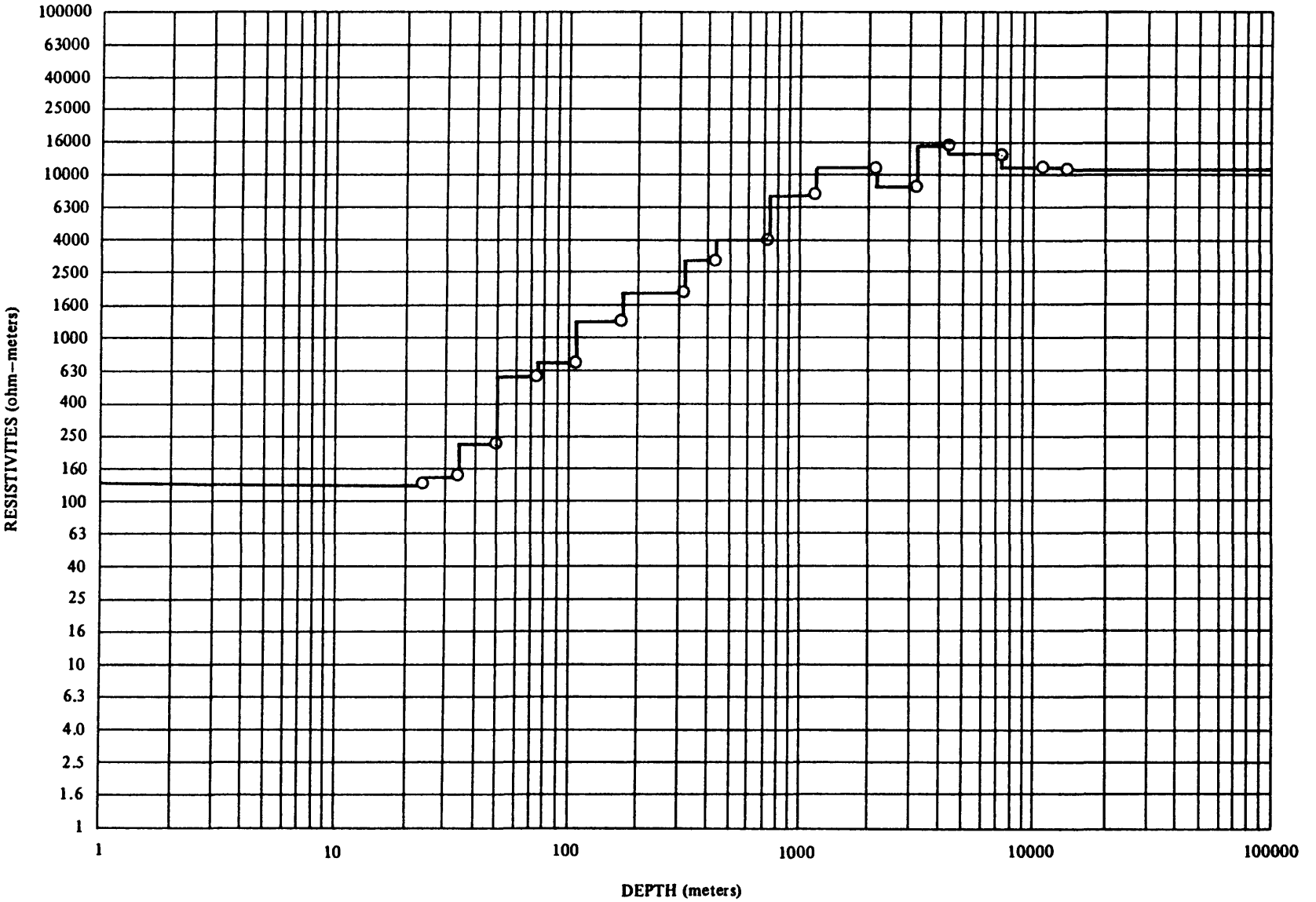

STATION—CM No. 66

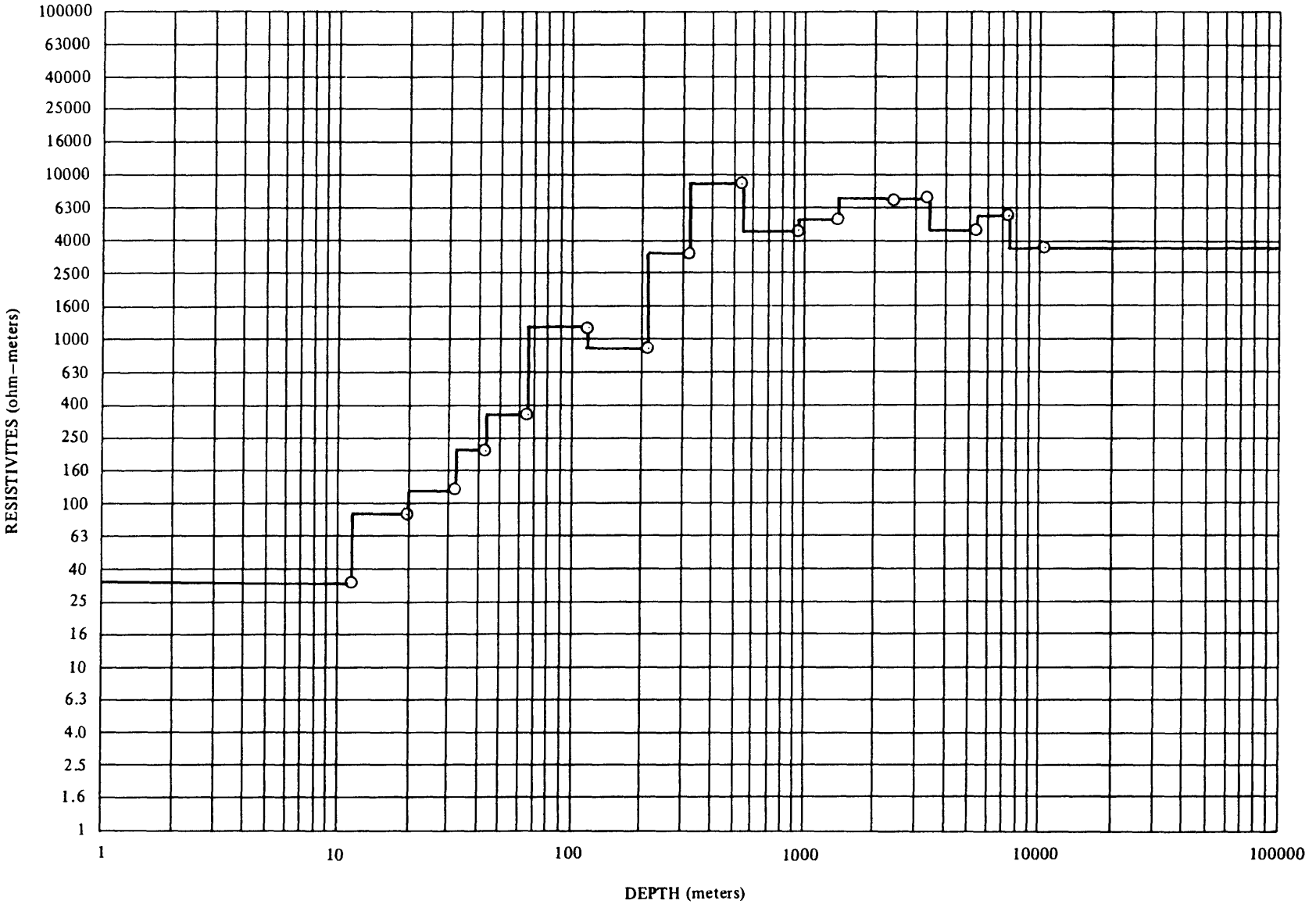

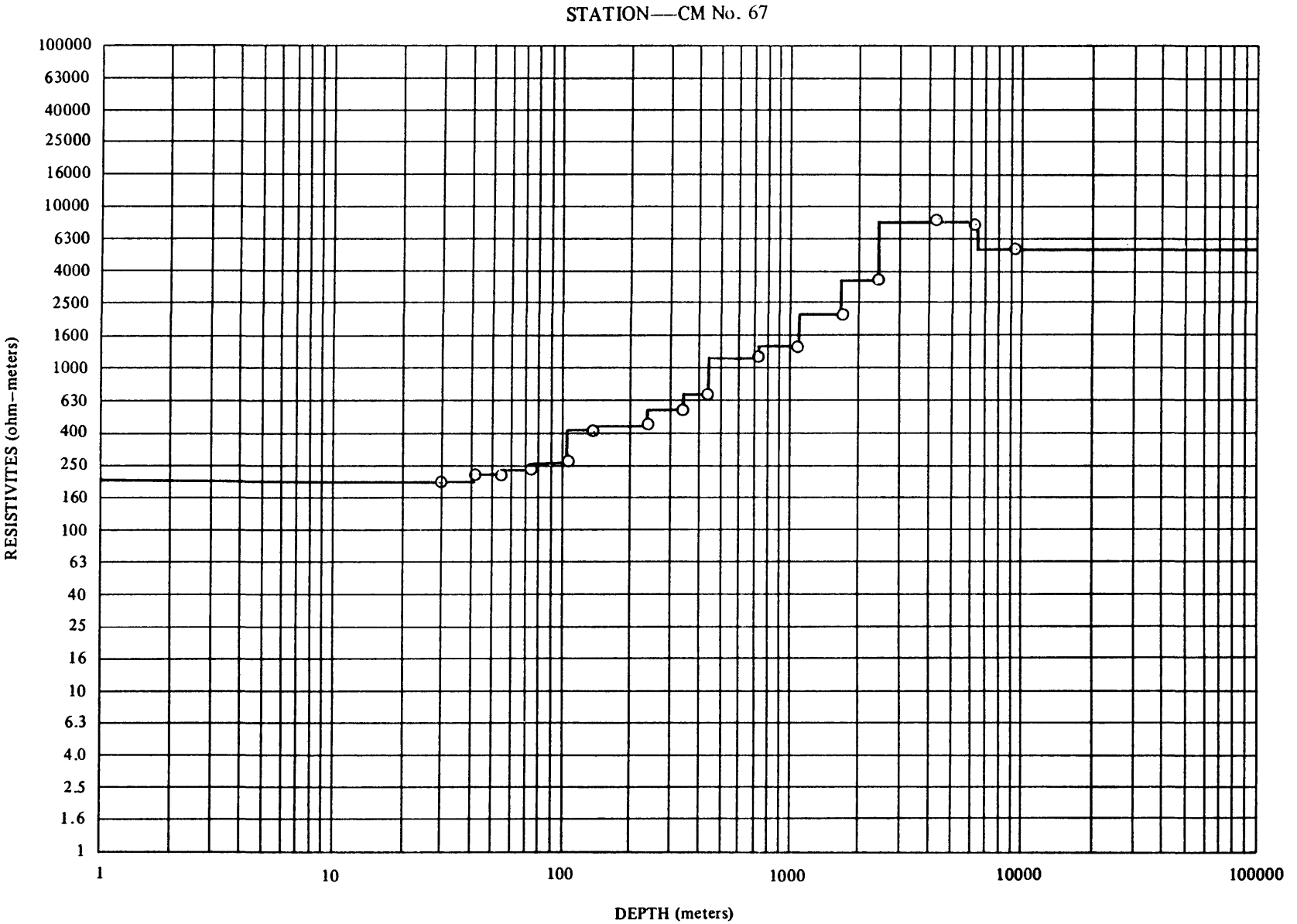
STATION—CM No. 67
RESISTIVITES (ohm-meters)
100000
63000
40000
25000
16000
10000
6300
4000
2500
1600
1000
630
400
250
160
100
63
40
25
16
10
6.3
4.0
2.5
1.6
1
1
10
100
1000
10000
100000
DEPTH (meters)

STATION—CM No. 68

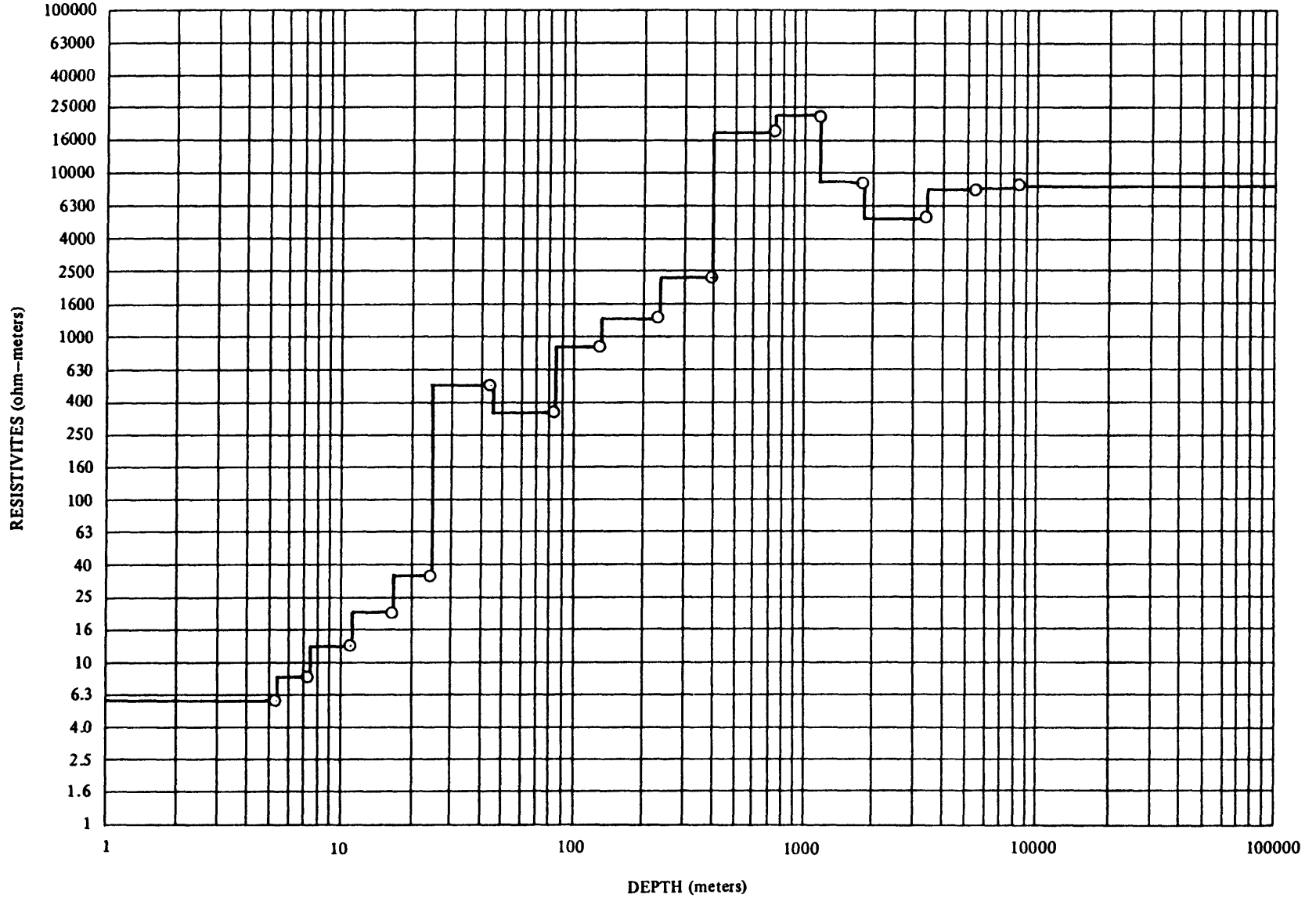

STATION—CM No. Y1

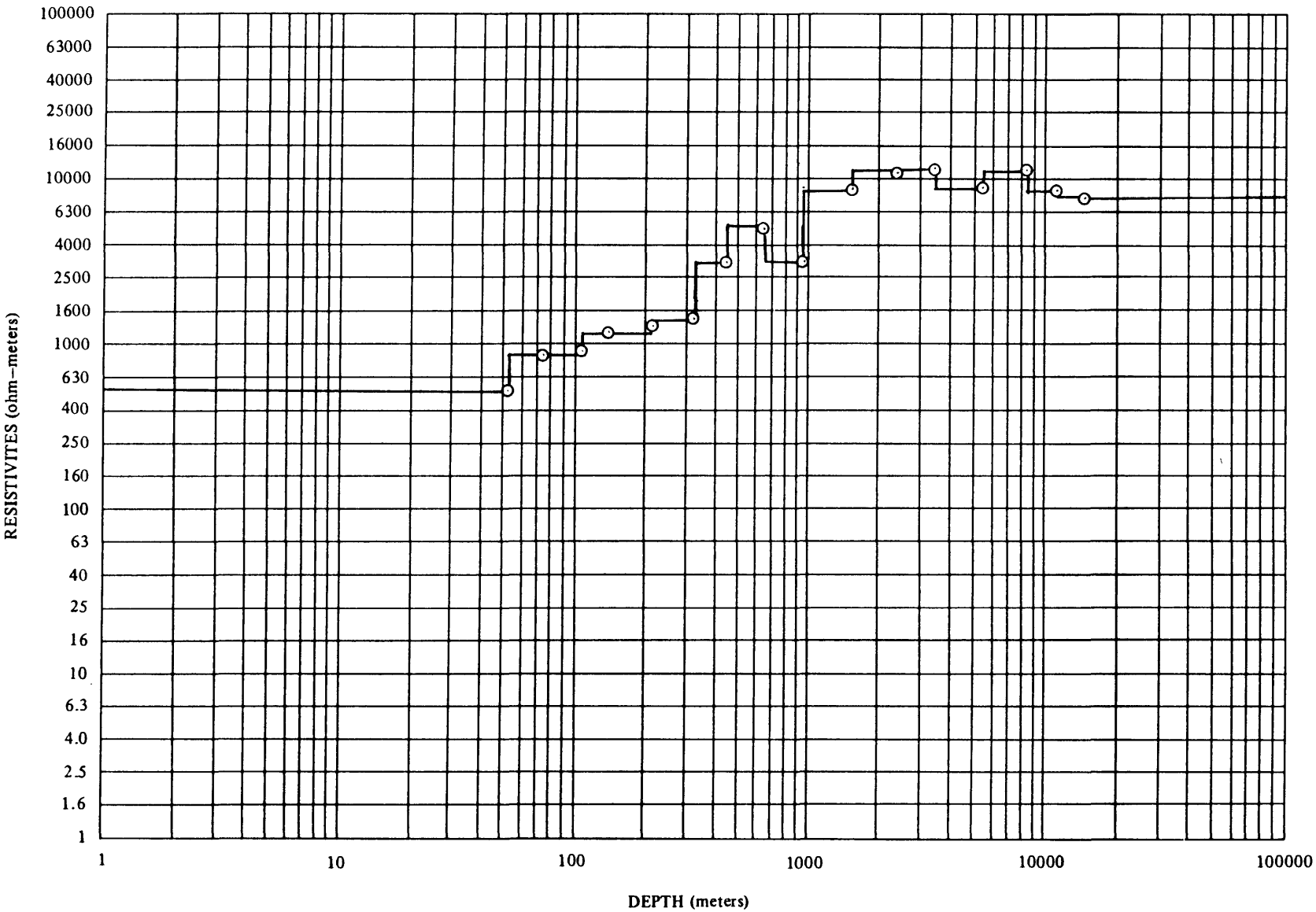

STATION—CM No. Y2

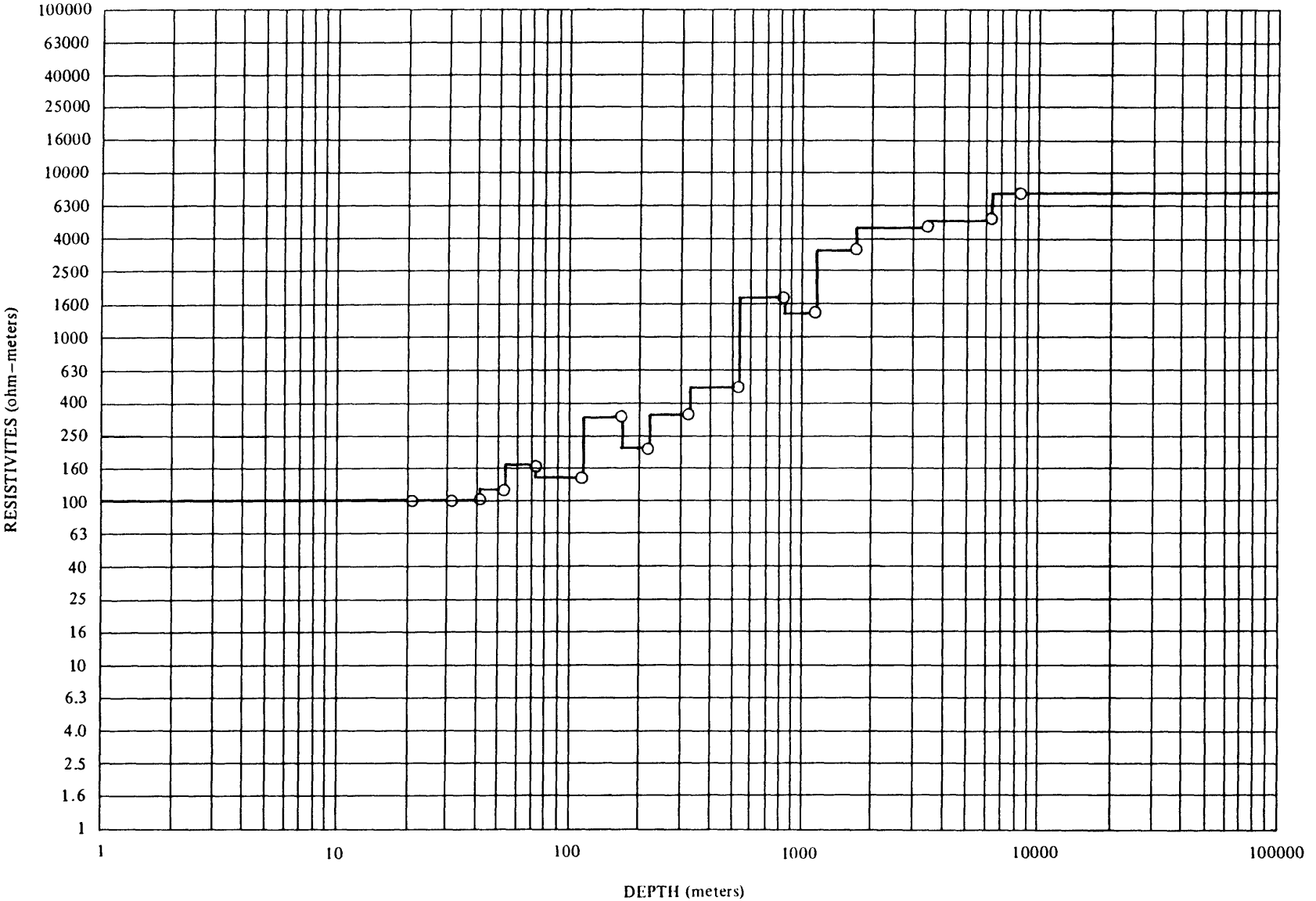

STATION—CM No. Y3

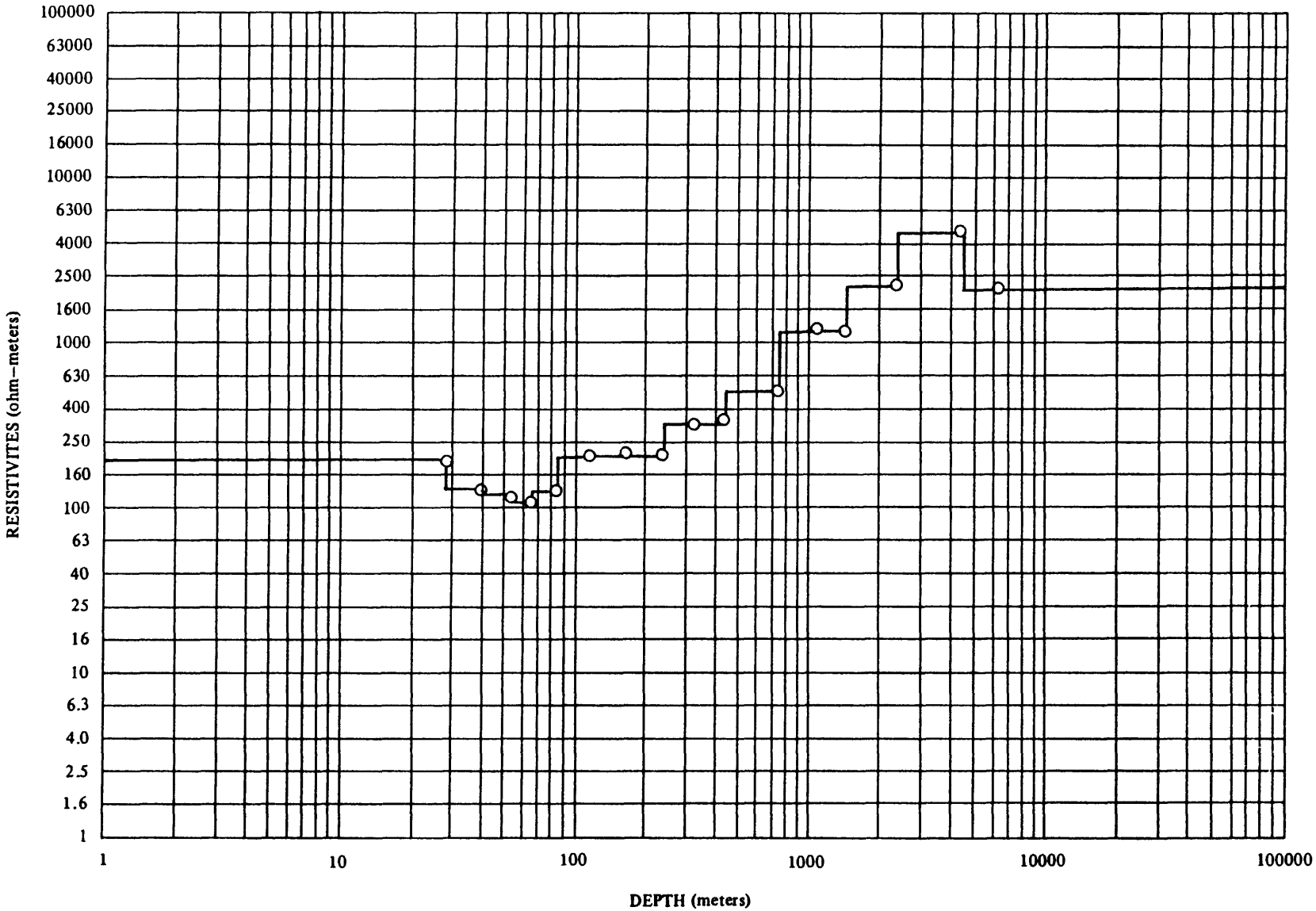

STATION—CM No. Y4

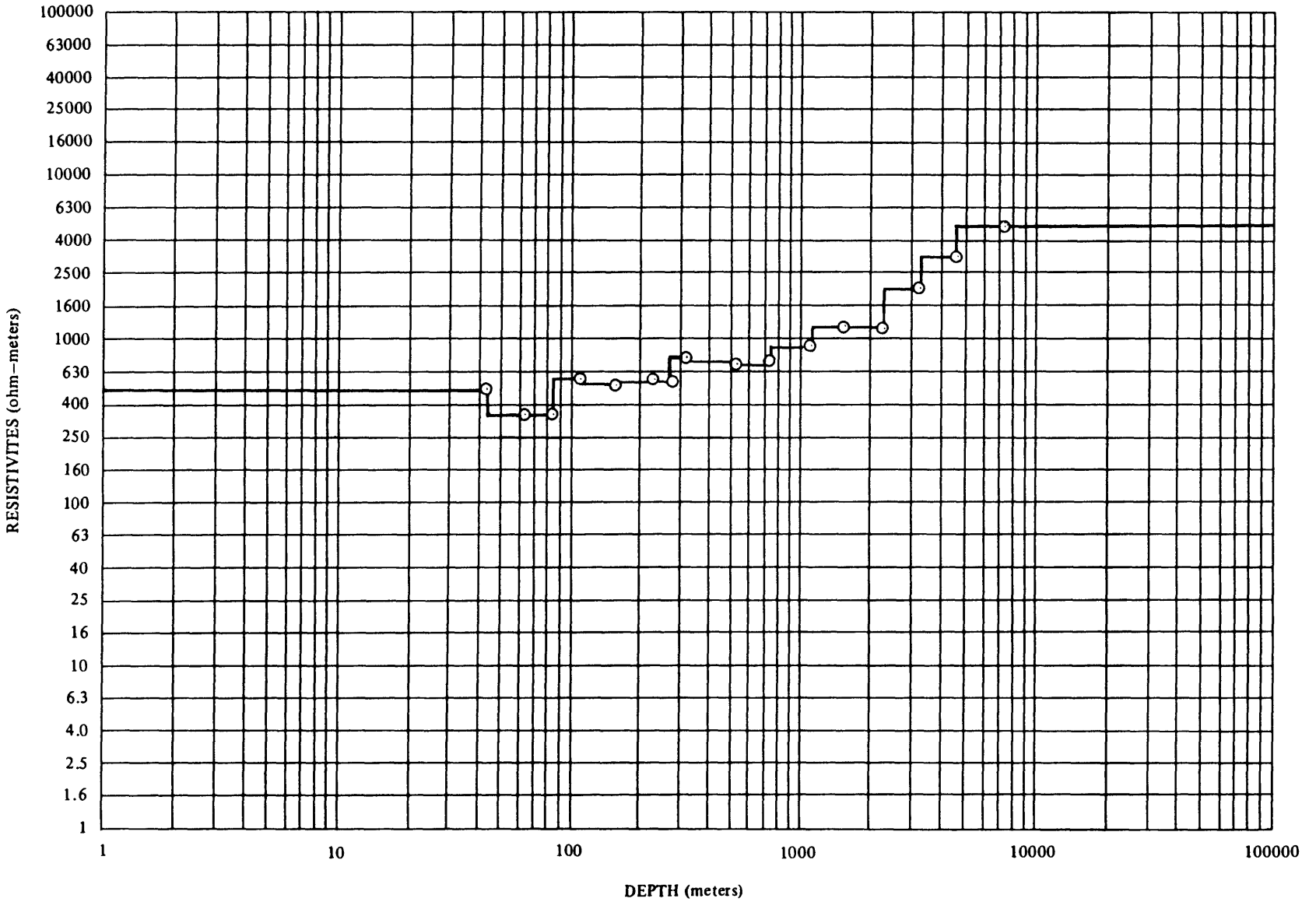

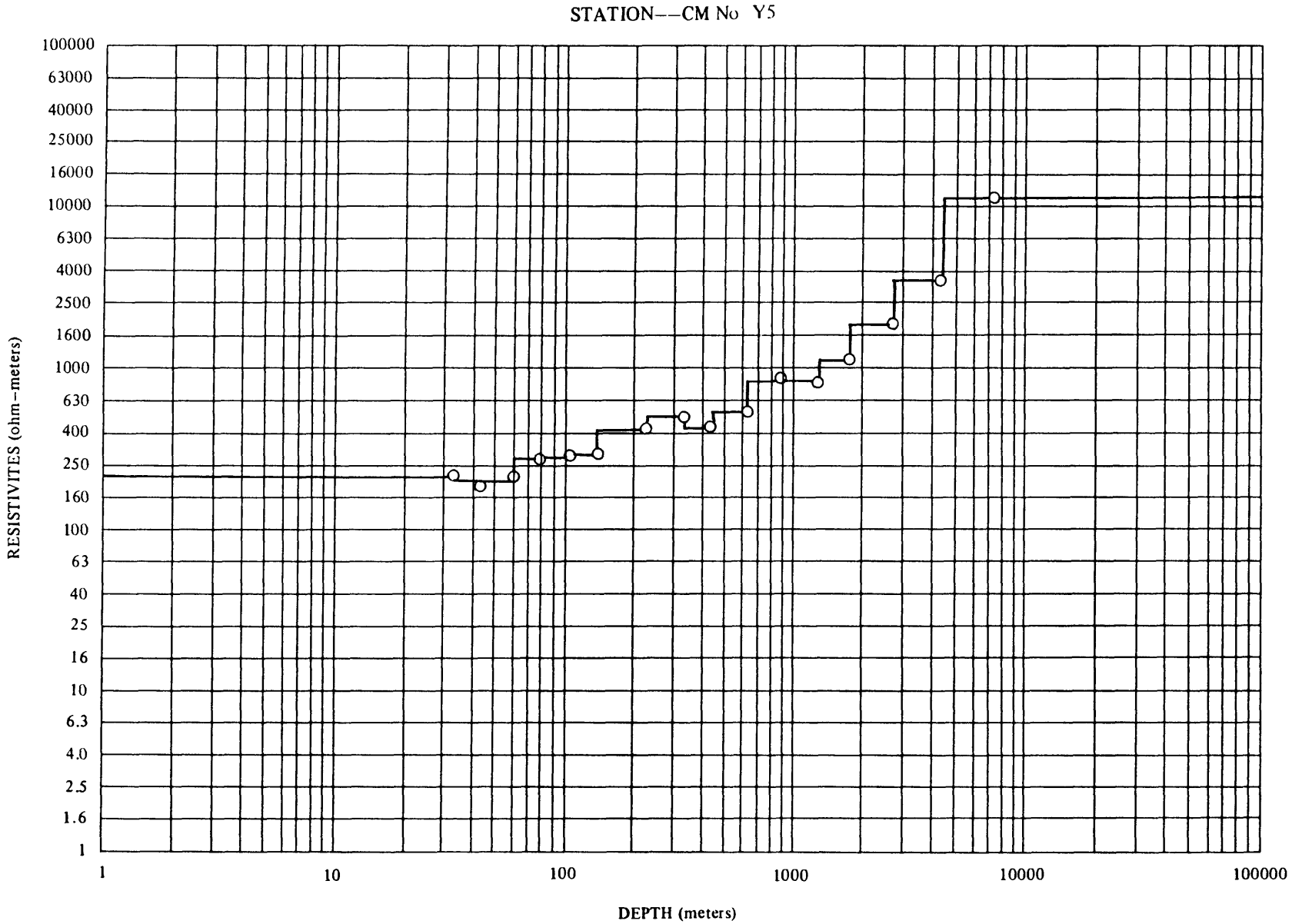
STATION--CM No Y5
RESISTIVITES (ohm-meters)
100000
63000
40000
25000
16000
10000
6300
4000
2500
1600
1000
630
400
250
160
100
63
40
25
16
10
6.3
4.0
2.5
1.6
1
1
10
100
1000
10000
100000
DEPTH (meters)

STATION—CM No. Y6

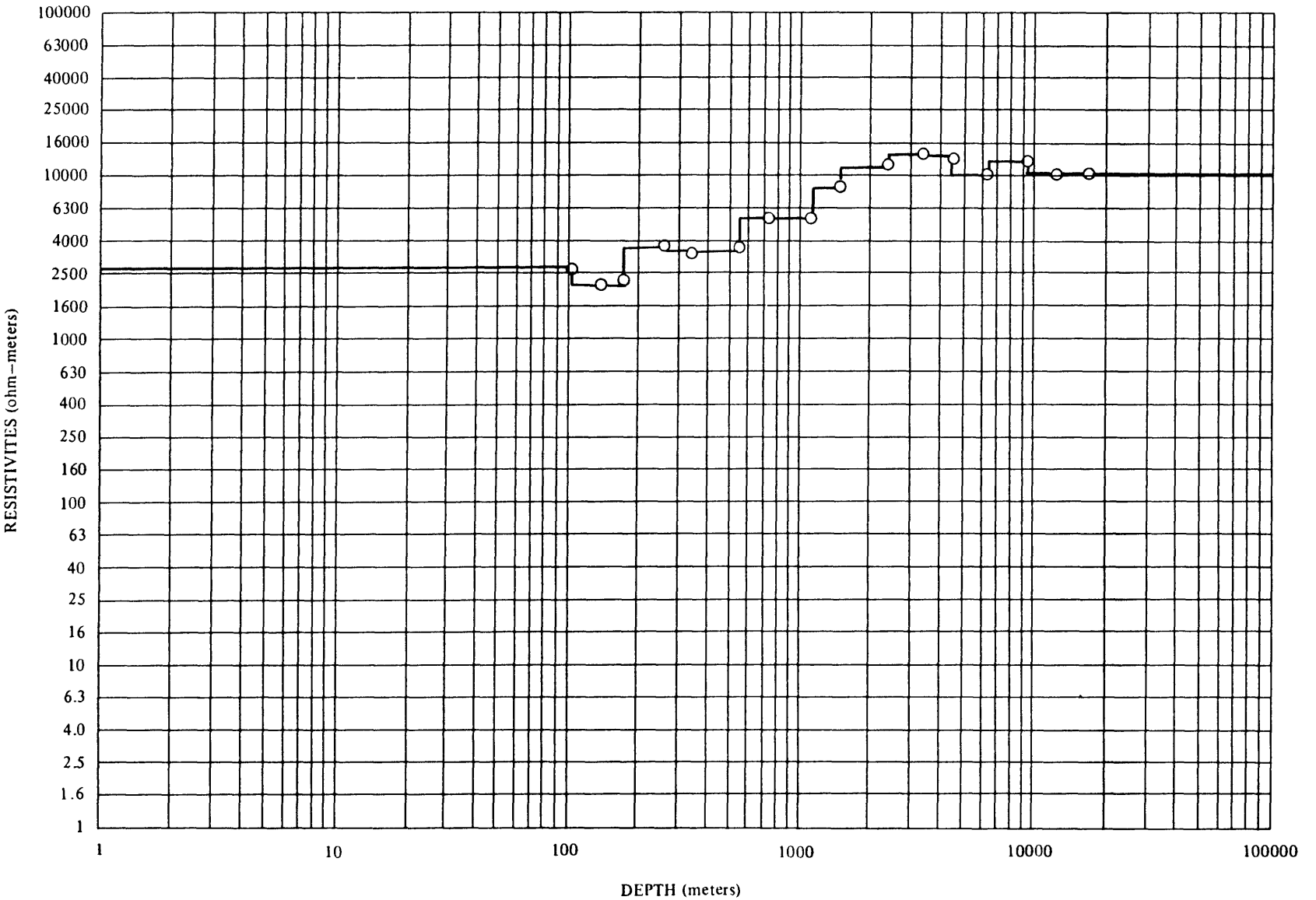

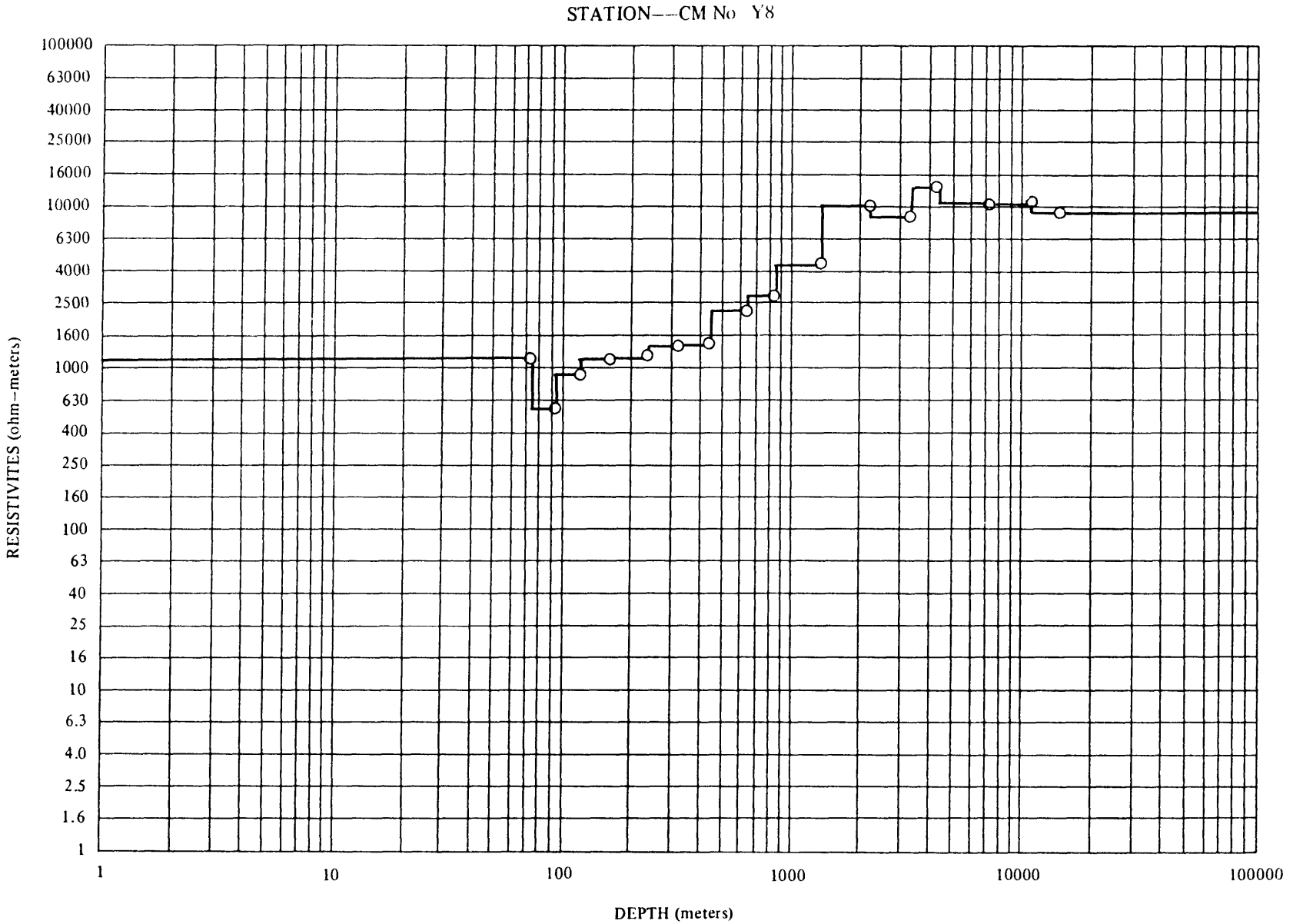
STATION--CM No Y8
RESISTIVITES (ohm-meters)
100000
63000
40000
25000
16000
10000
6300
4000
2500
1600
1000
630
400
250
160
100
63
40
25
16
10
6.3
4.0
2.5
1.6
1
1
10
100
1000
10000
100000
DEPTH (meters)

STATION—CM No. Y9